Quantum Monte Carlo simulations within dynamical mean-field theory

Nils Blümer, Univ. Mainz

Outline

Motivation: cooperative phenomena in solids

Approaches for correlated electron systems $\rightsquigarrow$ DMFT

Auxiliary-field quantum Monte Carlo algorithm

Update: orbital-selective Mott transitions

Efficiency of QMC DMFT solvers

Summary and outlook

Motivation: cooperative phenomena in solids

Itinerant ferromagnetism and half-metallicity

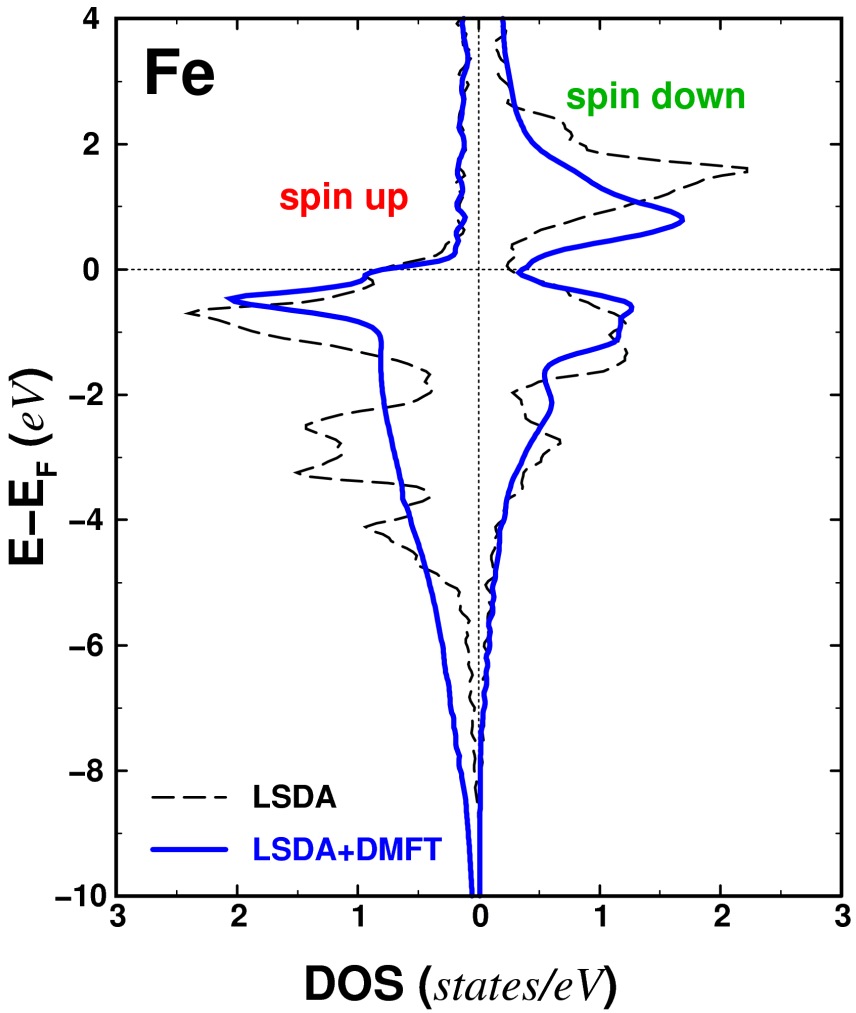

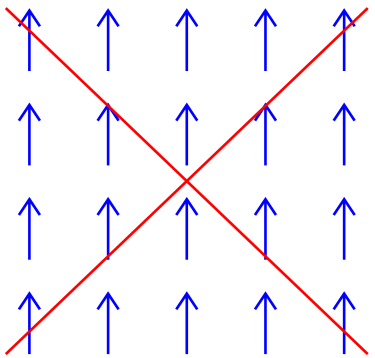

Spin models insufficient

[Chioncel et. al, PRB (2003)]

Motivation: cooperative phenomena in solids

Itinerant ferromagnetism and half-metallicity

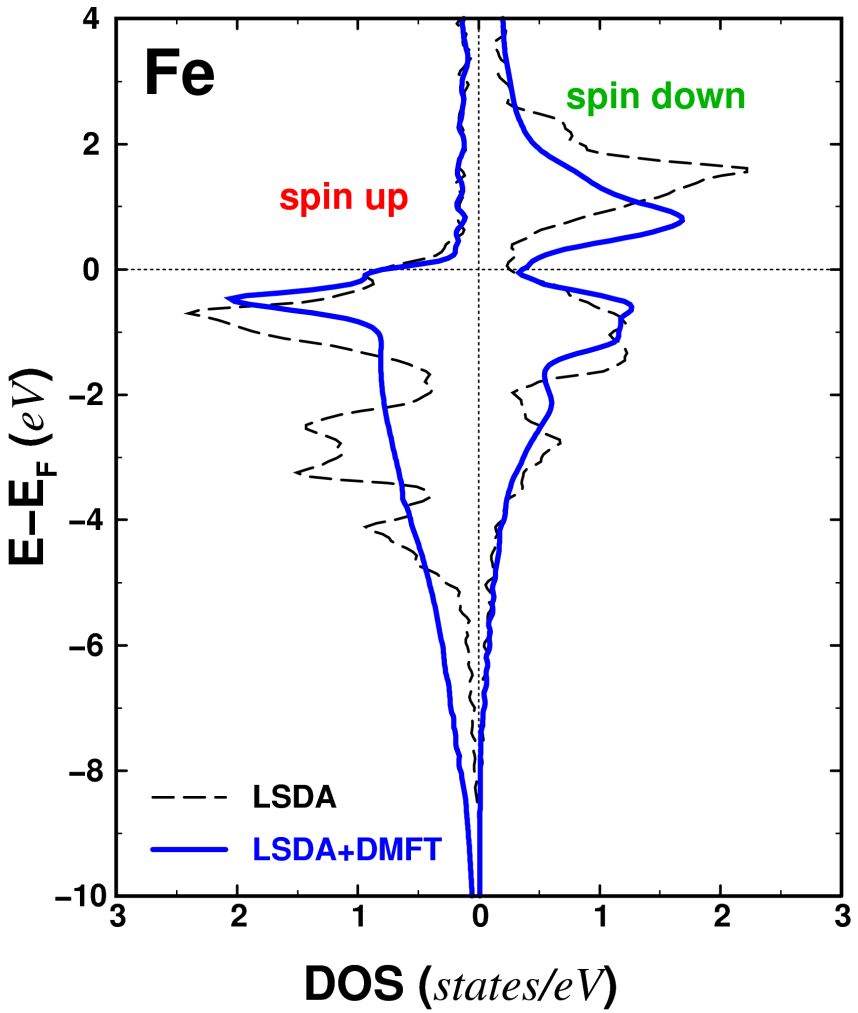

[Chioncel et. al, PRB (2003)]

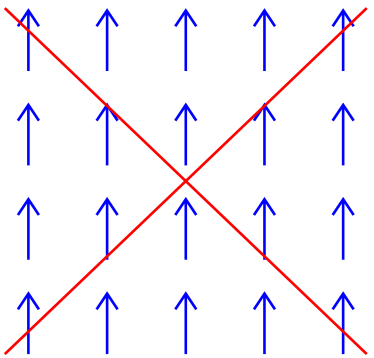

Spin models insufficient

Technological goal: TMR with half metals

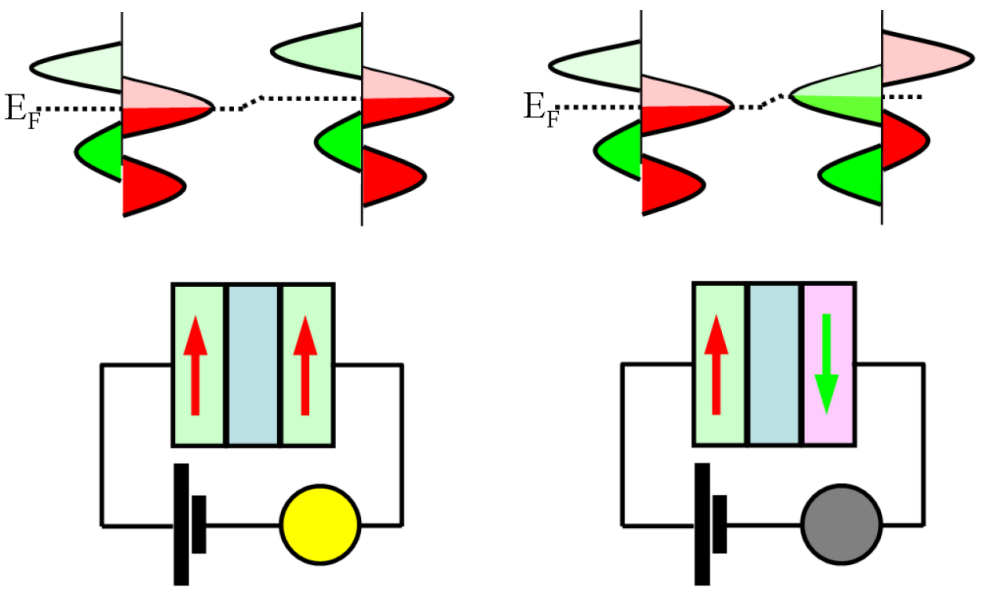

Complex phases of cuprate and organic superconductors

High-T_c physics contained in 2D Hubbard model?

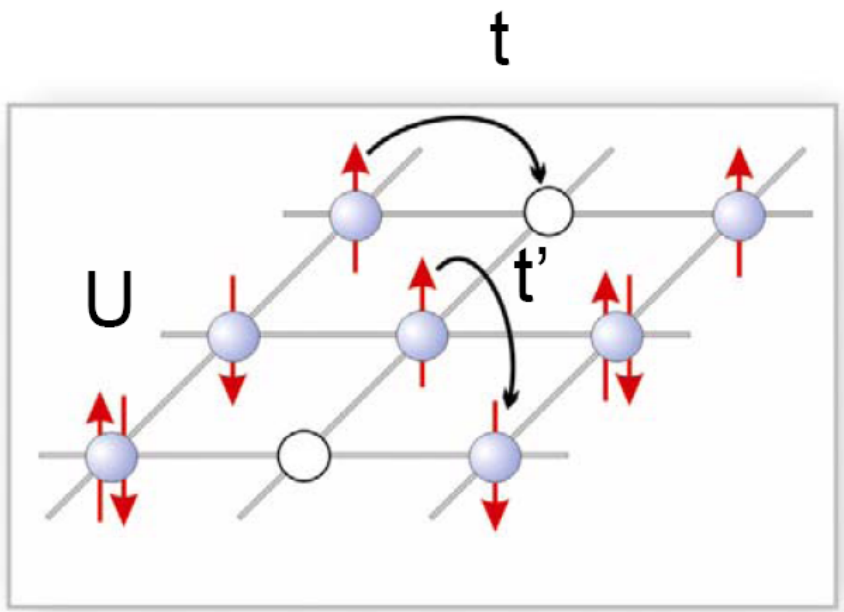

Are antiferromagnetic (AF) and Mott insulating phases essential for superconductivity?

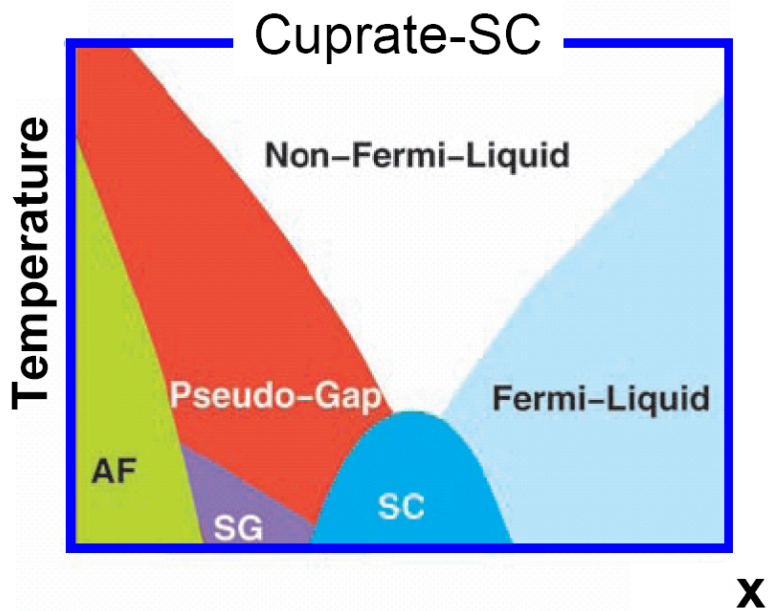

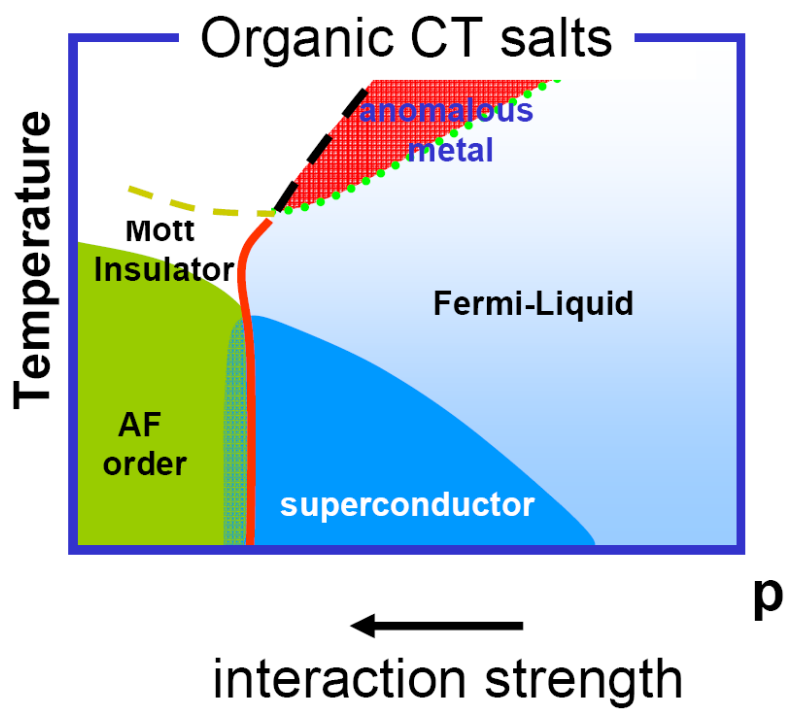

Mott metal-insulator transition

Prototype example: V_2O_3 doped
with Cr/Ti and/or under pressure

Phase diagram

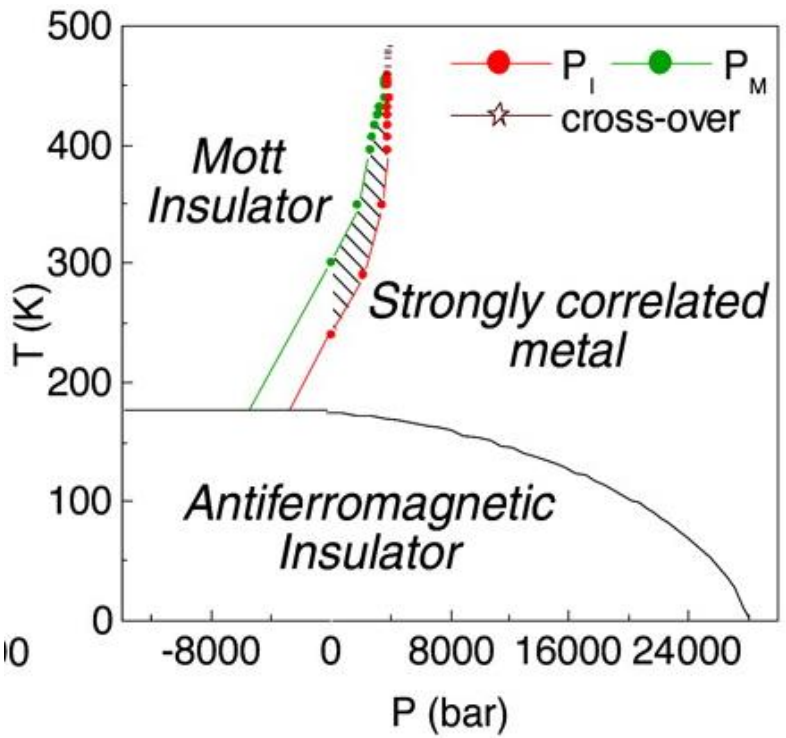

Mott metal-insulator transition

Prototype example: V_2O_3 doped with Cr/Ti and/or under pressure

Phase diagram

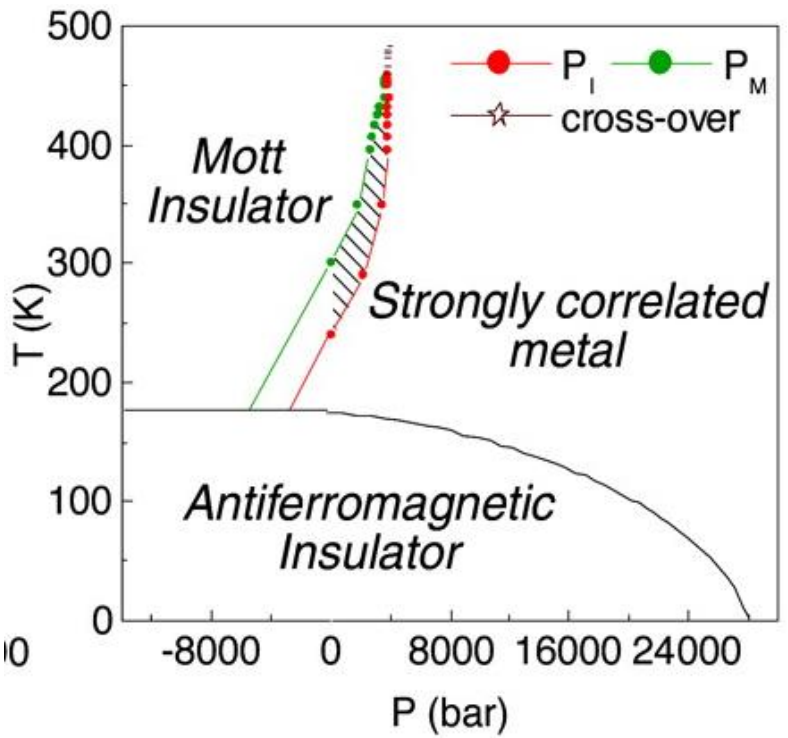

Electrical conductivity

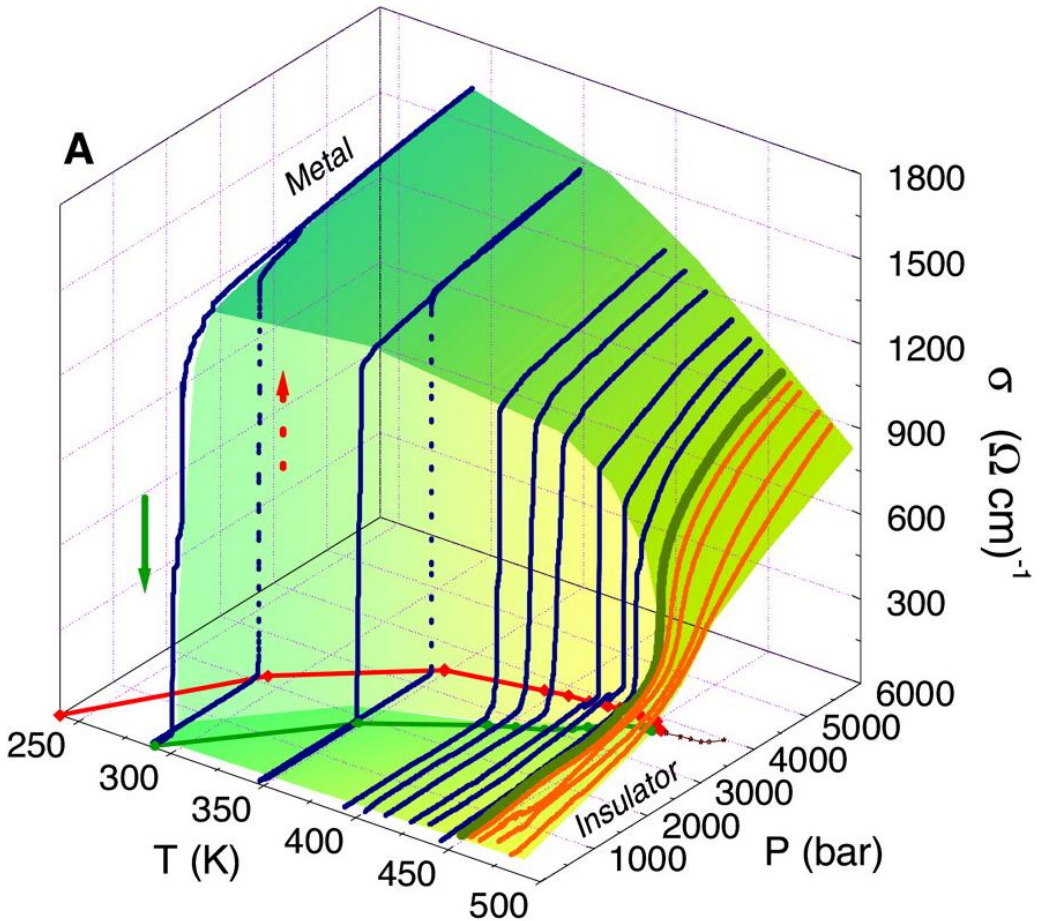

[Limelette et al., Science 302, 89 (2003)]

Bandwidth control of metal-insulator transitions

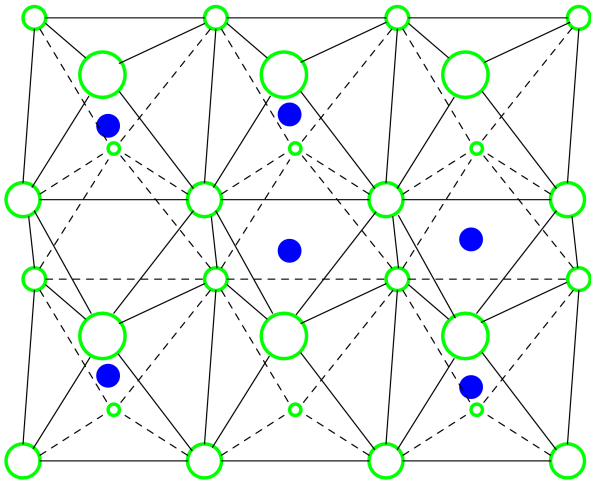

Corundum structure

Hydrostatic pressure or isovalent doping change

- lattice spacings
- bond angles

$\rightsquigarrow$ hopping amplitudes

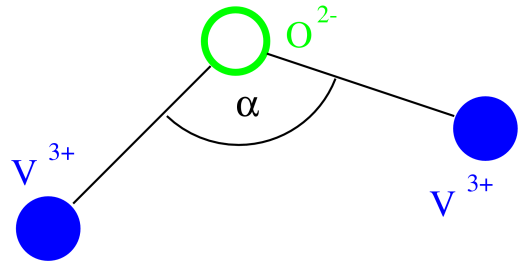

$\alpha_{Cr} < \alpha_{V} < \alpha_{Ti}$

Bond angles for V_2O_3 doped with Cr or Ti

Bandwidth control of metal-insulator transitions

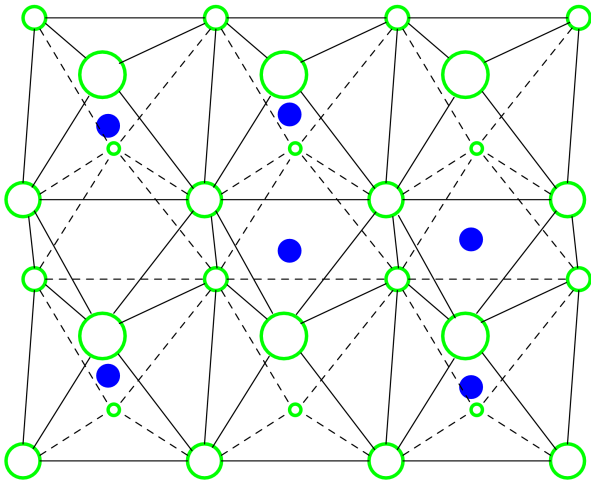

Corundum structure

Hydrostatic pressure or isovalent doping change

- lattice spacings
- bond angles

$\rightsquigarrow$ hopping amplitudes

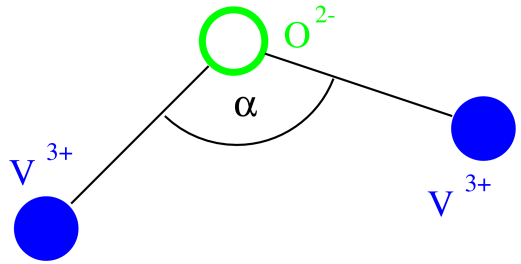

$\alpha_{Cr} < \alpha_{V} < \alpha_{Ti}$

Bond angles for V_2O_3 doped with Cr or Ti

Breakdown of Bloch band description at paramagnetic Mott transition

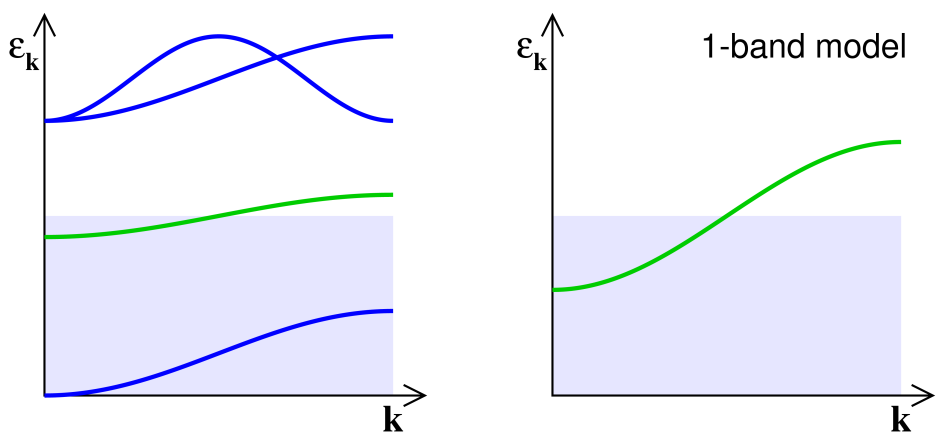

Bloch states near Fermi energy

Bandwidth control of metal-insulator transitions

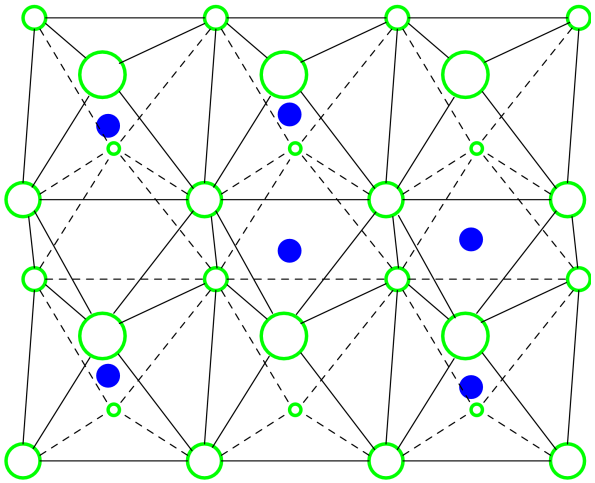

Corundum structure

Hydrostatic pressure or isovalent doping change

- lattice spacings
- bond angles

$\rightsquigarrow$ hopping amplitudes

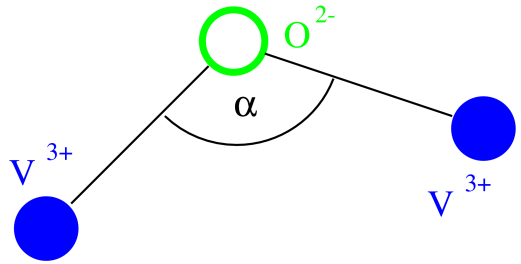

$\alpha_{Cr} < \alpha_{V} < \alpha_{Ti}$

Bond angles for V_2O_3 doped with Cr or Ti

Breakdown of Bloch band description at paramagnetic Mott transition

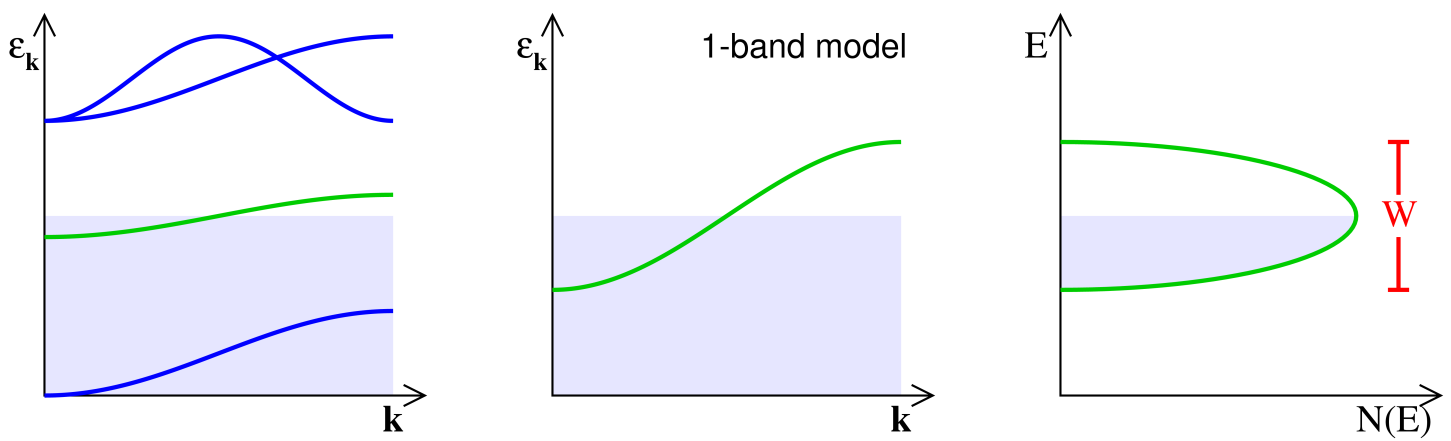

Bloch states near Fermi energy

Bandwidth control of metal-insulator transitions

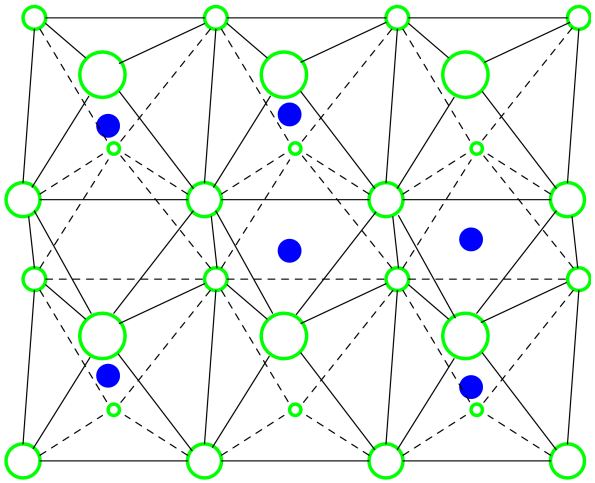

Corundum structure

Hydrostatic pressure or isovalent doping change

- lattice spacings
- bond angles

$\rightsquigarrow$ hopping amplitudes

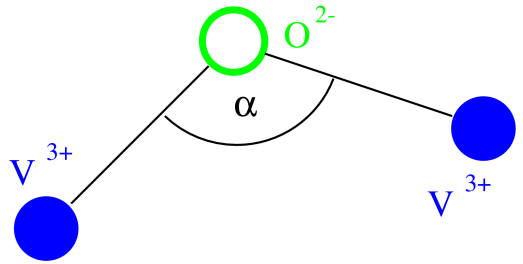

$\alpha_{Cr} < \alpha_{V} < \alpha_{Ti}$

Bond angles for V_2O_3 doped with Cr or Ti

Breakdown of Bloch band description at paramagnetic Mott transition

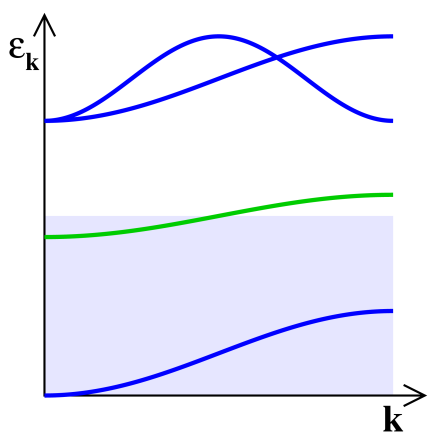

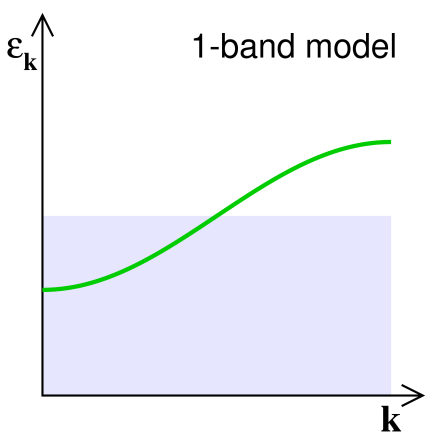

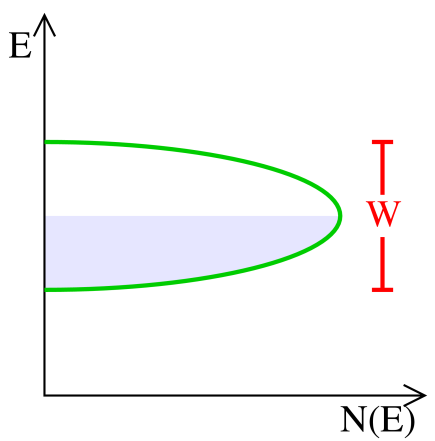

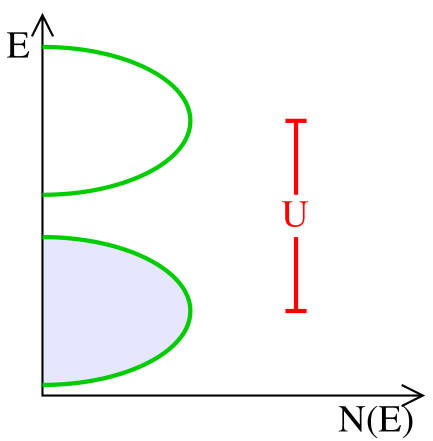

Bloch states near Fermi energy, band-splitting by Coulomb correlations

Approaches for correlated electron systems

Microscopic modeling I

General Hamiltonian for nuclei and electrons

$$H = \sum_{i=1}^{N_e} \frac{\boldsymbol{p}_i^{\,2}}{2m} + \sum_{k=1}^{L} \frac{\boldsymbol{P}_k^{\,2}}{2M_k} + \sum_{k<l} \frac{Z_k Z_l\, e^2}{|\boldsymbol{R}_k - \boldsymbol{R}_l|} - \sum_{i,k} \frac{Z_k\, e^2}{|\boldsymbol{r}_i - \boldsymbol{R}_k|} + \sum_{i<j} \frac{e^2}{|\boldsymbol{r}_i - \boldsymbol{r}_j|}$$

Approaches for correlated electron systems

Microscopic modeling I

General Hamiltonian for nuclei and electrons

$$H = \sum_{i=1}^{N_e} \frac{\boldsymbol{p}_i^{\,2}}{2m} + \sum_{k=1}^{L} \frac{\boldsymbol{P}_k^{\,2}}{2M_k} + \sum_{k<l} \frac{Z_k Z_l\, e^2}{|\boldsymbol{R}_k - \boldsymbol{R}_l|} - \sum_{i,k} \frac{Z_k\, e^2}{|\boldsymbol{r}_i - \boldsymbol{R}_k|} + \sum_{i<j} \frac{e^2}{|\boldsymbol{r}_i - \boldsymbol{r}_j|}$$

Born-Oppenheimer approximation (0^{th}order)

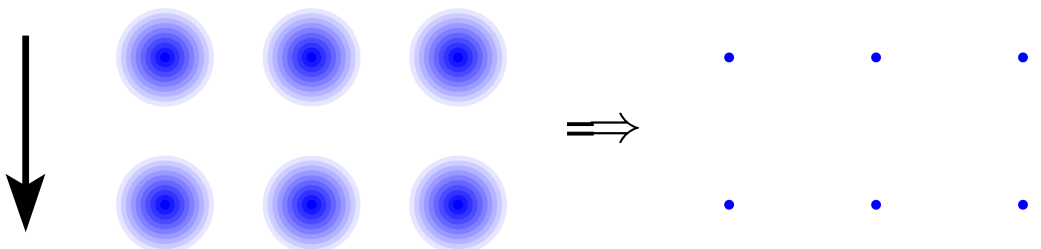

Approaches for correlated electron systems

Microscopic modeling I

General Hamiltonian for nuclei and electrons

$$H = \sum_{i=1}^{N_e} \frac{\boldsymbol{p}_i^2}{2m} + \sum_{k=1}^{L} \frac{\boldsymbol{P}_k^2}{2M_k} + \sum_{k<l} \frac{Z_k Z_l\, e^2}{|\boldsymbol{R}_k - \boldsymbol{R}_l|} - \sum_{i,k} \frac{Z_k\, e^2}{|\boldsymbol{r}_i - \boldsymbol{R}_k|} + \sum_{i<j} \frac{e^2}{|\boldsymbol{r}_i - \boldsymbol{r}_j|}$$

Born-Oppenheimer approximation (0^{th}order)

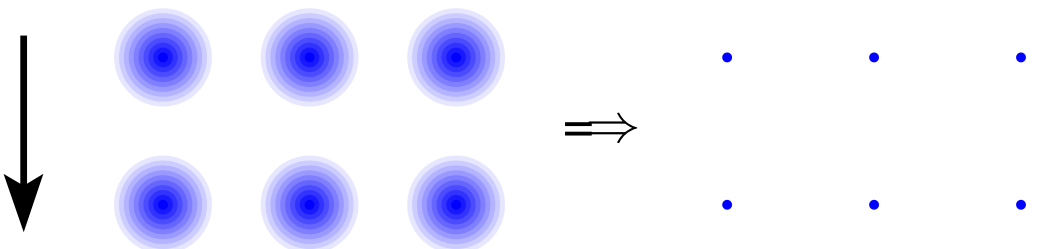

$$H = \sum_{i=1}^{N_e} \frac{\boldsymbol{p}_i^2}{2m} + \sum_{i} V(\boldsymbol{r}_i) + \sum_{i<j} \frac{e^2}{|\boldsymbol{r}_i - \boldsymbol{r}_j|}$$

Approaches for correlated electron systems

Microscopic modeling I

General Hamiltonian for nuclei and electrons

$$H = \sum_{i=1}^{N_e} \frac{\boldsymbol{p}_i^2}{2m} + \sum_{k=1}^{L} \frac{\boldsymbol{P}_k^2}{2M_k} + \sum_{k<l} \frac{Z_k Z_l\, e^2}{|\boldsymbol{R}_k - \boldsymbol{R}_l|} - \sum_{i,k} \frac{Z_k\, e^2}{|\boldsymbol{r}_i - \boldsymbol{R}_k|} + \sum_{i<j} \frac{e^2}{|\boldsymbol{r}_i - \boldsymbol{r}_j|}$$

Born-Oppenheimer approximation (0^{th}order)

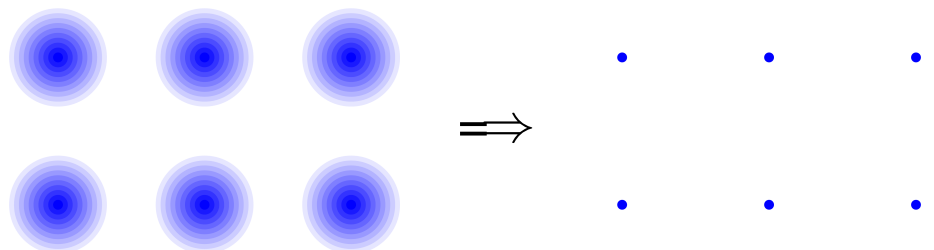

$$H = \sum_{i=1}^{N_e} \frac{\boldsymbol{p}_i^2}{2m} + \sum_{i} V(\boldsymbol{r}_i) + \sum_{i<j} \frac{e^2}{|\boldsymbol{r}_i - \boldsymbol{r}_j|}$$

Classes of theoretical approaches for electronic problem

- continuum methods: density functional theory (DFT), variational+diffusion QMC, . .
- methods for lattice electrons

Microscopic modeling II

$$H = \sum_{i=1}^{N_e} \frac{\boldsymbol{p}_i^2}{2m} + \sum_i V(\boldsymbol{r}_i) + \sum_{i<j} \frac{e^2}{|\boldsymbol{r}_i - \boldsymbol{r}_j|}$$

reduction to valence electrons

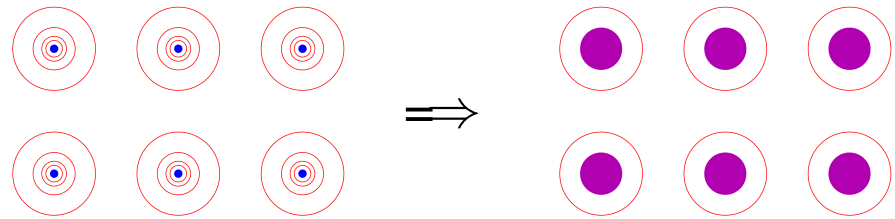

$$H = \sum_{i=1}^{N_v} \frac{\boldsymbol{p}_i^2}{2m} + \sum_{i=1}^{N_v} V^{\text{ion}}(\boldsymbol{r}_i) + \sum_{i=1}^{N_v-1} \sum_{j=i+1}^{N_v} V^{ee}(\boldsymbol{r}_i, \boldsymbol{r}_j)$$

Microscopic modeling II

$$H = \sum_{i=1}^{N_e} \frac{\boldsymbol{p}_i^2}{2m} + \sum_i V(\boldsymbol{r}_i) + \sum_{i<j} \frac{e^2}{|\boldsymbol{r}_i - \boldsymbol{r}_j|}$$

reduction to valence electrons ↓

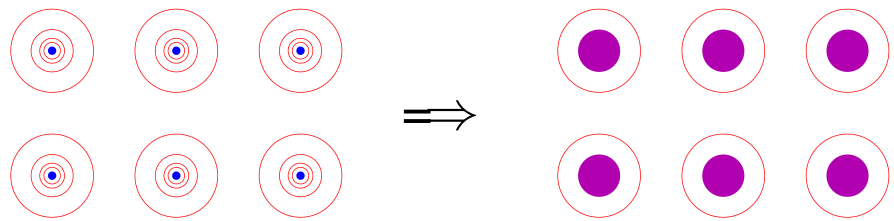

$$H = \sum_{i=1}^{N_v} \frac{\boldsymbol{p}_i^2}{2m} + \sum_{i=1}^{N_v} V^{\text{ion}}(\boldsymbol{r}_i) + \sum_{i=1}^{N_v-1} \sum_{j=i+1}^{N_v} V^{ee}(\boldsymbol{r}_i, \boldsymbol{r}_j)$$

occupation number formalism ↓ Wannier orbitals

$$\hat{H} = \sum_{i\nu j\sigma} t_{ij}^{\nu} \, \hat{c}_{i\nu\sigma}^{\dagger} \, \hat{c}_{j\nu\sigma} + \frac{1}{2} \sum_{\nu\nu'\mu\mu'} \sum_{ijmn} \sum_{\sigma\sigma'} \mathcal{V}_{ijmn}^{\nu\nu'\mu\mu'} \, \hat{c}_{i\nu\sigma}^{\dagger} \, \hat{c}_{j\nu'\sigma'}^{\dagger} \, \hat{c}_{n\mu'\sigma'} \, \hat{c}_{m\mu\sigma}$$

Microscopic modeling II

$$H = \sum_{i=1}^{N_e} \frac{\boldsymbol{p}_i^2}{2m} + \sum_i V(\boldsymbol{r}_i) + \sum_{i<j} \frac{e^2}{|\boldsymbol{r}_i - \boldsymbol{r}_j|}$$

reduction to valence electrons ↓

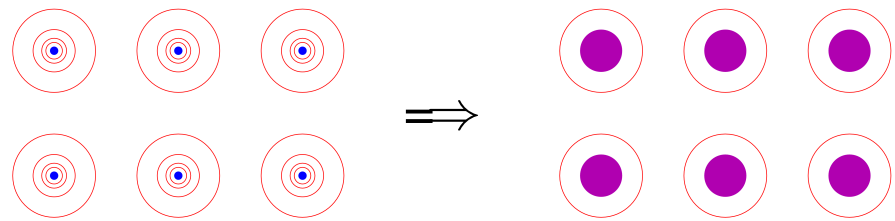

$$H = \sum_{i=1}^{N_v} \frac{\boldsymbol{p}_i^2}{2m} + \sum_{i=1}^{N_v} V^{\text{ion}}(\boldsymbol{r}_i) + \sum_{i=1}^{N_v-1} \sum_{j=i+1}^{N_v} V^{ee}(\boldsymbol{r}_i, \boldsymbol{r}_j)$$

occupation number formalism ↓ Wannier orbitals

$$\hat{H} = \sum_{i\nu j\sigma} t_{ij}^{\nu} \, \hat{c}_{i\nu\sigma}^{\dagger} \, \hat{c}_{j\nu\sigma} + \frac{1}{2} \sum_{\nu\nu'\mu\mu'} \sum_{ijmn} \sum_{\sigma\sigma'} \mathcal{V}_{ijmn}^{\nu\nu'\mu\mu'} \, \hat{c}_{i\nu\sigma}^{\dagger} \, \hat{c}_{j\nu'\sigma'}^{\dagger} \, \hat{c}_{n\mu'\sigma'} \, \hat{c}_{m\mu\sigma}$$

Hubbard model

$$\hat{H} = \sum_{(i,j),\sigma} t_{ij} \, (\hat{c}_{i\sigma}^{\dagger} \hat{c}_{j\sigma} + \text{h.c.}) + U \sum_i \hat{n}_{i\uparrow} \hat{n}_{i\downarrow}$$

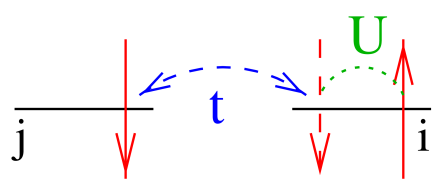

Approaches for Hubbard-type models

$$\hat{H} = \sum_{(i,j),\sigma} t_{ij} (\hat{c}^{\dagger}_{i\sigma} \hat{c}_{j\sigma} + \text{h.c.}) + U \sum_{i} \hat{n}_{i\uparrow} \hat{n}_{i\downarrow}$$

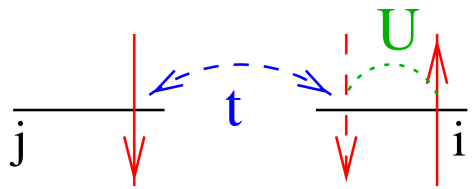

Perturbation theory

- $U \to 0$: Hartree-Fock
  2^{nd} order PT, . . .
- $t/U \to 0$ (for $n = 1$)
  $\rightsquigarrow$ Heisenberg model

finite clusters: ED, QMC

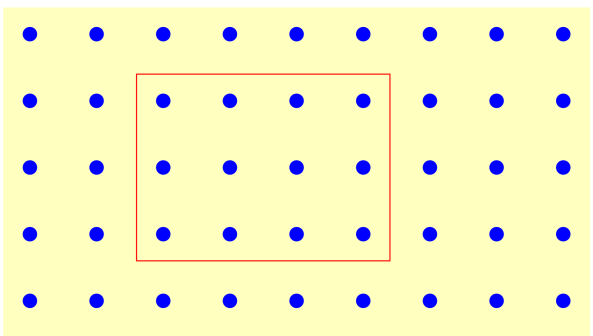

$d \to 1$: Bethe ansatz, DMRG

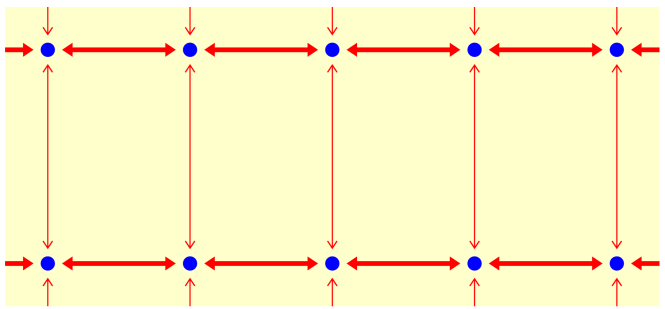

Approaches for Hubbard-type models

$$\hat{H} = \sum_{(i,j),\sigma} t_{ij} (\hat{c}^{\dagger}_{i\sigma} \hat{c}_{j\sigma} + \text{h.c.}) + U \sum_{i} \hat{n}_{i\uparrow} \hat{n}_{i\downarrow}$$

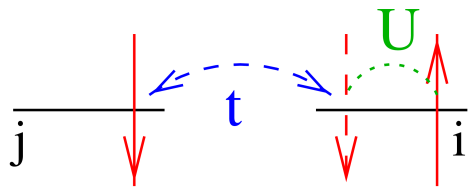

Perturbation theory

- $U \to 0$: Hartree-Fock
  2^{nd} order PT, . . .
- $t/U \to 0$ (for $n = 1$)
  $\rightsquigarrow$ Heisenberg model

finite clusters: ED, QMC

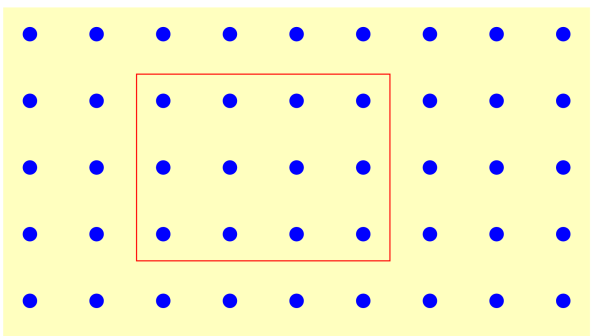

$d \to 1$: Bethe ansatz, DMRG

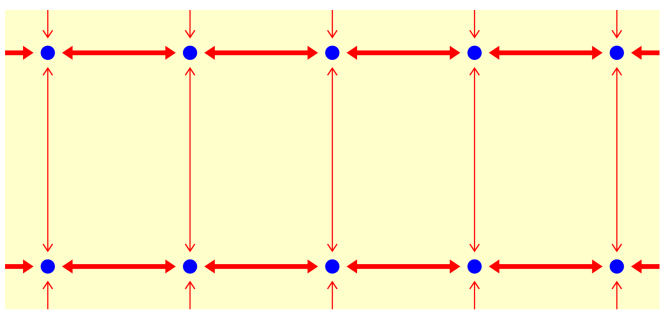

Dynamical mean-field theory (DMFT): local self-energy $\Sigma(\boldsymbol{k}, \omega) \equiv \Sigma(\omega)$

[Metzner, Vollhardt, PRL (1989), Georges, Kotliar, PRL (1992), Jarrell, PRL (1992)]

\+ non-perturbative $\rightsquigarrow$ valid at MIT

\+ dynamical on-site correlations preserved

\+ in thermodynamic limit

+/− exact for coordination $Z \to \infty$

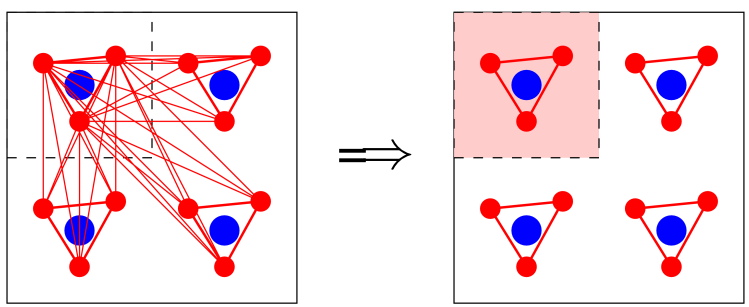

Excursus: Green function and self-energy

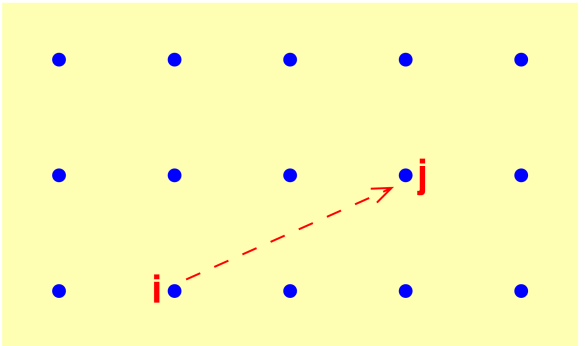

Single-particle Green function (lattice sites i, j):

$$G_{ij}(t_1, t_2) = -\langle c_j(t_2)\, c_i^\dagger(t_1)\rangle$$

Translation invariance in space and time: $G_{ij}(t_1, t_2) \equiv G_{j-i}(t_2 - t_1) \overset{\text{Fourier}}{\longrightarrow} G(\boldsymbol{k}, \omega)$

Excursus: Green function and self-energy

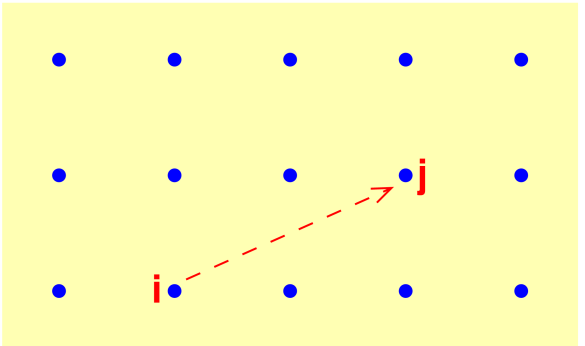

Single-particle Green function (lattice sites i, j):

$$G_{ij}(t_1, t_2) = -\langle c_j(t_2)\, c_i^\dagger(t_1)\rangle$$

Translation invariance in space and time: $G_{ij}(t_1, t_2) \equiv G_{j-i}(t_2 - t_1) \overset{\text{Fourier}}{\longrightarrow} G(\boldsymbol{k}, \omega)$

Noninteracting limit (dispersion $\epsilon_{\boldsymbol{k}}$): $G_0(\boldsymbol{k}, \omega) = \dfrac{1}{\omega + \mu - \epsilon_{\boldsymbol{k}}}$

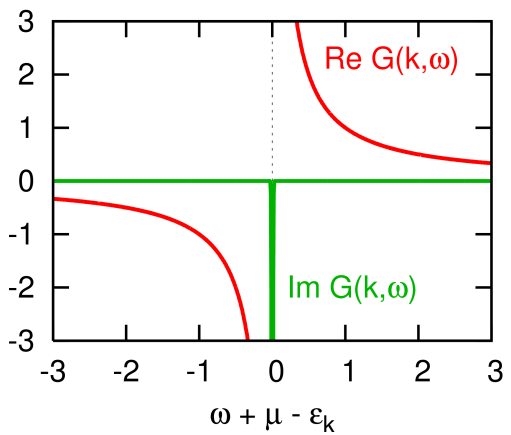

Excursus: Green function and self-energy

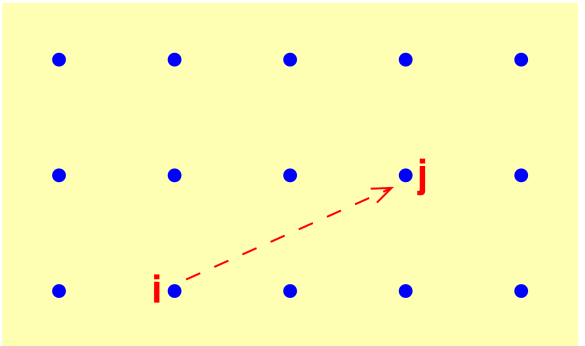

Single-particle Green function (lattice sites i, j):

$$G_{ij}(t_1, t_2) = -\langle c_j(t_2)\, c_i^\dagger(t_1)\rangle$$

Translation invariance in space and time: $G_{ij}(t_1, t_2) \equiv G_{j-i}(t_2 - t_1) \overset{\text{Fourier}}{\longrightarrow} G(\boldsymbol{k}, \omega)$

Noninteracting limit (dispersion $\epsilon_{\boldsymbol{k}}$): $G_0(\boldsymbol{k}, \omega) = \dfrac{1}{\omega + \mu - \epsilon_{\boldsymbol{k}}}$

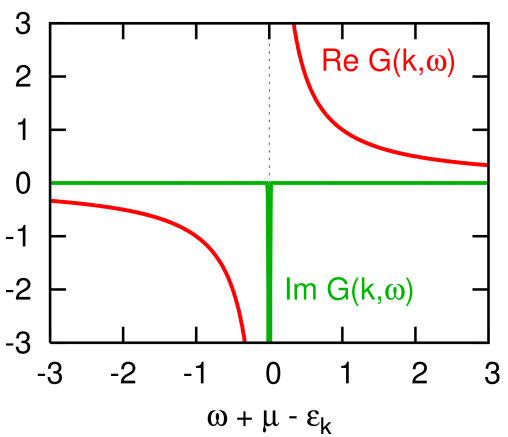

Self-energy Σ quantifies impact of interactions:

$$G(\boldsymbol{k}, \omega) = \frac{1}{\omega + \mu - \epsilon_{\boldsymbol{k}} - \Sigma(\boldsymbol{k}, \omega)}$$

Excursus: Green function and self-energy

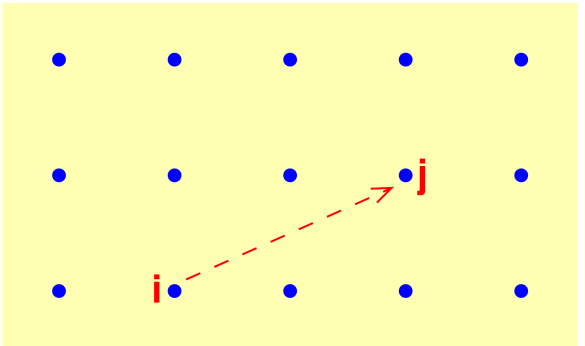

Single-particle Green function (lattice sites i, j):

$$G_{ij}(t_1, t_2) = -\langle c_j(t_2)\, c_i^\dagger(t_1)\rangle$$

Translation invariance in space and time: $G_{ij}(t_1, t_2) \equiv G_{j-i}(t_2 - t_1) \overset{\text{Fourier}}{\longrightarrow} G(\boldsymbol{k}, \omega)$

Noninteracting limit (dispersion $\epsilon_{\boldsymbol{k}}$): $G_0(\boldsymbol{k}, \omega) = \dfrac{1}{\omega + \mu - \epsilon_{\boldsymbol{k}}}$

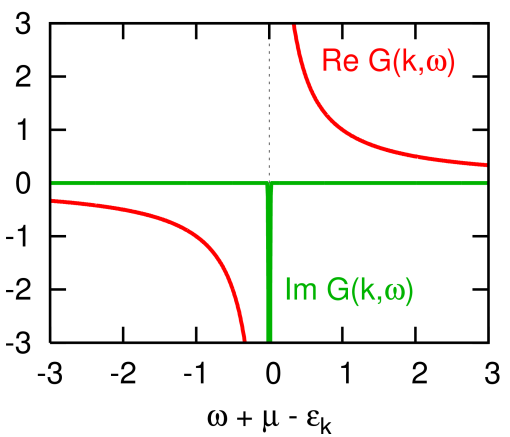

Self-energy Σ quantifies impact of interactions:

$$G(\boldsymbol{k}, \omega) = \frac{1}{\omega + \mu - \epsilon_{\boldsymbol{k}} - \Sigma(\boldsymbol{k}, \omega)}$$

Locality of self-energy $\Sigma(\boldsymbol{k}, \omega) \equiv \Sigma(\omega)$ within DMFT simplifies local Green function:

$$G(\omega) \equiv G_{ii}(\omega) = \int d\epsilon \, \frac{\rho(\epsilon)}{\omega + \mu - \epsilon - \Sigma(\omega)}; \qquad \rho(\epsilon) = \frac{1}{N} \sum_{\boldsymbol{k}} \delta(\epsilon - \epsilon_{\boldsymbol{k}})$$

$\boldsymbol{k}$ integrated Dyson equation — noninteracting DOS

Brief History of DMFT

1989 Metzner, Vollhardt: **limit** $\boldsymbol{d} \to \infty$: Gutzwiller approximation exact

Müller-Hartmann: local self-energy: $\Sigma(\boldsymbol{q}, \omega) \to \Sigma(\omega)$

Brandt, Mielsch: exact solution of Falicov-Kimball model

Brief History of DMFT

1989 Metzner, Vollhardt: **limit** $\boldsymbol{d} \to \infty$: Gutzwiller approximation exact

Müller-Hartmann: local self-energy: $\Sigma(\boldsymbol{q}, \omega) \to \Sigma(\omega)$

Brandt, Mielsch: exact solution of Falicov-Kimball model

1992 Georges, Kotliar: mapping to Anderson impurity model + self consistency

Brief History of DMFT

1989 Metzner, Vollhardt: **limit** $\boldsymbol{d \to \infty}$: Gutzwiller approximation exact
Müller-Hartmann: local self-energy: $\Sigma(\boldsymbol{q}, \omega) \to \Sigma(\omega)$
Brandt, Mielsch: exact solution of Falicov-Kimball model

1992 Georges, Kotliar: mapping to Anderson impurity model + self consistency
Jarrell: quantum Monte Carlo $\rightsquigarrow$ antiferromagnetism, Mott-Hubbard behavior

1993 Georges et al., Kotliar et al.: frustrated Bethe lattice $\rightsquigarrow$ Mott transition

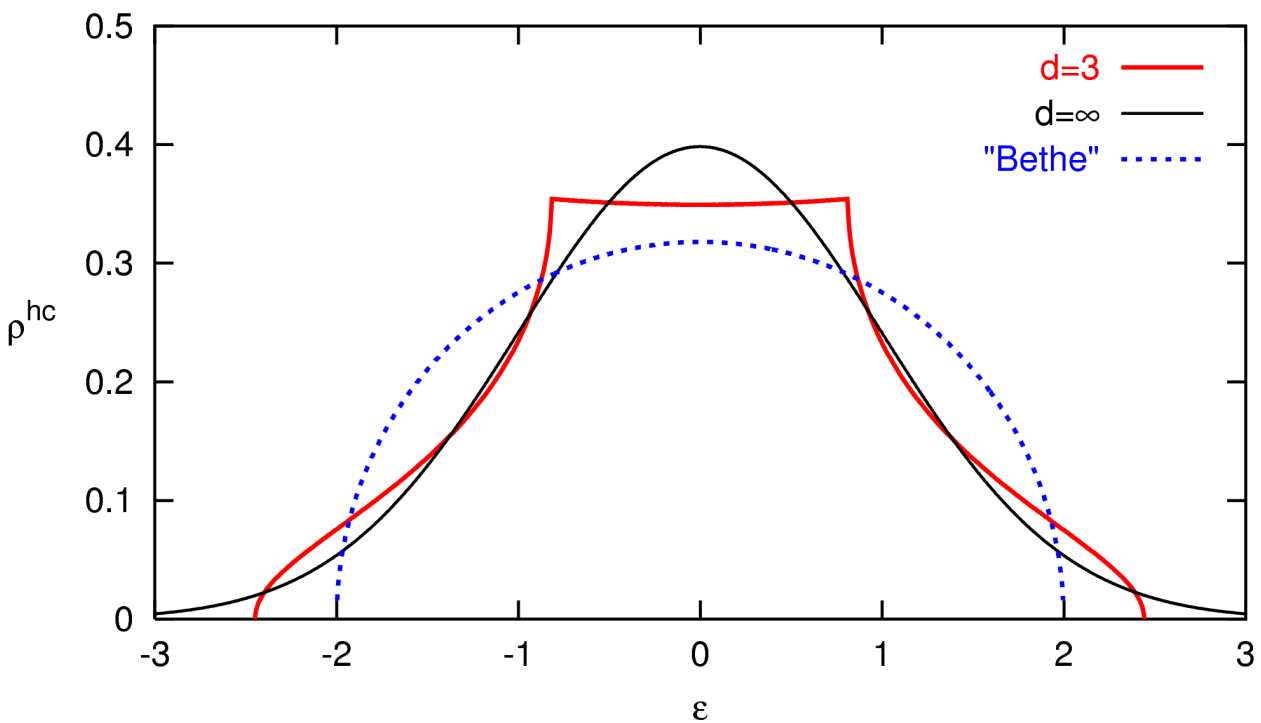

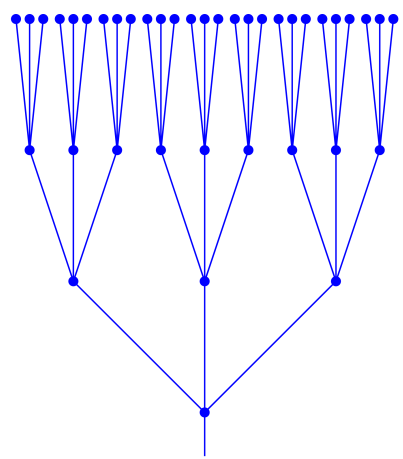

Brief History of DMFT

1989 Metzner, Vollhardt: **limit** $\boldsymbol{d} \to \infty$: Gutzwiller approximation exact
Müller-Hartmann: local self-energy: $\Sigma(\boldsymbol{q}, \omega) \to \Sigma(\omega)$
Brandt, Mielsch: exact solution of Falicov-Kimball model

1992 Georges, Kotliar: mapping to Anderson impurity model + self consistency
Jarrell: quantum Monte Carlo $\rightsquigarrow$ antiferromagnetism, Mott-Hubbard behavior

1993 Georges et al., Kotliar et al.: frustrated Bethe lattice $\rightsquigarrow$ Mott transition

1996 Georges, Kotliar, Krauth, Rozenberg: **Rev. Mod. Phys.** article
Vollhardt group: ferro/metamagnetism

Brief History of DMFT

1989 Metzner, Vollhardt: **limit** $\boldsymbol{d} \to \infty$: Gutzwiller approximation exact
Müller-Hartmann: local self-energy: $\Sigma(\boldsymbol{q}, \omega) \to \Sigma(\omega)$
Brandt, Mielsch: exact solution of Falicov-Kimball model

1992 Georges, Kotliar: mapping to Anderson impurity model + self consistency
Jarrell: quantum Monte Carlo $\rightsquigarrow$ antiferromagnetism, Mott-Hubbard behavior

1993 Georges et al., Kotliar et al.: frustrated Bethe lattice $\rightsquigarrow$ Mott transition

1996 Georges, Kotliar, Krauth, Rozenberg: **Rev. Mod. Phys.** article
Vollhardt group: ferro/metamagnetism

1997 Anisimov, Kotliar: LDA+DMFT(IPT) $\rightsquigarrow$ photo emission spectra (PES)

2000 Vollhardt+Anisimov groups: LDA+DMFT(QMC) $\rightsquigarrow$ PES for $La_{1-x}Sr_xTiO_3$

Brief History of DMFT

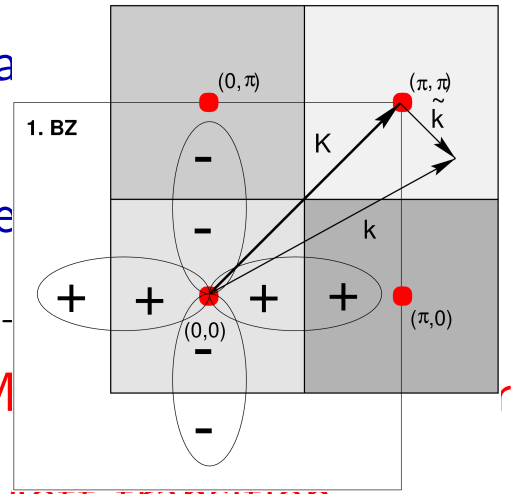

1989 Metzner, Vollhardt: **limit** $d \to \infty$: Gutzwiller approxima
Müller-Hartmann: local self-energy: $\Sigma(\boldsymbol{q}, \omega) \longrightarrow \Sigma(\omega)$
Brandt, Mielsch: exact solution of Falicov-Kimball mode

1992 Georges, Kotliar: mapping to Anderson impurity model -
Jarrell: quantum Monte Carlo $\rightsquigarrow$ antiferromagnetism, M

1993 Georges et al., Kotliar et al.: frustrated Bethe lattice $\rightsquigarrow$ Mott transition

1996 Georges, Kotliar, Krauth, Rozenberg: **Rev. Mod. Phys.** article
Vollhardt group: ferro/metamagnetism

1997 Anisimov, Kotliar: LDA+DMFT(IPT) $\rightsquigarrow$ photo emission spectra (PES)

2000 Vollhardt+Anisimov groups: LDA+DMFT(QMC) $\rightsquigarrow$ PES for $La_{1-x}Sr_xTiO_3$
Jarrell group: dynamical cluster approximation (DCA) $\rightsquigarrow$ d-wave sc

Brief History of DMFT

1989 Metzner, Vollhardt: **limit** $d \to \infty$: Gutzwiller approximation exact
Müller-Hartmann: local self-energy: $\Sigma(\boldsymbol{q}, \omega) \to \Sigma(\omega)$
Brandt, Mielsch: exact solution of Falicov-Kimball model

1992 Georges, Kotliar: mapping to Anderson impurity model + self consistency
Jarrell: quantum Monte Carlo $\rightsquigarrow$ antiferromagnetism, Mott-Hubbard behavior

1993 Georges et al., Kotliar et al.: frustrated Bethe lattice $\rightsquigarrow$ Mott transition

1996 Georges, Kotliar, Krauth, Rozenberg: **Rev. Mod. Phys.** article
Vollhardt group: ferro/metamagnetism

1997 Anisimov, Kotliar: LDA+DMFT(IPT) $\rightsquigarrow$ photo emission spectra (PES)

2000 Vollhardt+Anisimov groups: LDA+DMFT(QMC) $\rightsquigarrow$ PES for $La_{1-x}Sr_xTiO_3$
Jarrell group: dynamical cluster approximation (DCA) $\rightsquigarrow$ d-wave sc

today new DMFT solvers, multi-orbital physics
realistic calculations (LDA+DMFT), cluster methods (DCA, CDMFT)

Iterative solution of DMFT equations

0. Initialize self-energy
1. Solve Dyson equation
2. Solve single impurity Anderson model (SIAM)

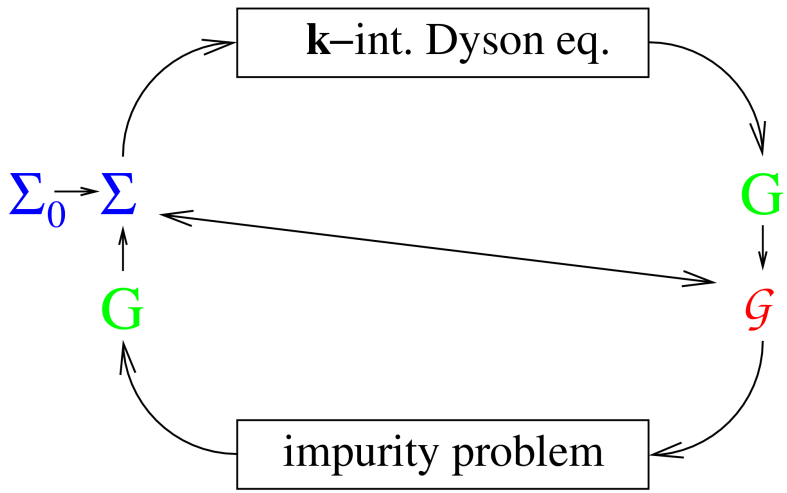

$\longleftarrow$ DOS / t_{ij} / $\epsilon_{\nu \boldsymbol{k}}$

$\longleftarrow$ local interactions

Iterative solution of DMFT equations

0. Initialize self-energy
1. Solve Dyson equation
2. Solve single impurity Anderson model (SIAM)

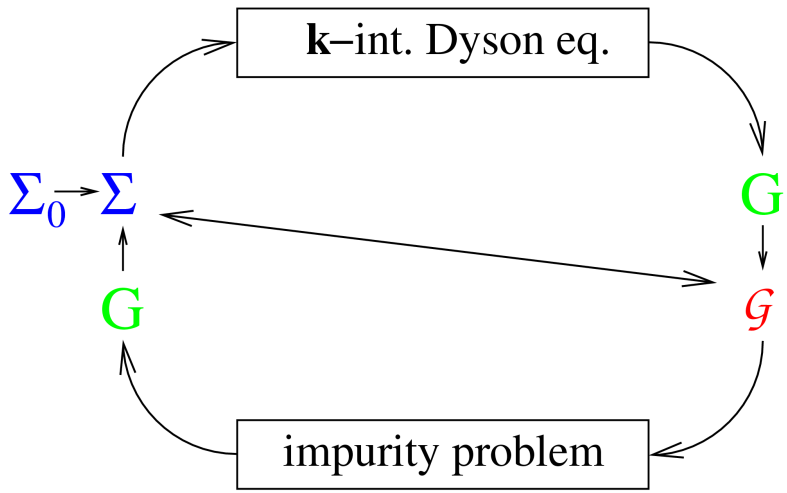

⟵ DOS / t_{ij} / $\epsilon_{\nu \boldsymbol{k}}$

⟵ local interactions

Impurity solver:

- Iterative perturbation theory (IPT; not controlled)
- Quantum Monte-Carlo (QMC)

Iterative solution of DMFT equations

0. Initialize self-energy
1. Solve Dyson equation
2. Solve single impurity Anderson model (SIAM)

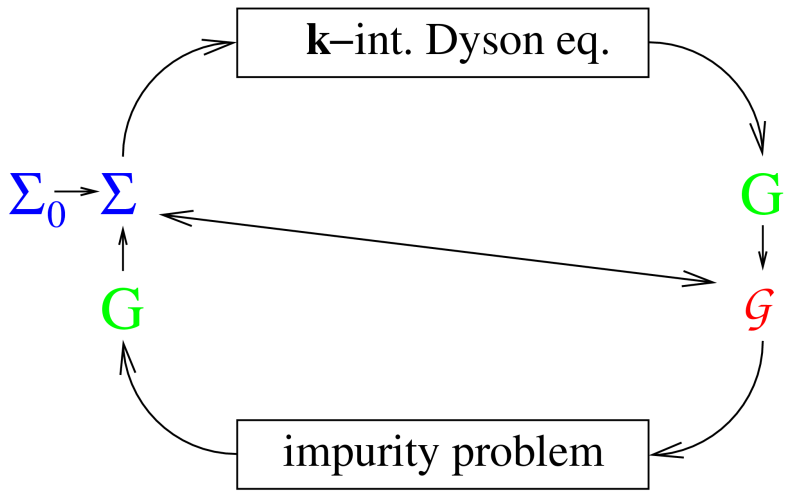

⟵ DOS / t_{ij} / $\epsilon_{\nu \boldsymbol{k}}$

⟵ local interactions

Impurity solver:

- Iterative perturbation theory (IPT; not controlled)
- Quantum Monte-Carlo (QMC)
- Exact diagonalization (ED; large finite-size errors)
- Numerical renormalization group (NRG; 1-2 bands)
- Density matrix renormalization group (DMRG)
- Self-energy functional theory (SFT) + ED

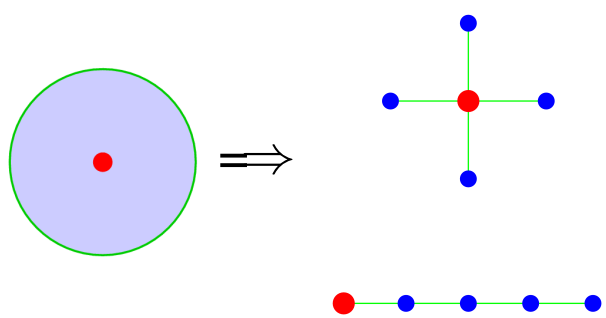

Auxiliary-field QMC algorithm [Hirsch, Fye (1986)]

Green-Funktion G in imaginary time (fermionic Grassmann variables ψ, ψ^*):

$$G_\sigma(\tau_2 - \tau_1) = \frac{1}{\mathcal{Z}} \int \mathcal{D}[\psi]\, \mathcal{D}[\psi^*]\ \psi_\sigma(\tau_1)\psi^*_\sigma(\tau_2)\ \exp\Big[\mathcal{A}_0 - U \sum_{\sigma\sigma'} \int_0^\beta d\tau\, \psi^*_\sigma \psi_\sigma \psi^*_{\sigma'} \psi_{\sigma'}\Big]$$

Auxiliary-field QMC algorithm [Hirsch, Fye (1986)]

Green-Funktion G in imaginary time (fermionic Grassmann variables ψ, ψ^*):

$$G_\sigma(\tau_2 - \tau_1) = \frac{1}{\mathcal{Z}} \int \mathcal{D}[\psi]\, \mathcal{D}[\psi^*]\ \psi_\sigma(\tau_1)\psi^*_\sigma(\tau_2)\ \exp\Big[\mathcal{A}_0 - U \sum_{\sigma\sigma'} \int_0^\beta d\tau\, \psi^*_\sigma \psi_\sigma \psi^*_{\sigma'} \psi_{\sigma'}\Big]$$

Discretization $\beta = \Lambda\, \Delta\tau$, Trotter decoupling $e^{-\beta(\hat{T}+\hat{V})} = \lim_{\Lambda\to\infty} \left[e^{-\Delta\tau \hat{T}} e^{-\Delta\tau \hat{V}}\right]^\Lambda$

Auxiliary-field QMC algorithm [Hirsch, Fye (1986)]

Green-Funktion G in imaginary time (fermionic Grassmann variables ψ, ψ^*):

$$G_\sigma(\tau_2-\tau_1) = \frac{1}{\mathcal{Z}} \int \mathcal{D}[\psi]\,\mathcal{D}[\psi^*]\ \psi_\sigma(\tau_1)\psi^*_\sigma(\tau_2)\ \exp\Big[\mathcal{A}_0 - U\sum_{\sigma\sigma'}\int_0^\beta d\tau\,\psi^*_\sigma\psi_\sigma\psi^*_{\sigma'}\psi_{\sigma'}\Big]$$

Discretization $\beta = \Lambda\,\Delta\tau$, Trotter decoupling $e^{-\beta(\hat{T}+\hat{V})} = \lim_{\Lambda\to\infty}\left[e^{-\Delta\tau\hat{T}}e^{-\Delta\tau\hat{V}}\right]^\Lambda$

Use $\hat{n}_\uparrow\hat{n}_\downarrow = \frac{1}{2}\left[\hat{n}_\uparrow + \hat{n}_\downarrow - \left(\hat{n}_\uparrow - \hat{n}_\downarrow\right)^2\right]$; discrete Hubbard-Stratonovich transformation

$$\exp\left[\Delta\tau U\left(\hat{n}_\uparrow - \hat{n}_\downarrow\right)^2/2\right] = \frac{1}{2}\sum_{s=\pm1}\exp\left[\lambda s\left(\hat{n}_\uparrow - \hat{n}_\downarrow\right)\right]; \qquad \cosh(\lambda) = \exp(\Delta\tau U/2)$$

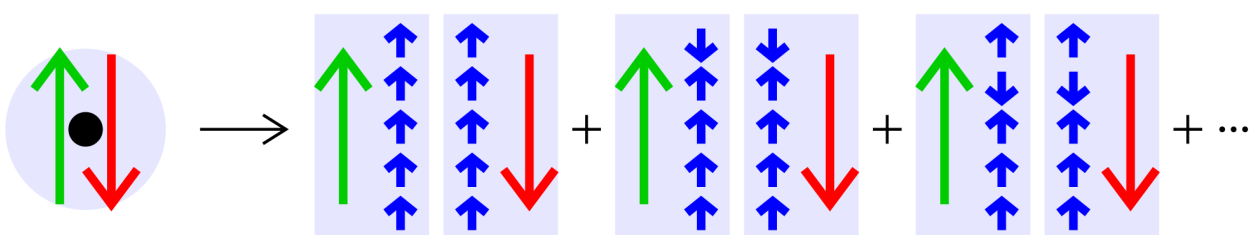

Wick theorem:

$$G = \frac{\sum M \det\{M\}}{\sum \det\{M\}}$$

Auxiliary-field QMC algorithm [Hirsch, Fye (1986)]

Green-Funktion G in imaginary time (fermionic Grassmann variables ψ, ψ^*):

$$G_\sigma(\tau_2-\tau_1) = \frac{1}{\mathcal{Z}} \int \mathcal{D}[\psi]\,\mathcal{D}[\psi^*]\ \psi_\sigma(\tau_1)\psi^*_\sigma(\tau_2)\ \exp\Big[\mathcal{A}_0 - U\sum_{\sigma\sigma'}\int_0^\beta d\tau\,\psi^*_\sigma\psi_\sigma\psi^*_{\sigma'}\psi_{\sigma'}\Big]$$

Discretization $\beta = \Lambda\,\Delta\tau$, Trotter decoupling $e^{-\beta(\hat{T}+\hat{V})} = \lim_{\Lambda\to\infty}\left[e^{-\Delta\tau\hat{T}}e^{-\Delta\tau\hat{V}}\right]^\Lambda$

Use $\hat{n}_\uparrow\hat{n}_\downarrow = \frac{1}{2}\left[\hat{n}_\uparrow + \hat{n}_\downarrow - \left(\hat{n}_\uparrow - \hat{n}_\downarrow\right)^2\right]$; discrete Hubbard-Stratonovich transformation

$$\exp\left[\Delta\tau U\left(\hat{n}_\uparrow - \hat{n}_\downarrow\right)^2/2\right] = \frac{1}{2}\sum_{s=\pm1}\exp\left[\lambda s\left(\hat{n}_\uparrow - \hat{n}_\downarrow\right)\right]; \qquad \cosh(\lambda) = \exp(\Delta\tau U/2)$$

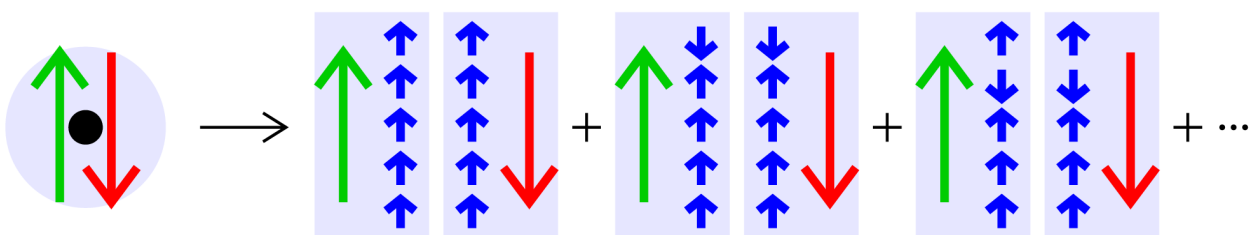

Wick theorem:

$$G = \frac{\sum M \det\{M\}}{\sum \det\{M\}}$$

Metropolis MC importance sampling over auxiliary Ising field $\{s\}$: 2^Λ configurations

\+ numerically exact, + no sign problem, − effort scales as T^{-3},

Problems with Fourier transformations in DMFT-QMC cycle

Iterative solution of DMFT equations (for imaginary-time impurity solver)

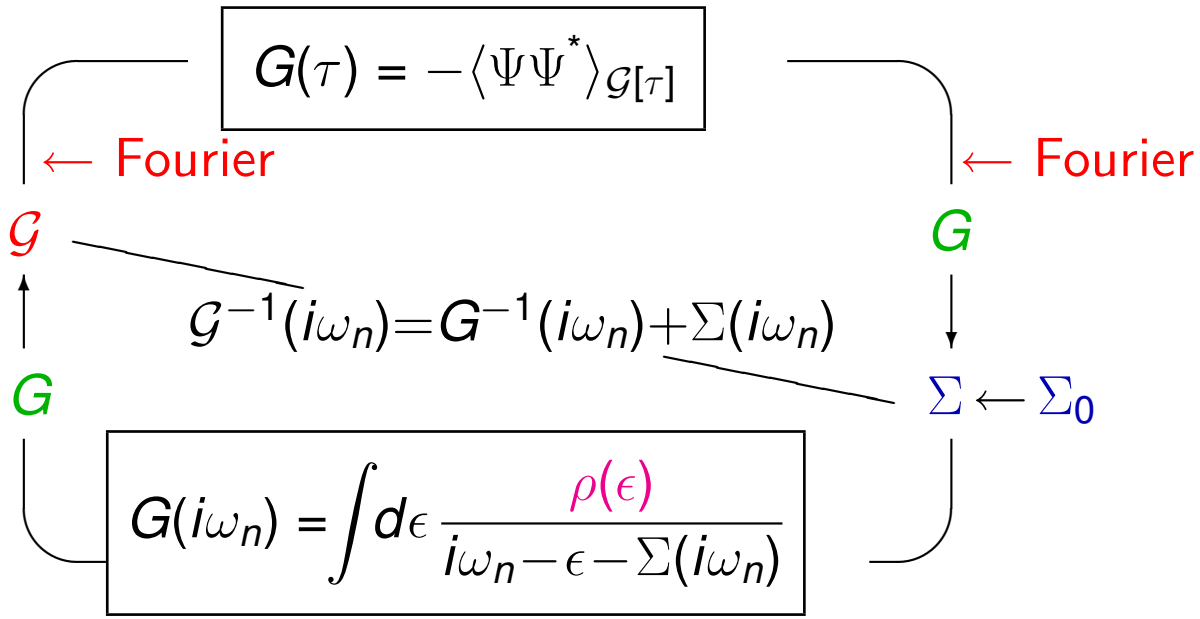

Problems with Fourier transformations in DMFT-QMC cycle

Iterative solution of DMFT equations (for imaginary-time impurity solver)

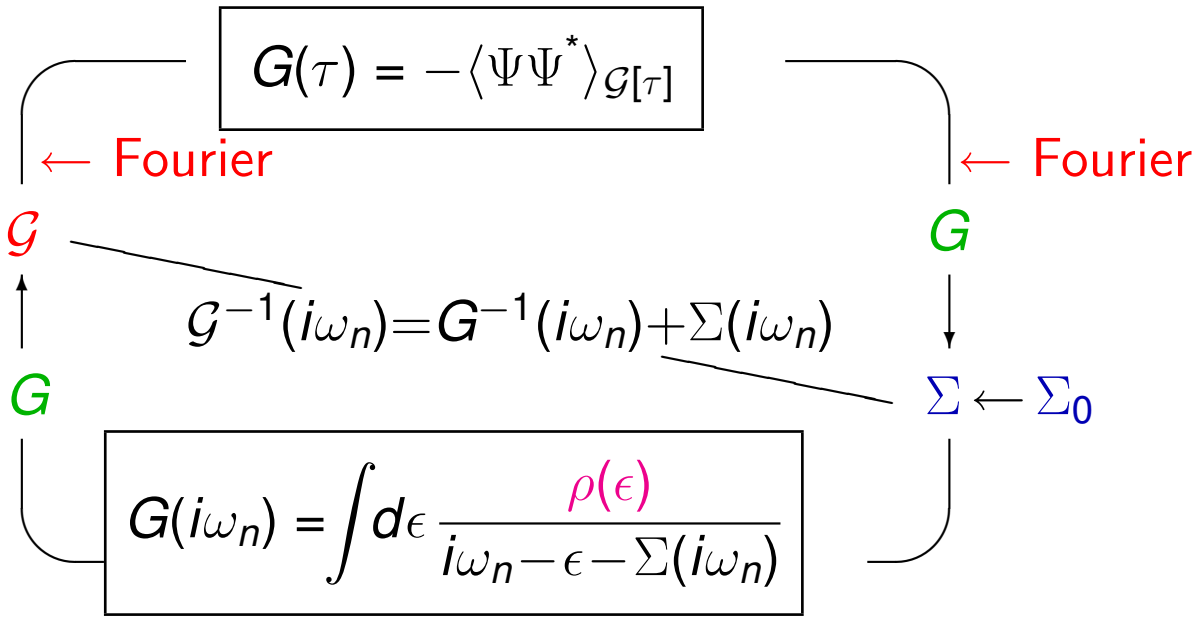

Naive discrete Fourier transformation $\rightsquigarrow$ oscillations (instead of $G(\omega) \overset{\omega\to\infty}{\longrightarrow} 1/\omega$)

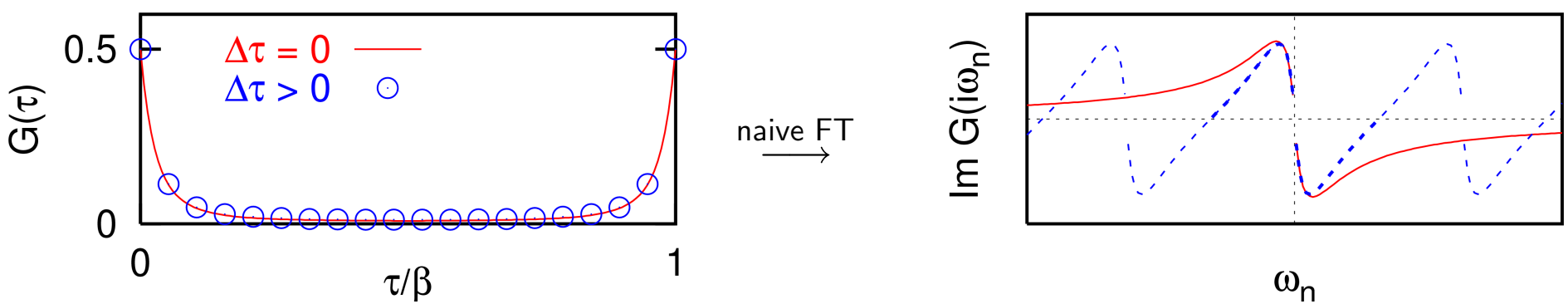

Problems with Fourier transformations in DMFT-QMC cycle

Iterative solution of DMFT equations (for imaginary-time impurity solver)

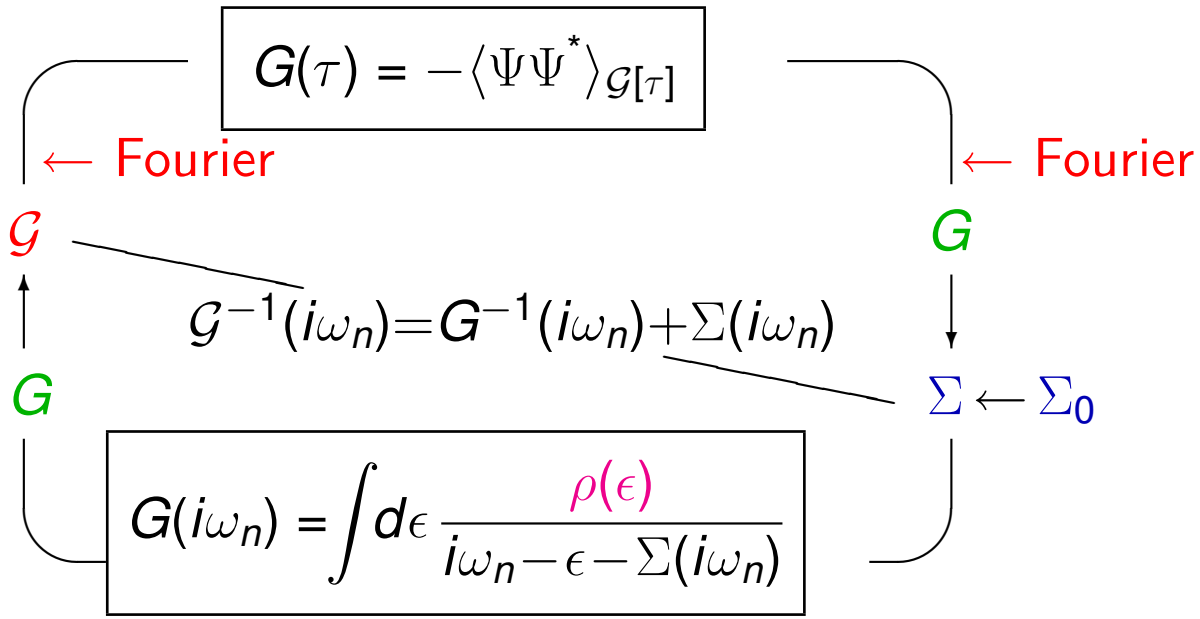

Naive discrete Fourier transformation $\rightsquigarrow$ oscillations (instead of $G(\omega) \overset{\omega\to\infty}{\longrightarrow} 1/\omega$)

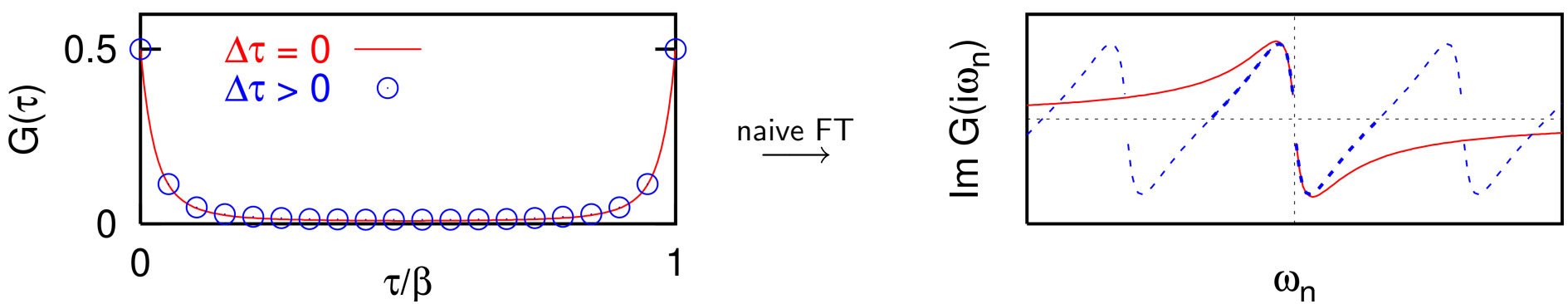

1st solution: correct unphysical behavior for $|\omega| \lesssim \omega_{\text{Nyquist}}$ by transformation [Ulmke]

2^{nd} solution: interpolate $G_{\text{QMC}}(\tau)$ by cubic splines [Jarrell, Krauth, Gull, . . .]

But: $\dfrac{d^2G(\tau)}{d\tau^2}$ maximal for $\tau \longrightarrow 0, \beta$ $\quad \rightsquigarrow$ natural boundary conditions inappropriate

2^{nd} solution: interpolate $G_{\text{QMC}}(\tau)$ by cubic splines [Jarrell, Krauth, Gull, . . .]

But: $\dfrac{d^2G(\tau)}{d\tau^2}$ maximal for $\tau \to 0, \beta$ $\rightsquigarrow$ natural boundary conditions inappropriate

- adjust boundary cond. [Oudovenko]
- spline-fit only difference w.r.t. reference problem:
  - IPT [Jarrell]

2nd solution: interpolate $G_{\mathrm{QMC}}(\tau)$ by cubic splines [Jarrell, Krauth, Gull, . . .]

But: $\dfrac{d^2G(\tau)}{d\tau^2}$ maximal for $\tau \to 0, \beta$ $\rightsquigarrow$ natural boundary conditions inappropriate

- adjust boundary cond. [Oudovenko]
- spline-fit only difference w.r.t. reference problem:
  - IPT [Jarrell]
  - high-frequency expansion for $\Sigma(\omega)$ + param. [Knecht, NB]

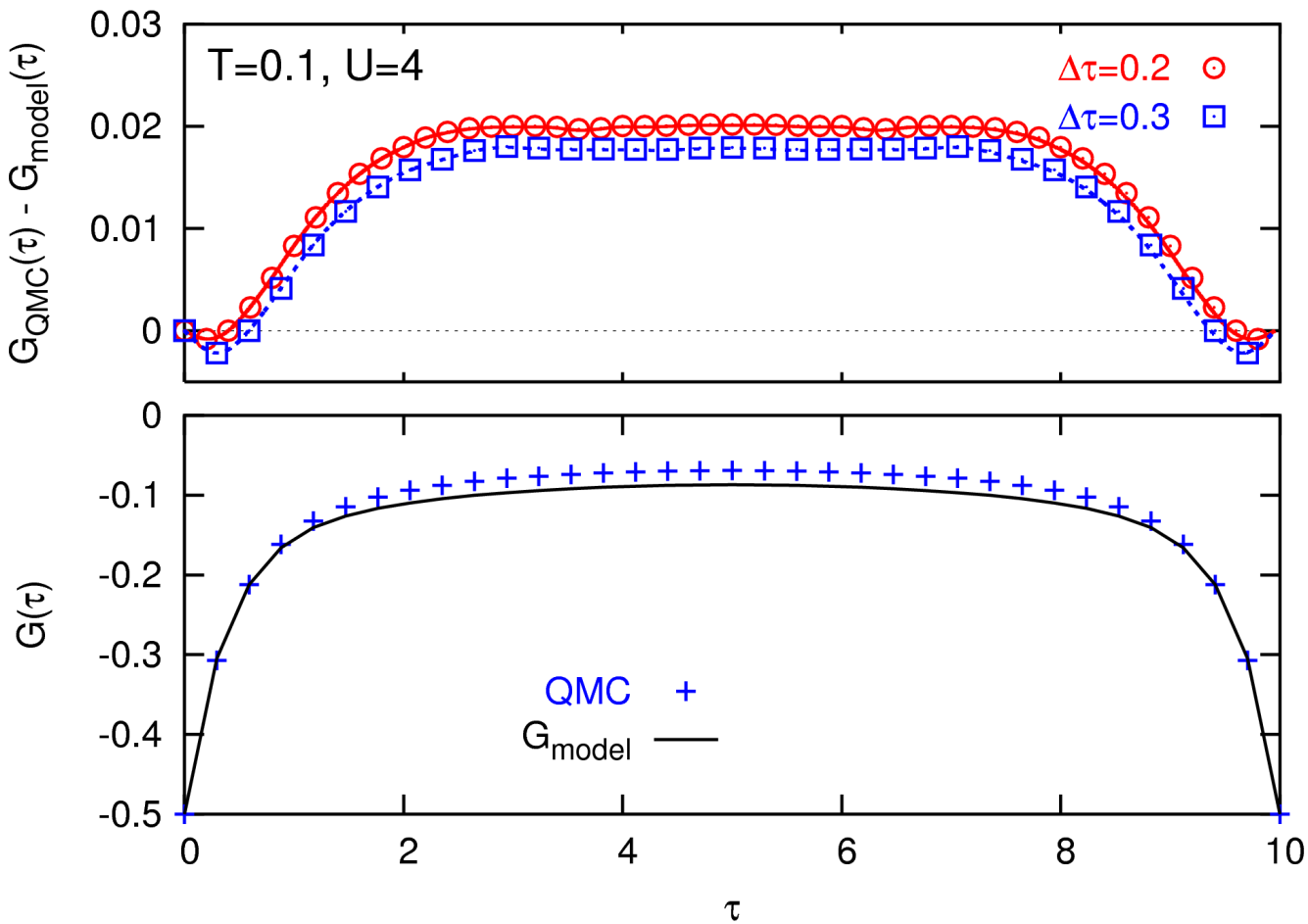

$$\Sigma_\sigma(\omega) = U\left(\langle \hat{n}_{-\sigma}\rangle - \tfrac{1}{2}\right)\omega^0 + U^2\langle \hat{n}_{-\sigma}\rangle\left(1 - \langle \hat{n}_{-\sigma}\rangle\right)\omega^{-1} + \mathcal{O}(\omega^{-2})$$

Sensitive test: self-energy $\Sigma(i\omega_n)$ for insulating phase ($T = 0.1$, $U = 5.0$)

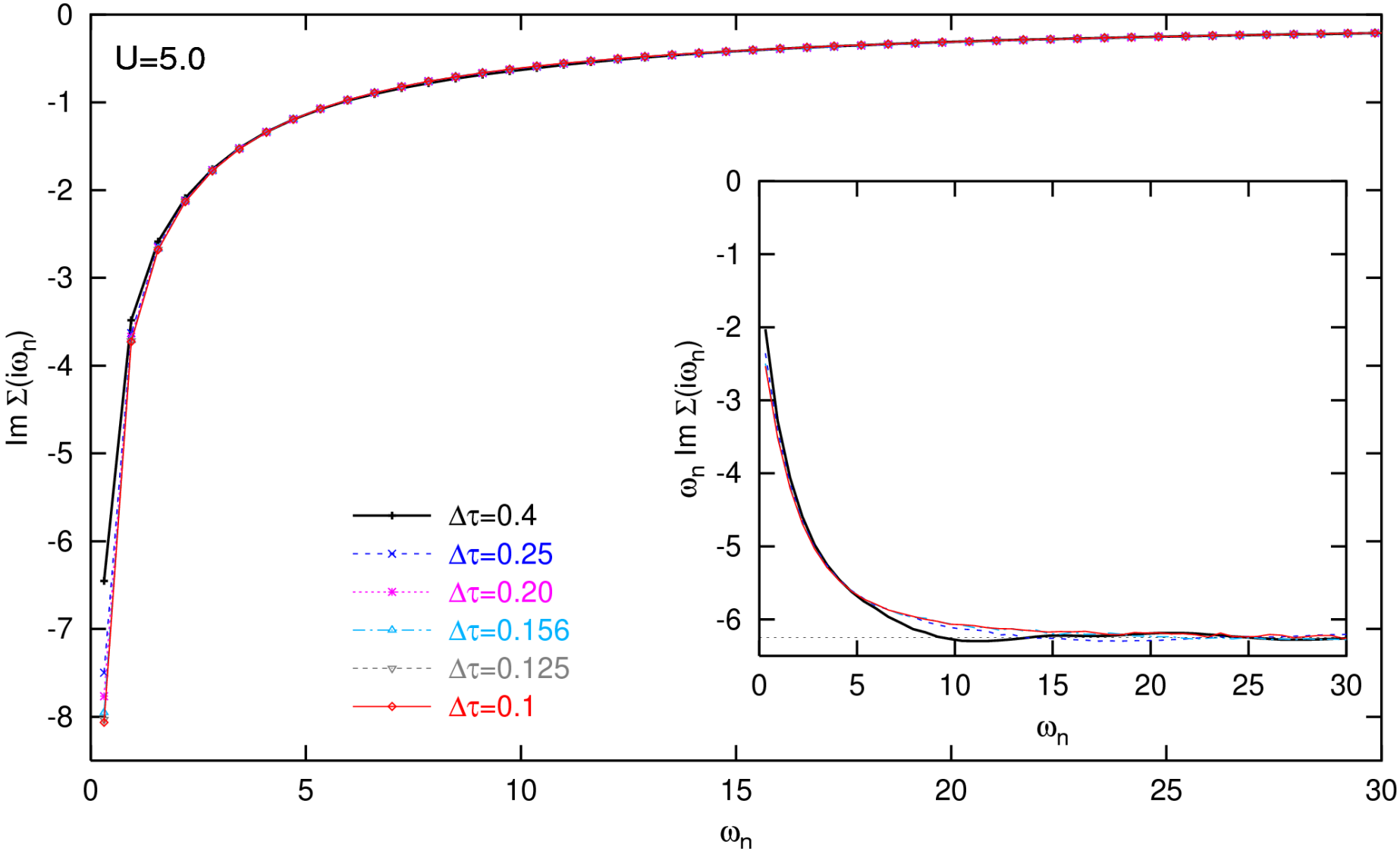

Rapid convergence at all frequencies for "QMC + $1/\omega$" DMFT solver

Update: Orbital-selective Mott transitions

Step back: Mott transition in frustrated 1-band Hubbard model

$$H = -t \sum_{\langle i,j \rangle,\sigma} c^{\dagger}_{i\sigma} c_{j\sigma} + U \sum_{i} n_{i\uparrow} n_{i\downarrow}$$

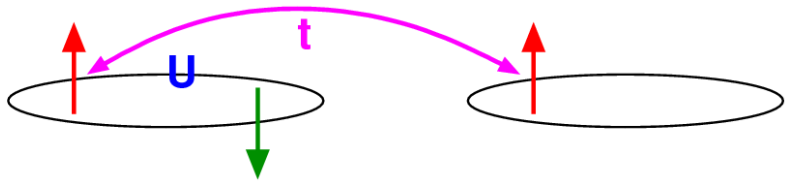

Fundamental question: smooth crossover from metal to insulator or
transition at $U_c(T)$ (within DMFT)?

Update: Orbital-selective Mott transitions

Step back: Mott transition in frustrated 1-band Hubbard model

$$H = -t \sum_{\langle i,j \rangle,\sigma} c^{\dagger}_{i\sigma} c_{j\sigma} + U \sum_{i} n_{i\uparrow} n_{i\downarrow}$$

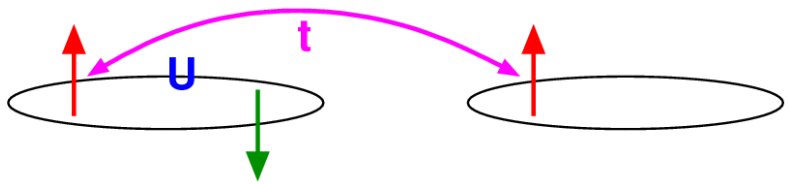

Fundamental question: smooth crossover from metal to insulator or transition at $U_c(T)$ (within DMFT)?

No conclusive answer up to 1999

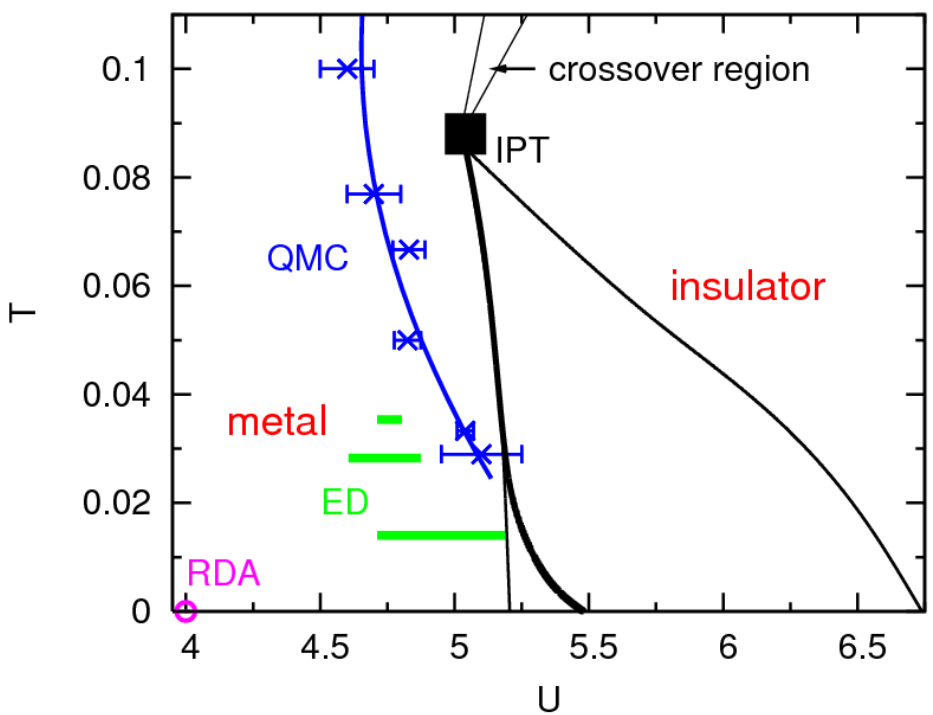

Update: Orbital-selective Mott transitions

Step back: Mott transition in frustrated 1-band Hubbard model

$$H = -t \sum_{\langle i,j \rangle,\sigma} c^{\dagger}_{i\sigma} c_{j\sigma} + U \sum_{i} n_{i\uparrow} n_{i\downarrow}$$

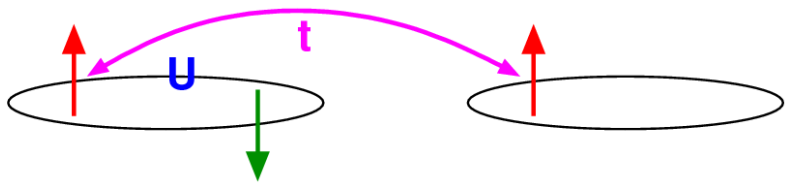

Fundamental question: smooth crossover from metal to insulator or transition at $U_c(T)$ (within DMFT)?

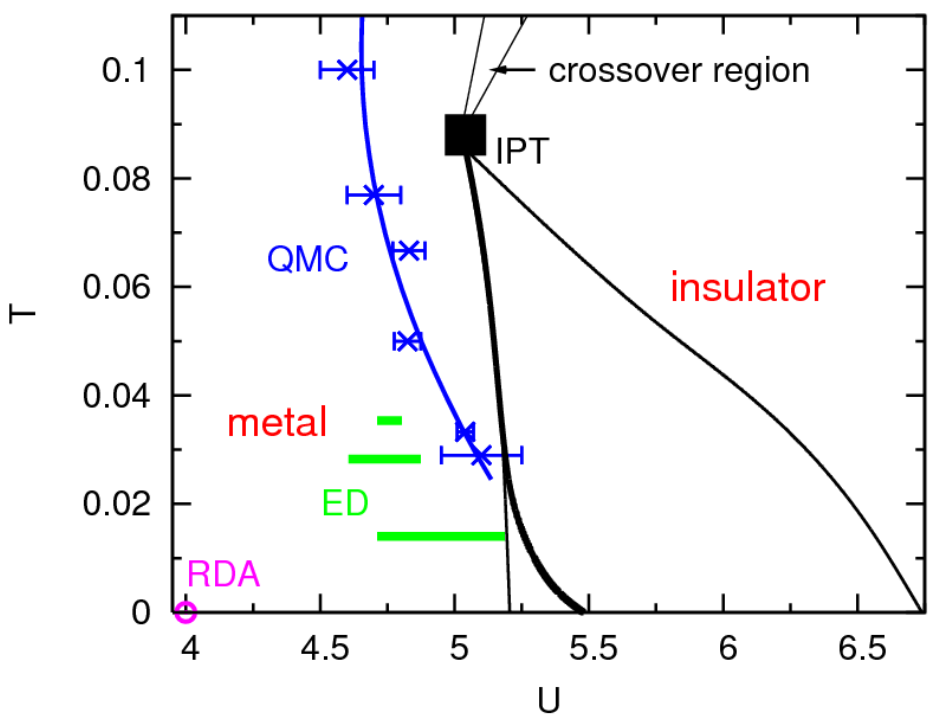

No conclusive answer up to 1999

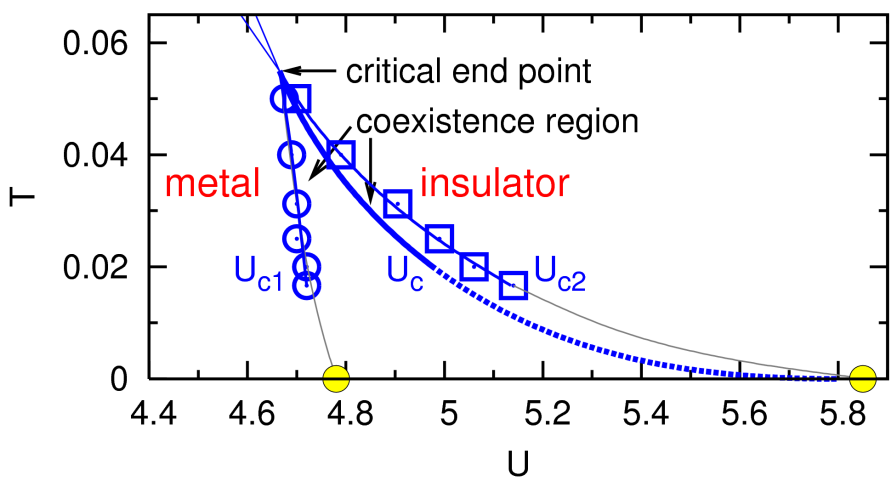

Now accepted: 1st order transition for $0 < T < T^*$ (QMC + ePT, 2000-2005)

Update: Orbital-selective Mott transitions

Step back: Mott transition in frustrated 1-band Hubbard model

$$H = -t \sum_{\langle i,j \rangle,\sigma} c^{\dagger}_{i\sigma} c_{j\sigma} + U \sum_{i} n_{i\uparrow} n_{i\downarrow}$$

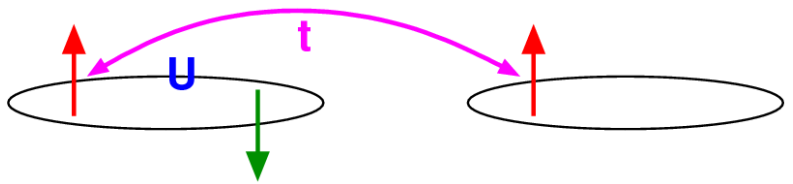

F ...om metal to insulator or
(within DMFT)?

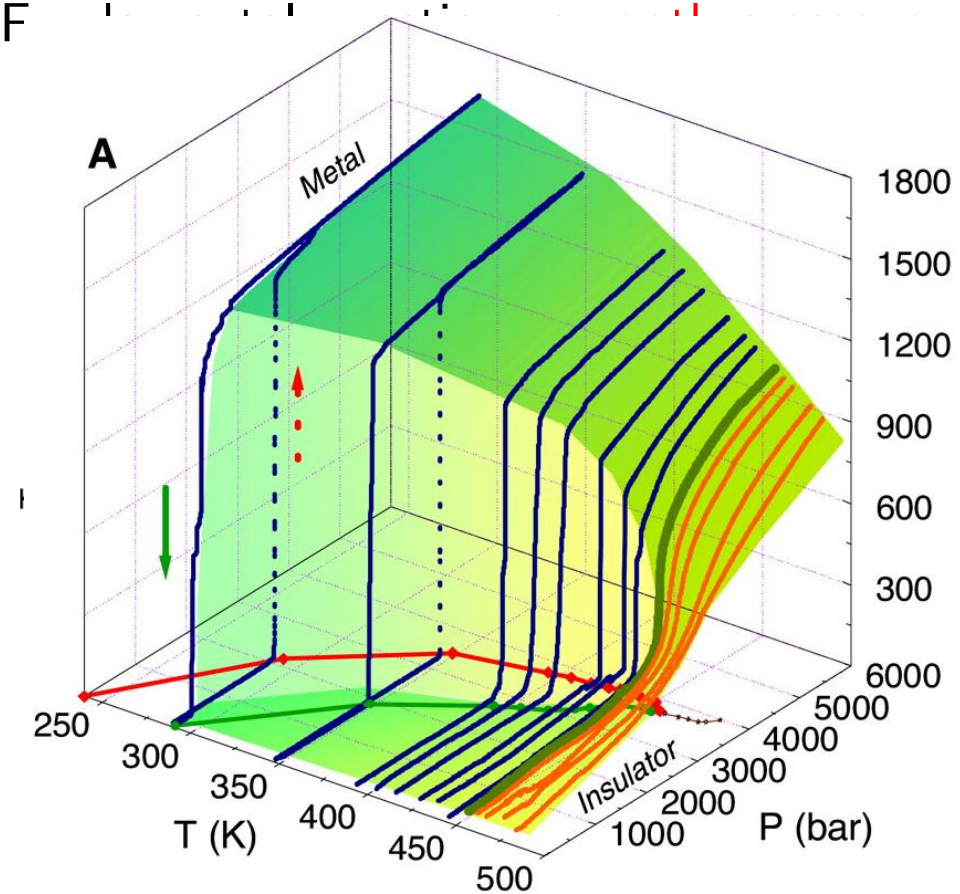

No conclusive answer up to 1999

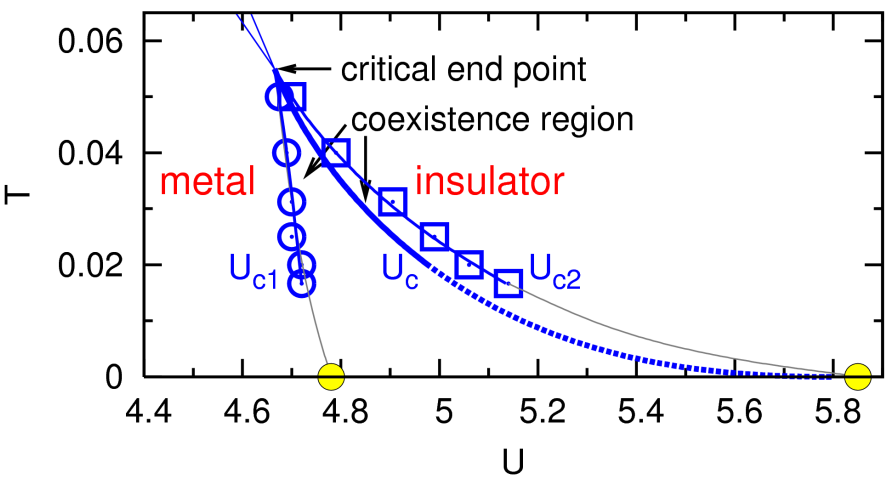

Now accepted: 1st order transition for $0 < T < T^*$ (QMC + ePT, 2000-2005)

Multiorbital case ($M > 1$ orbitals, half filling $n = M$)?

Extension without additional parameters: SU(2M) symmetric case:

$$H = -t \sum_{\langle i,j \rangle, m, \sigma} c^{\dagger}_{im\sigma} c_{jm\sigma} + \frac{U}{2} \sum_{i} \sum_{(m,\sigma) \neq (m'\sigma')} n_{im\sigma} n_{im\sigma'}$$

Multiorbital case ($M > 1$ orbitals, half filling $n = M$)?

Extension without additional parameters: SU(2M) symmetric case:

$$H = -t \sum_{\langle i,j \rangle, m, \sigma} c^{\dagger}_{im\sigma} c_{jm\sigma} + \frac{U}{2} \sum_{i} \sum_{(m,\sigma) \neq (m'\sigma')} n_{im\sigma} n_{im\sigma'}$$

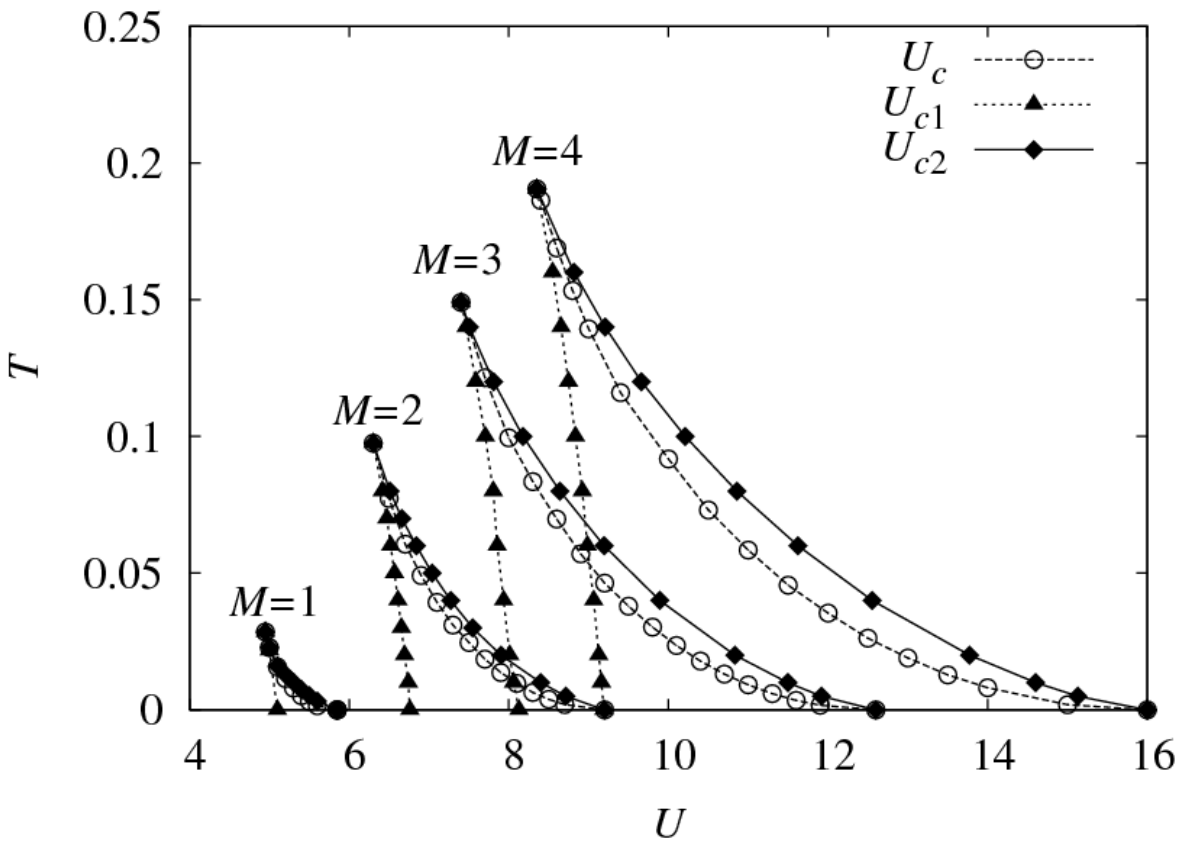

$U_c(M) \propto \sqrt{M}$

[Koch et al., PRB(1999)]

[Inaba, Koga, Suga, Kawakami, PRB **72**, 085112 (2005)]

Multiorbital case ($M > 1$ orbitals, half filling $n = M$)?

Extension without additional parameters: SU(2M) symmetric case:

$$H = -t \sum_{\langle i,j\rangle,m,\sigma} c^{\dagger}_{im\sigma}\, c_{jm\sigma} + \frac{U}{2} \sum_{i} \sum_{(m,\sigma)\neq(m'\sigma')} n_{im\sigma}\, n_{im\sigma'}$$

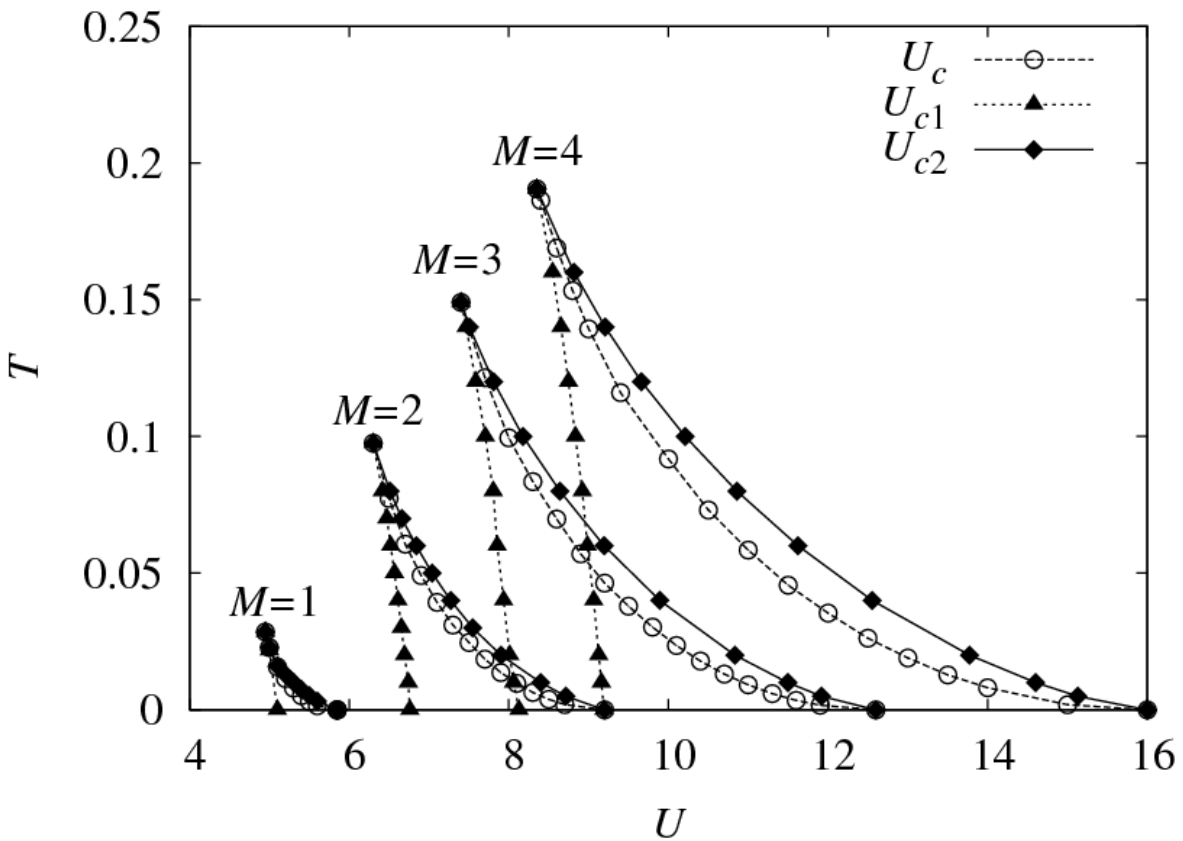

$U_c(M) \propto \sqrt{M}$

[Koch et al., PRB(1999)]

$U_{c1} \propto \sqrt{M}$, $U_{c2}(M) \sim 2M\, E^0_{\rm kin}$

[Florens et al., PRB (2002)]

[Inaba, Koga, Suga, Kawakami, PRB **72**, 085112 (2005)]

Multiorbital case ($M > 1$ orbitals, half filling $n = M$)?

Extension without additional parameters: SU(2M) symmetric case:

$$H = -t \sum_{\langle i,j \rangle, m, \sigma} c^{\dagger}_{im\sigma} c_{jm\sigma} + \frac{U}{2} \sum_{i} \sum_{(m,\sigma) \neq (m'\sigma')} n_{im\sigma} n_{im\sigma'}$$

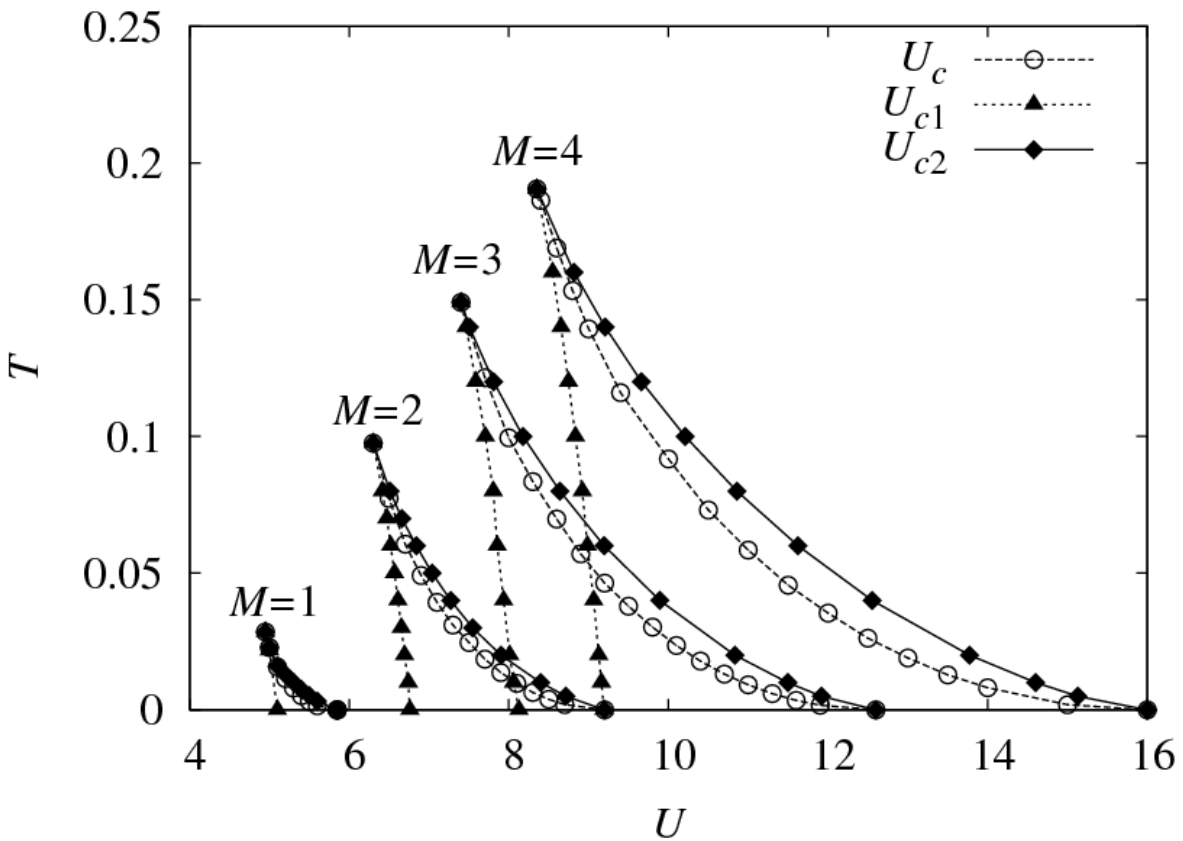

$U_c(M) \propto \sqrt{M}$

[Koch et al., PRB(1999)]

$U_{c1} \propto \sqrt{M}$, $U_{c2}(M) \sim 2M\, E^0_{\text{kin}}$

[Florens et al., PRB (2002)]

but still single Mott transition

[Inaba, Koga, Suga, Kawakami, PRB **72**, 085112 (2005)]

OSMTs in $Ca_{2-x}Sr_xRuO_4$

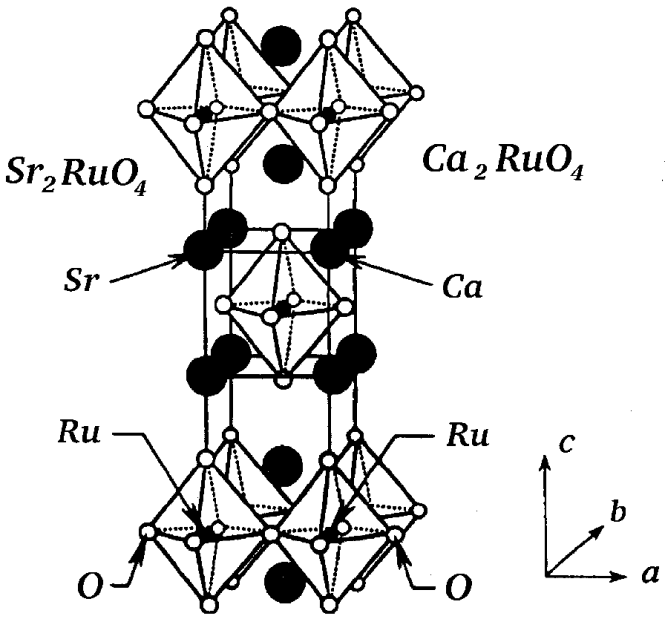

isostructural to $La_{2-x}Sr_xCuO_4$

4 valence electrons in 3 Ru t_{2g} orbitals

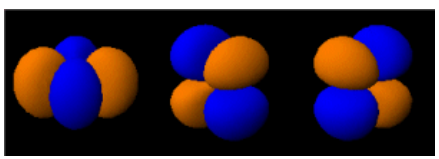

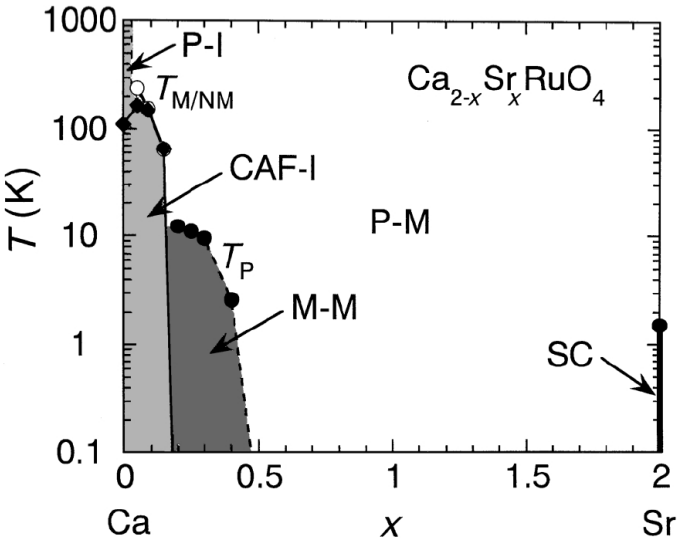

[Nakatsuji, Maeno, PRL (2000)]

OSMTs in $Ca_{2-x}Sr_xRuO_4$

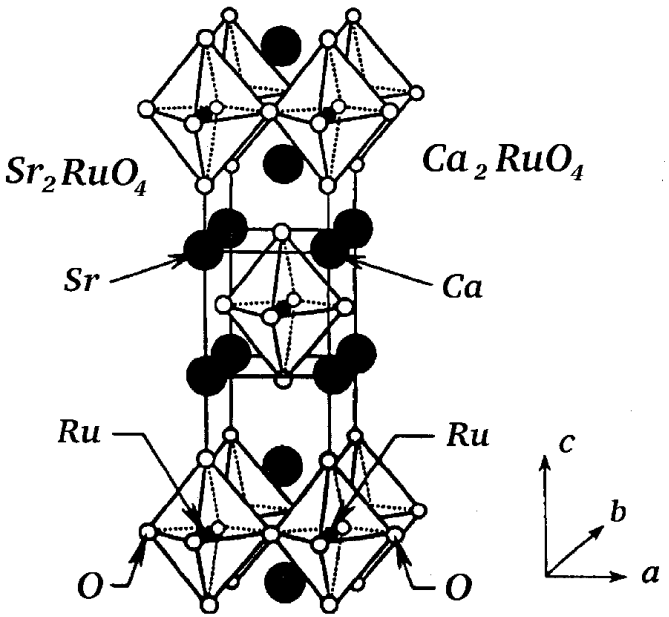

isostructural to $La_{2-x}Sr_xCuO_4$

4 valence electrons in 3 Ru t_{2g} orbitals

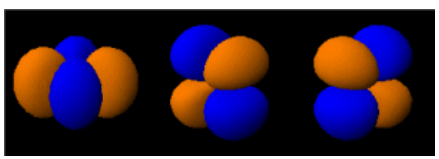

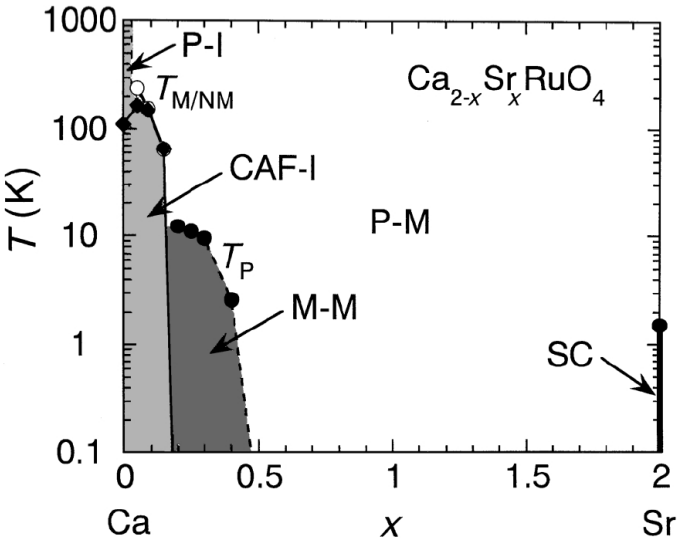

[Nakatsuji, Maeno, PRL (2000)]

susceptibility, MR $\rightsquigarrow$ $S = 1/2$ system (+ easy axis) for $0.2 < x \lesssim 0.5$ (not $S = 1$)

orbital-selective Mott metal-insulator transitions for $x \approx 0.5$, $x \approx 0.2$?

OSMTs in $Ca_{2-x}Sr_xRuO_4$

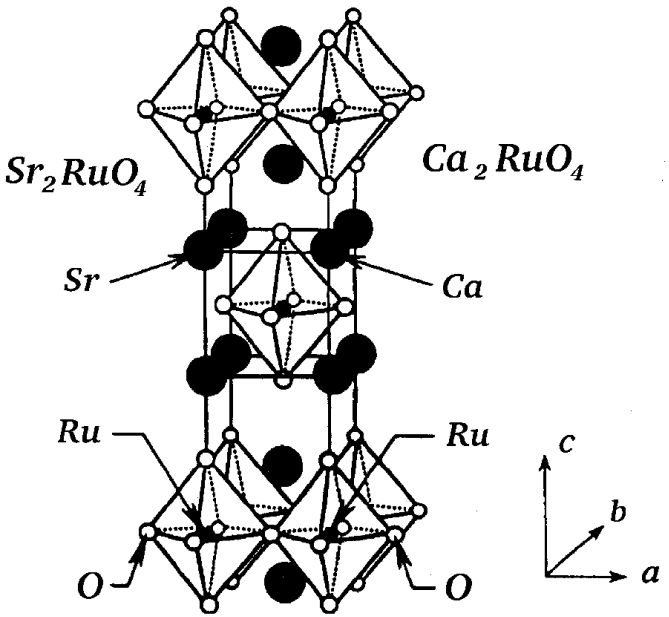

isostructural to $La_{2-x}Sr_xCuO_4$

4 valence electrons in 3 Ru t_{2g} orbitals

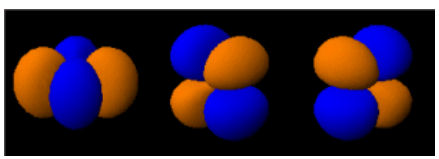

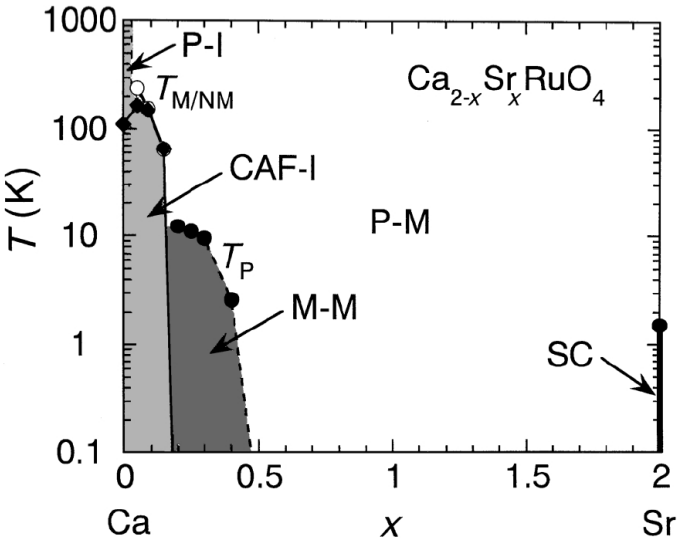

[Nakatsuji, Maeno, PRL (2000)]

susceptibility, MR $\rightsquigarrow$ $S = 1/2$ system (+ easy axis) for $0.2 < x \lesssim 0.5$ (not $S = 1$)

orbital-selective Mott metal-insulator transitions for $x \approx 0.5$, $x \approx 0.2$?

Possible mechanism: different effective hopping amplitudes for in-plane and out-of-plane orbitals [Anisimov et al., EPJB (2002)]

2-band model with orbital-dependent hopping

$$H = \sum_{m=1}^{2} \Big[-\sum_{\langle ij\rangle\sigma} t_m c^{\dagger}_{im\sigma} c_{jm\sigma} + U \sum_i n_{im\uparrow} n_{im\downarrow} \Big]$$

$$+ \sum_{i\sigma\sigma'} (U' - \delta_{\sigma\sigma'} J_z)\, n_{i1\sigma}\, n_{i2\sigma'}$$

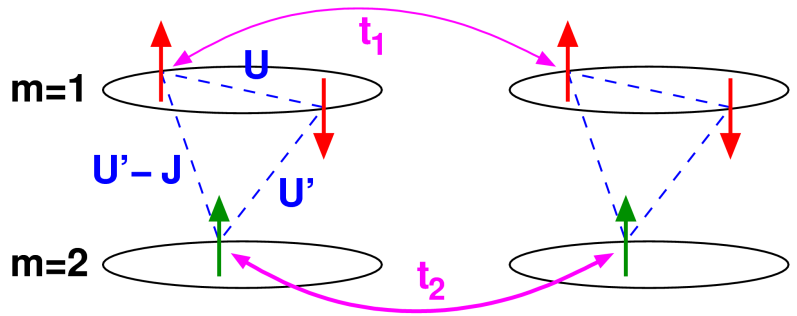

Ising-type Hund couplings with $t_2/t_1 = 2$ and $U' = U/2$, $J_z = U/4$ [Liebsch, PRB (2004)]

2-band model with orbital-dependent hopping

$$H = \sum_{m=1}^{2} \left[-\sum_{\langle ij \rangle \sigma} t_m c^{\dagger}_{im\sigma} c_{jm\sigma} + U \sum_i n_{im\uparrow} n_{im\downarrow} \right]$$

$$+ \sum_{i\sigma\sigma'} (U' - \delta_{\sigma\sigma'} J_z)\, n_{i1\sigma}\, n_{i2\sigma'}$$

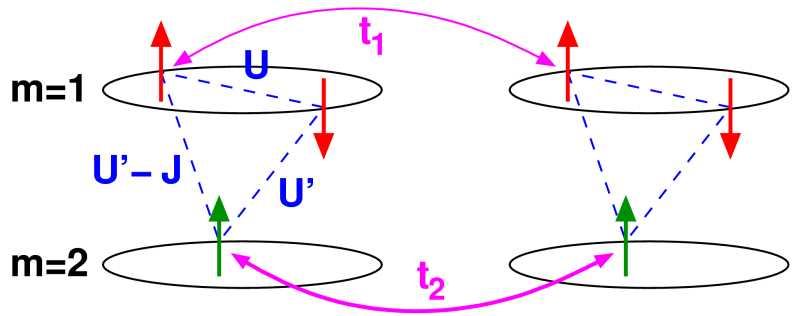

Ising-type Hund couplings with $t_2/t_1 = 2$ and $U' = U/2$, $J_z = U/4$ [Liebsch, PRB (2004)]

2 well-defined phase transitions

[Knecht et al. (PRB 2005), de' Medici et al. (PRB 2005), Rüegg et al. (EPJB 2005)]

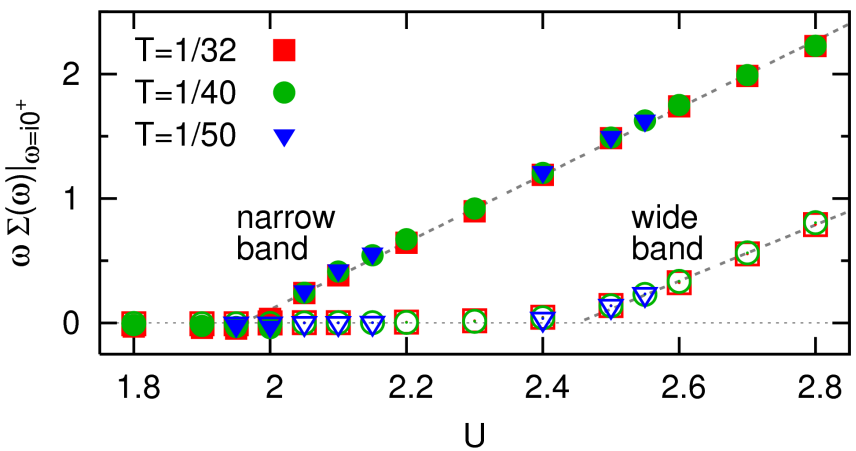

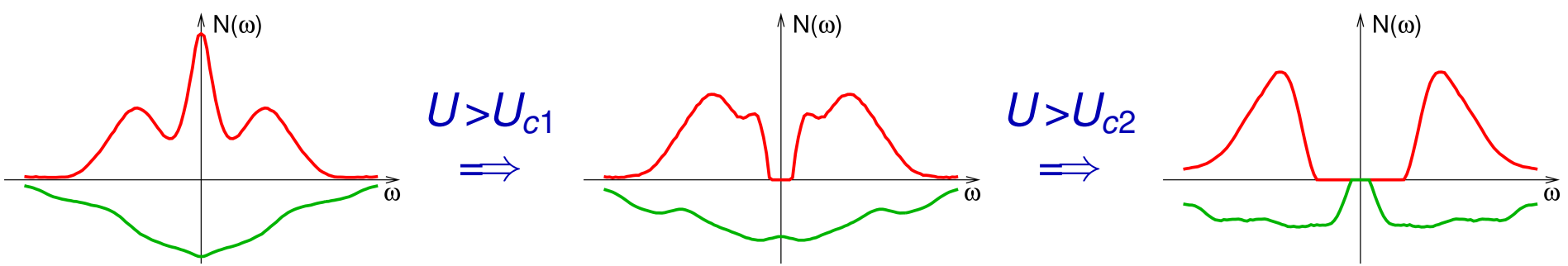

Order of wide-band transition in anisotropic model

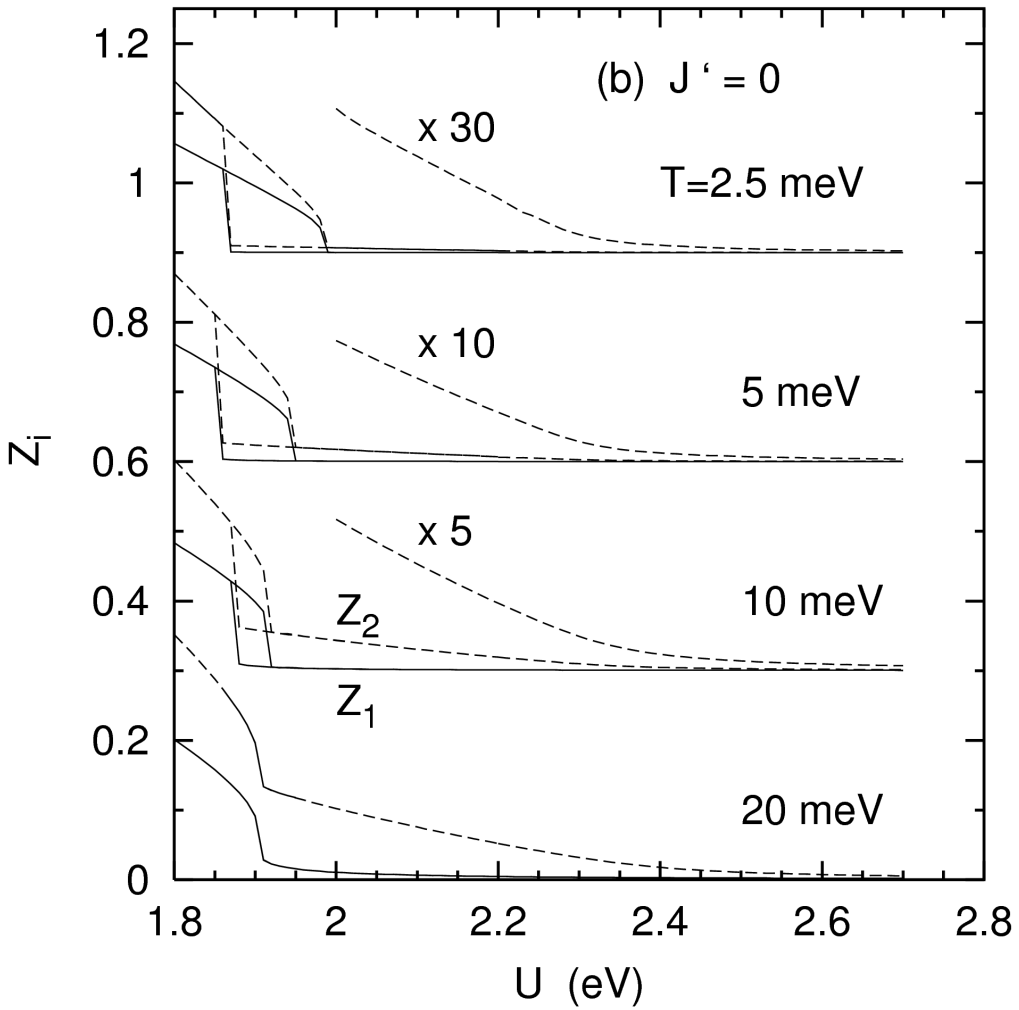

ED $\rightsquigarrow$ no hysteresis at low T for wide-band transition [Liebsch, PRL (2005)]

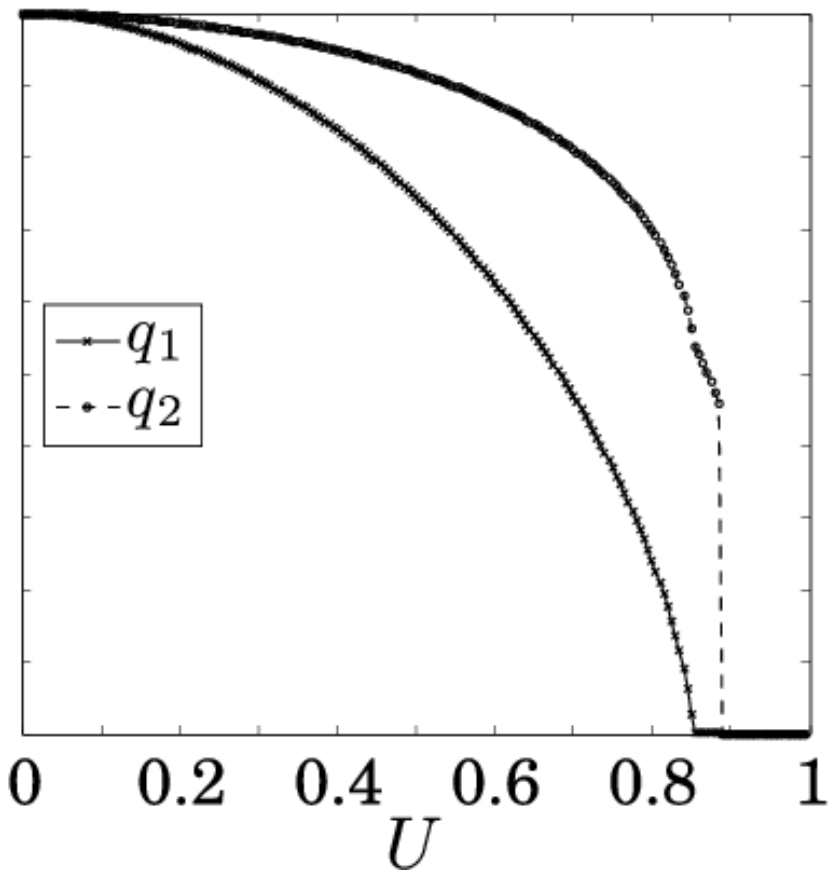

Slave-boson MF $\rightsquigarrow$ 1st order wide-band transition (at $T = 0$) [Rüegg, Indergand, Pilgram, Sigrist, EPJB (2005)]

Systematic study: effect of inter-orbital coupling

$$H = \sum_{m=1}^{2} \left[-\sum_{\langle ij \rangle \sigma} t_m c^{\dagger}_{im\sigma} c_{jm\sigma} + U \sum_i n_{im\uparrow} n_{im\downarrow} \right] + \alpha \sum_{i\sigma\sigma'} (U/2 - \delta_{\sigma\sigma'} U/4)\, n_{i1\sigma}\, n_{i2\sigma'}$$

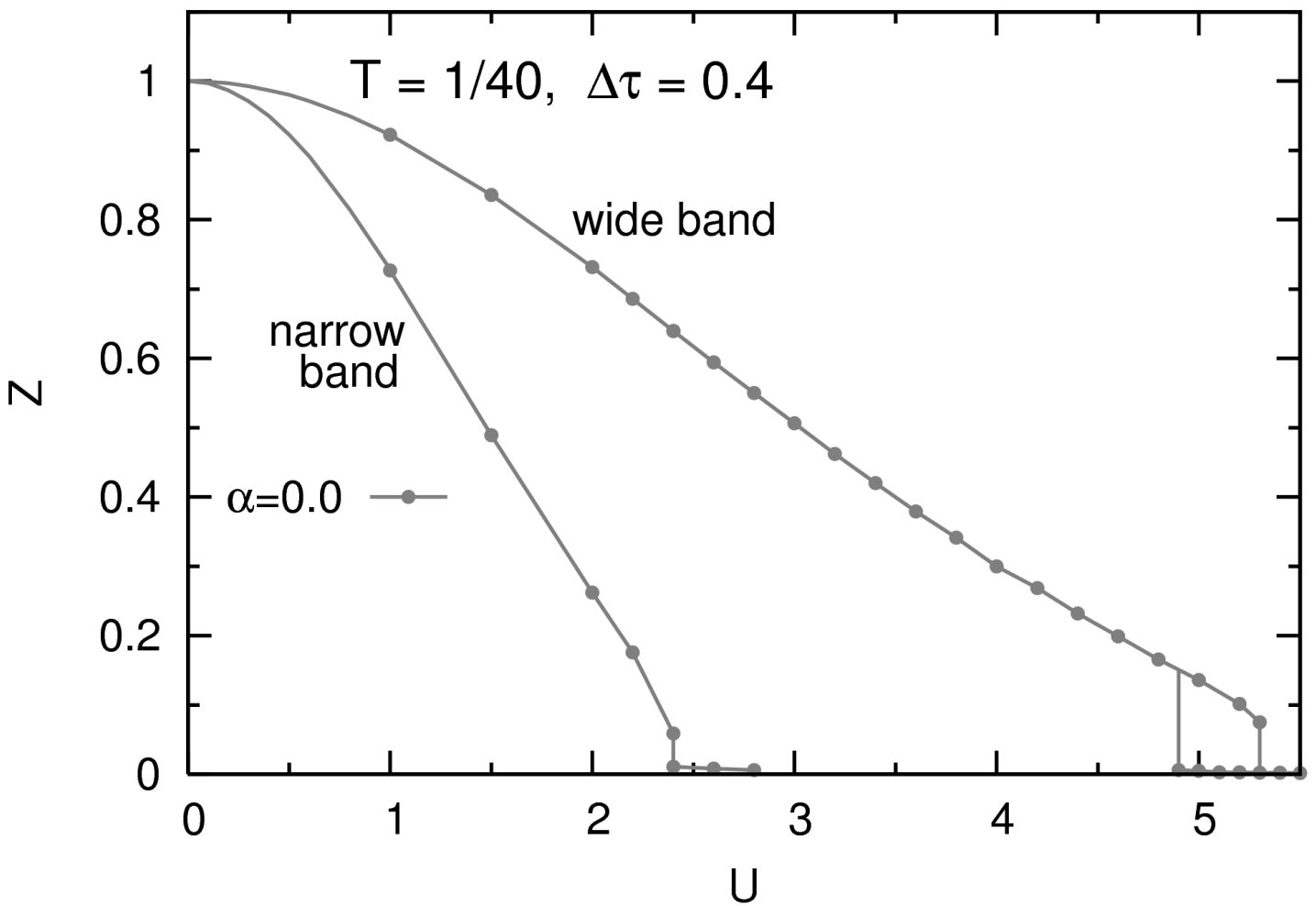

Systematic study: effect of inter-orbital coupling

$$H = \sum_{m=1}^{2} \left[-\sum_{\langle ij \rangle \sigma} t_m c^{\dagger}_{im\sigma} c_{jm\sigma} + U \sum_i n_{im\uparrow} n_{im\downarrow} \right] + \alpha \sum_{i\sigma\sigma'} (U/2 - \delta_{\sigma\sigma'} U/4)\, n_{i1\sigma}\, n_{i2\sigma'}$$

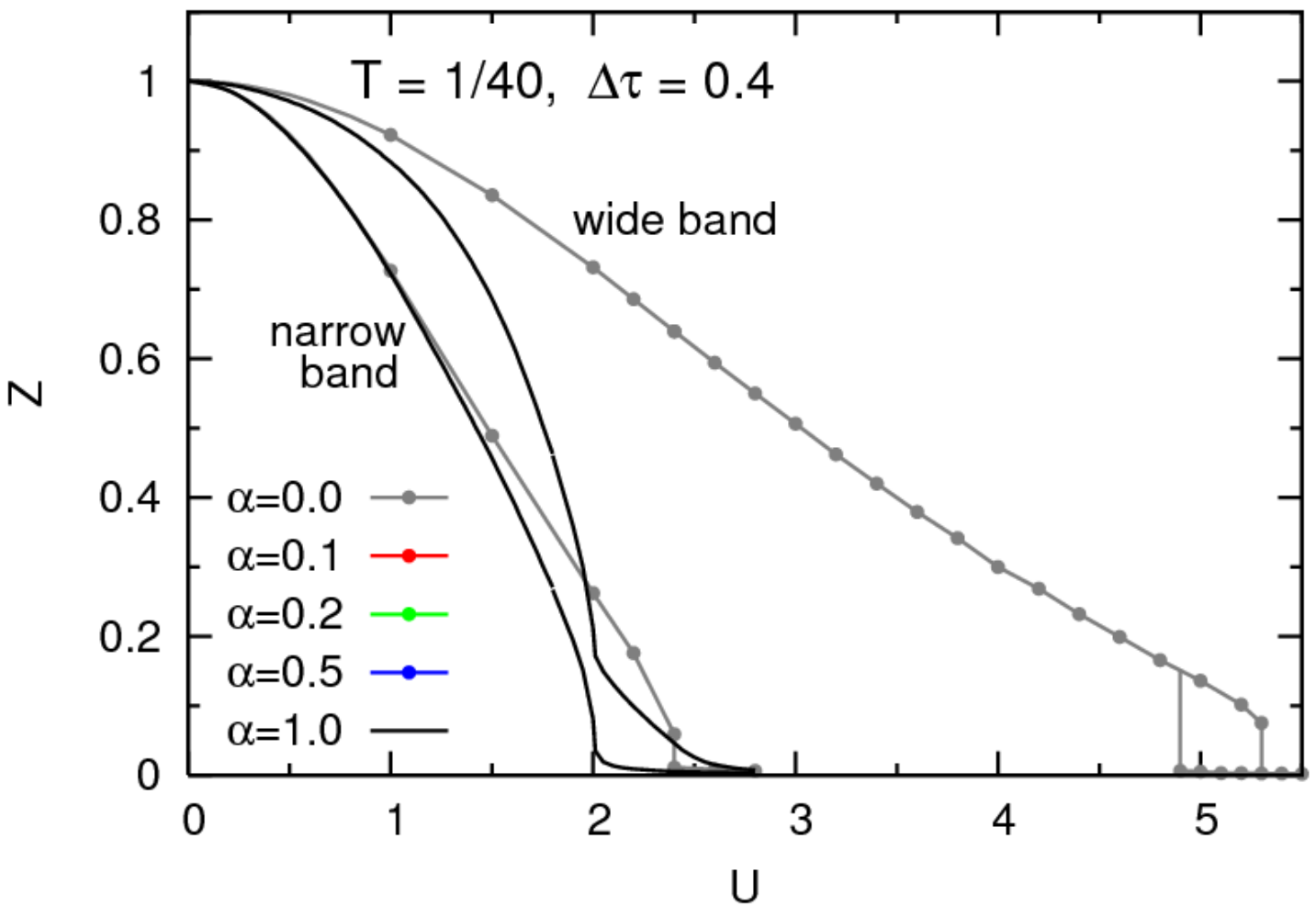

Systematic study: effect of inter-orbital coupling

$$H = \sum_{m=1}^{2} \left[-\sum_{\langle ij \rangle \sigma} t_m c^{\dagger}_{im\sigma} c_{jm\sigma} + U \sum_i n_{im\uparrow} n_{im\downarrow} \right] + \alpha \sum_{i\sigma\sigma'} (U/2 - \delta_{\sigma\sigma'} U/4)\, n_{i1\sigma}\, n_{i2\sigma'}$$

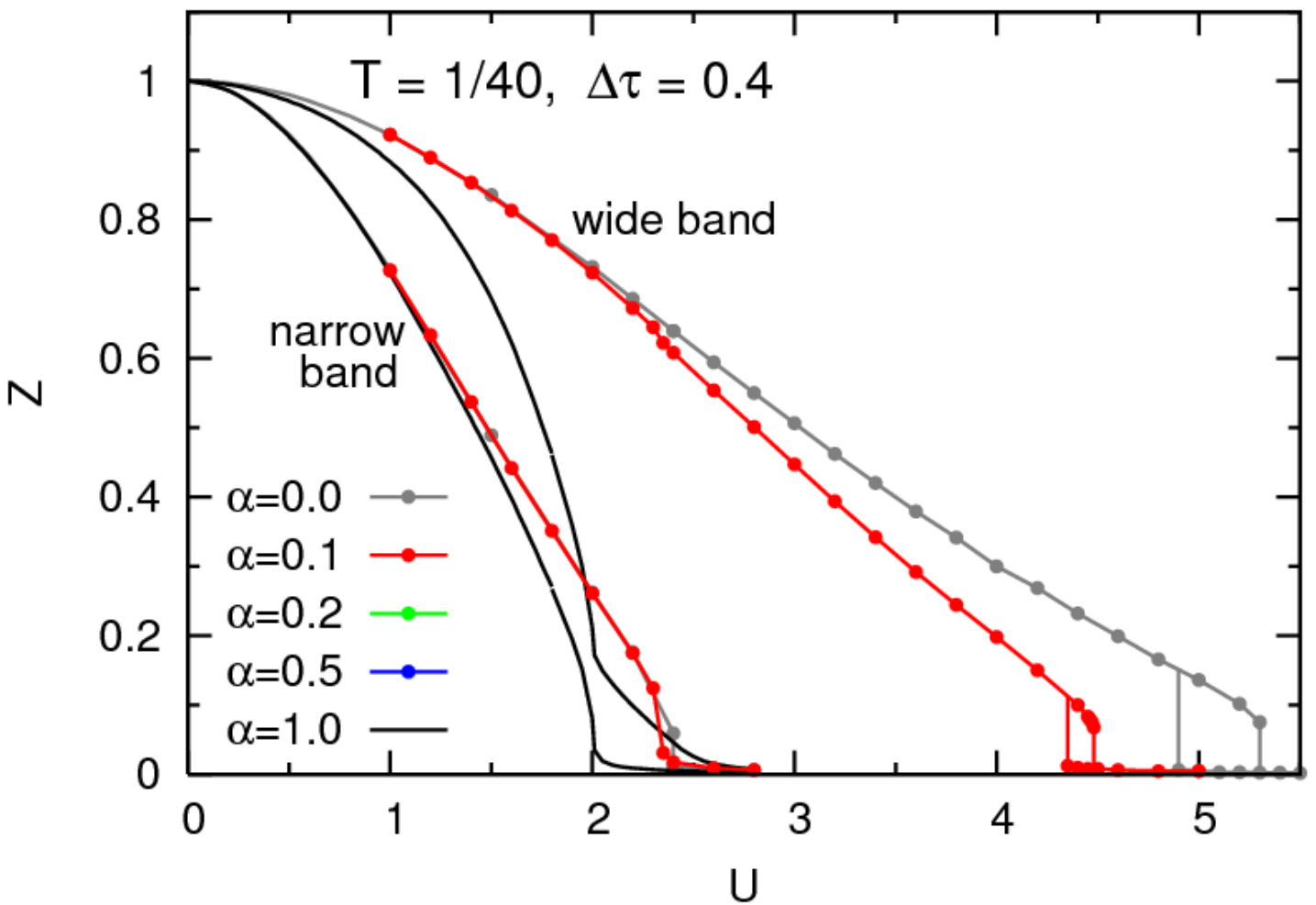

Systematic study: effect of inter-orbital coupling

$$H = \sum_{m=1}^{2} \Big[- \sum_{\langle ij \rangle \sigma} t_m c^{\dagger}_{im\sigma} c_{jm\sigma} + U \sum_i n_{im\uparrow} n_{im\downarrow} \Big] + \alpha \sum_{\cdot} (U/2 - \delta_{\sigma\sigma'} U/4)\, n_{i1\sigma}\, n_{i2\sigma'}$$

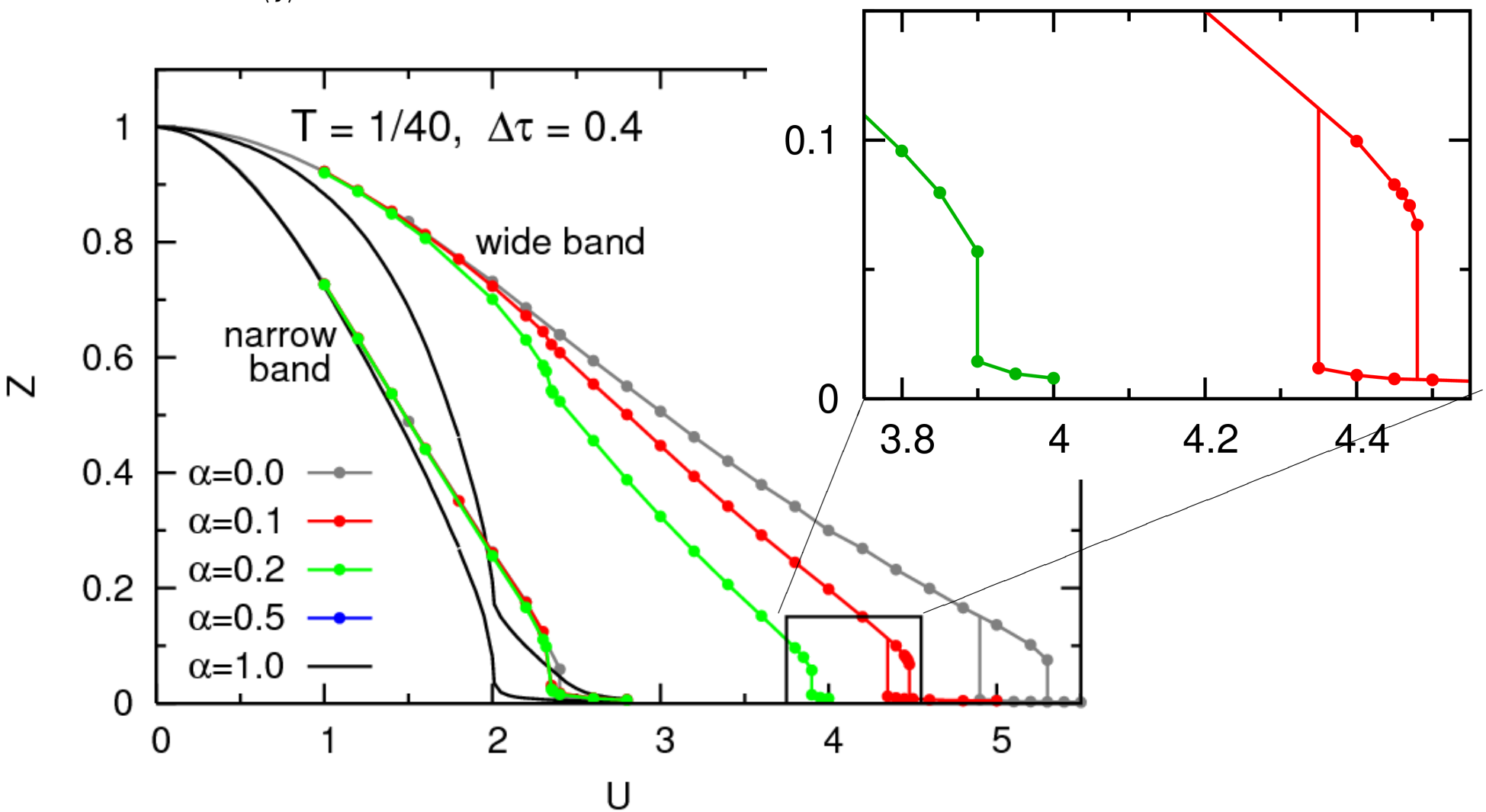

Systematic study: effect of inter-orbital coupling

$$H = \sum_{m=1}^{2} \Big[- \sum_{\langle ij \rangle \sigma} t_m c^{\dagger}_{im\sigma} c_{jm\sigma} + U \sum_i n_{im\uparrow} n_{im\downarrow} \Big] + \alpha \sum_{\cdot} (U/2 - \delta_{\sigma\sigma'} U/4)\, n_{i1\sigma}\, n_{i2\sigma'}$$

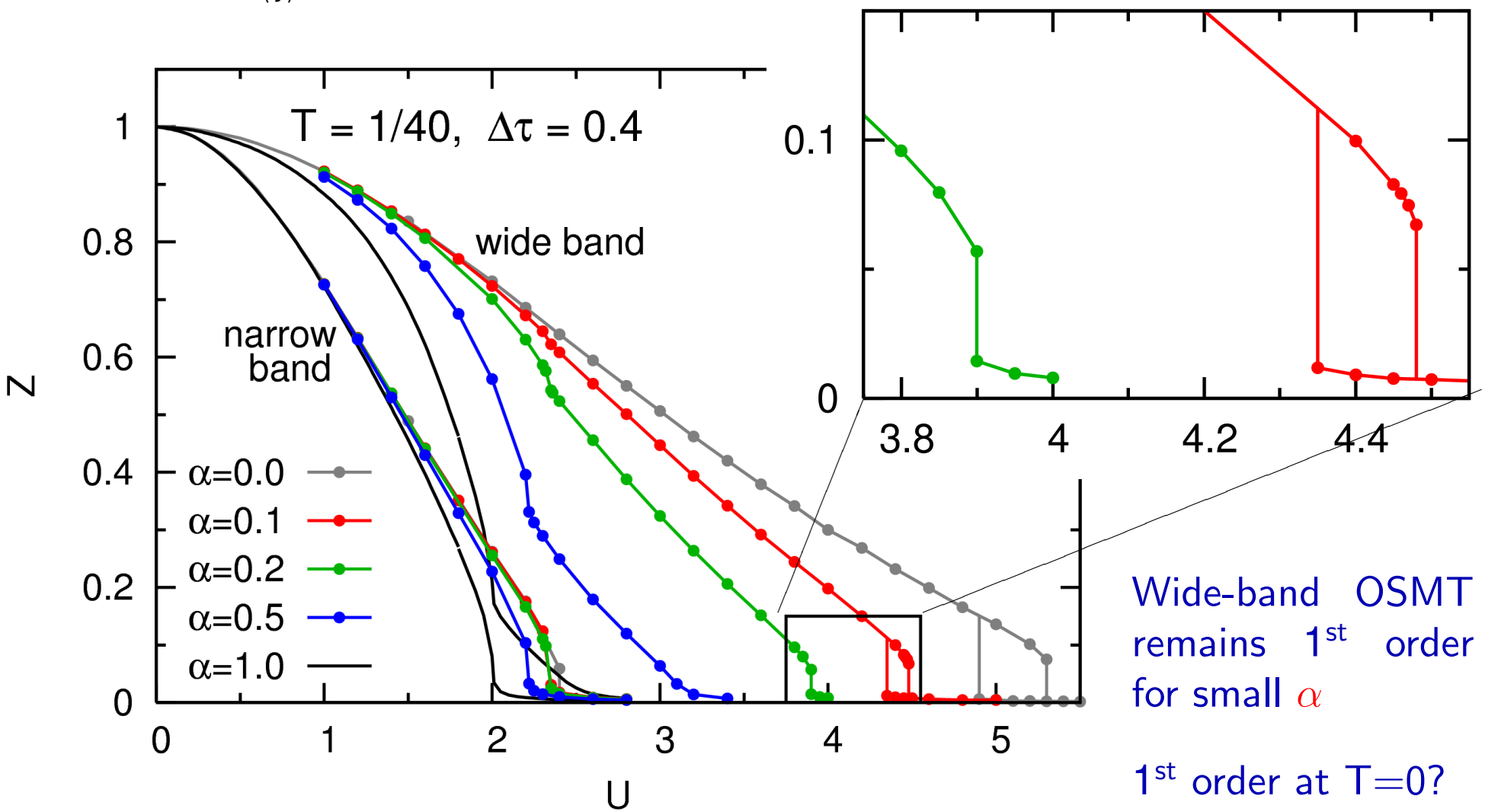

Wide-band OSMT remains 1st order for small α

1st order at T=0?

Self-energy functional theory (SFT+ED) with 1 bath site per orbital

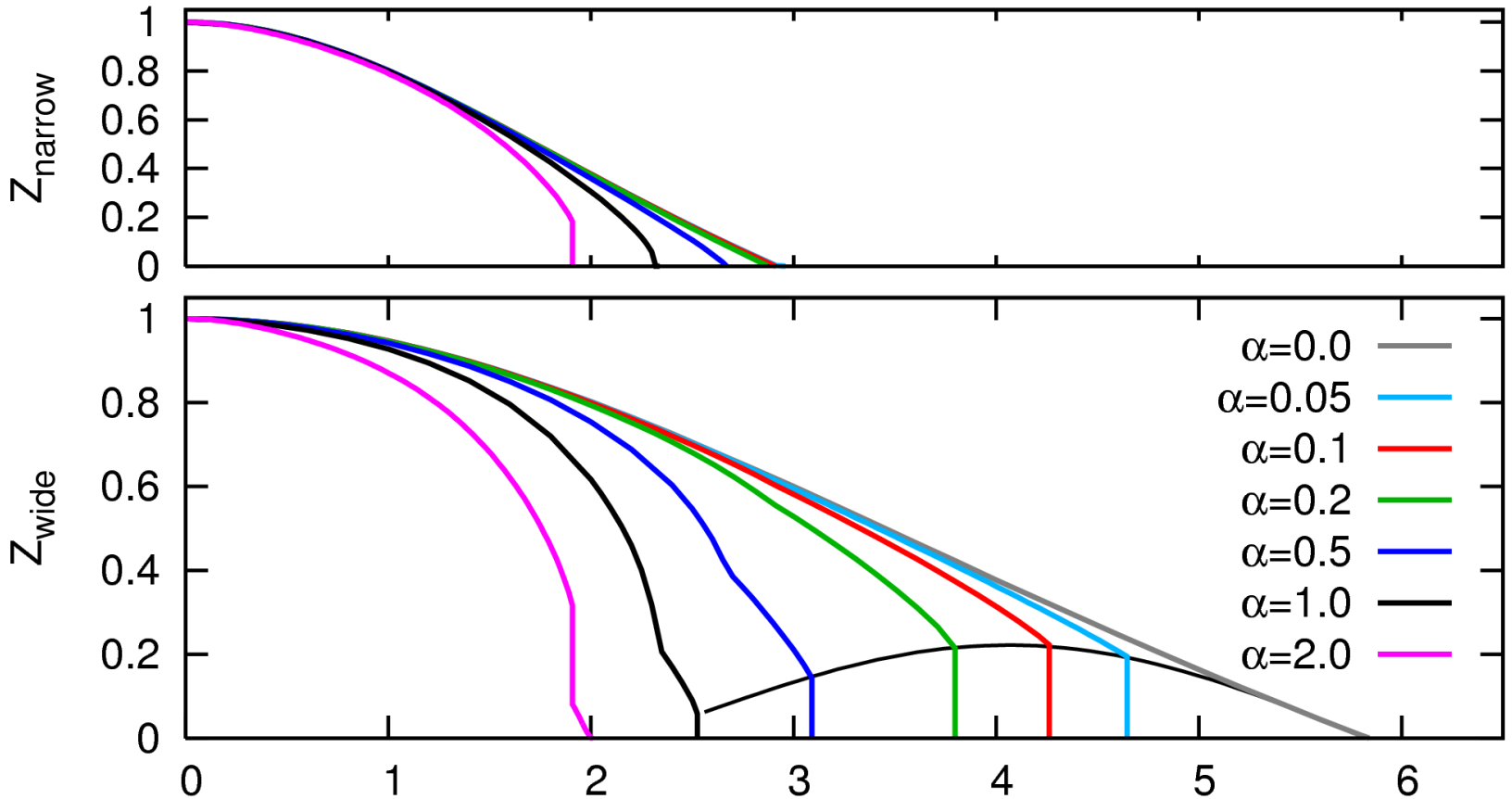

[K. Požgajčić, 8/2005, unpublished]

- 1st order wide-band transition for $0 < \alpha \lesssim 1.5$
- larger α: 2nd order $\leftrightarrow$ 1st order

Self-energy functional theory (SFT+ED) with 1 bath site per orbital

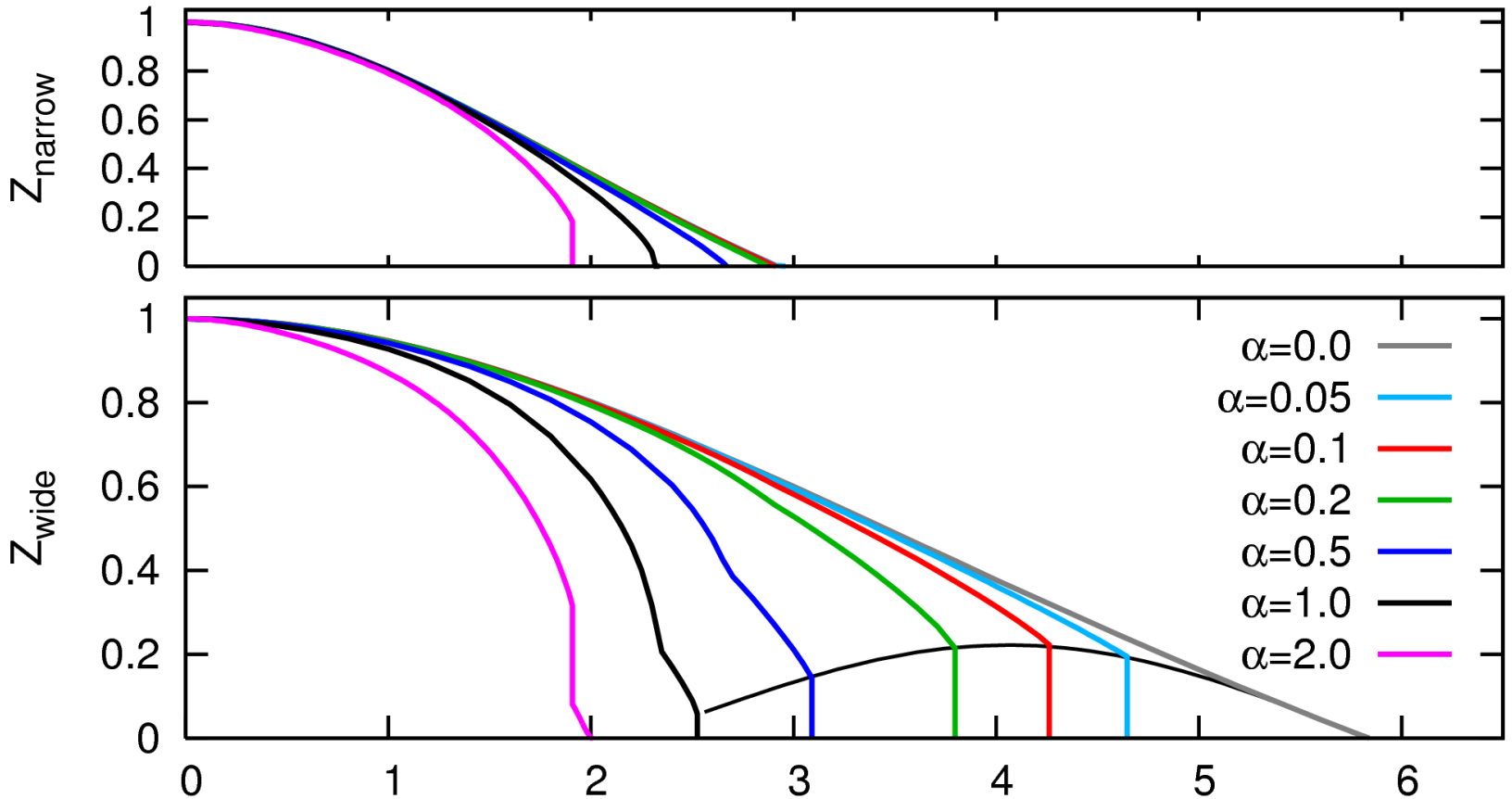

[K. Požgajčić, 8/2005, unpublished]

◦ 1st order wide-band transition for $0 < \alpha \lesssim 1.5$ ◦ larger α: 2nd order $\leftrightarrow$ 1st order

Problems: ◦ Low-frequency part of $\Sigma(\omega)$ inconsistent with QMC

◦ Z ill-defined in OSM phase ◦ strong finite-size effects

Double occupancy (1st order derivative of Ω)

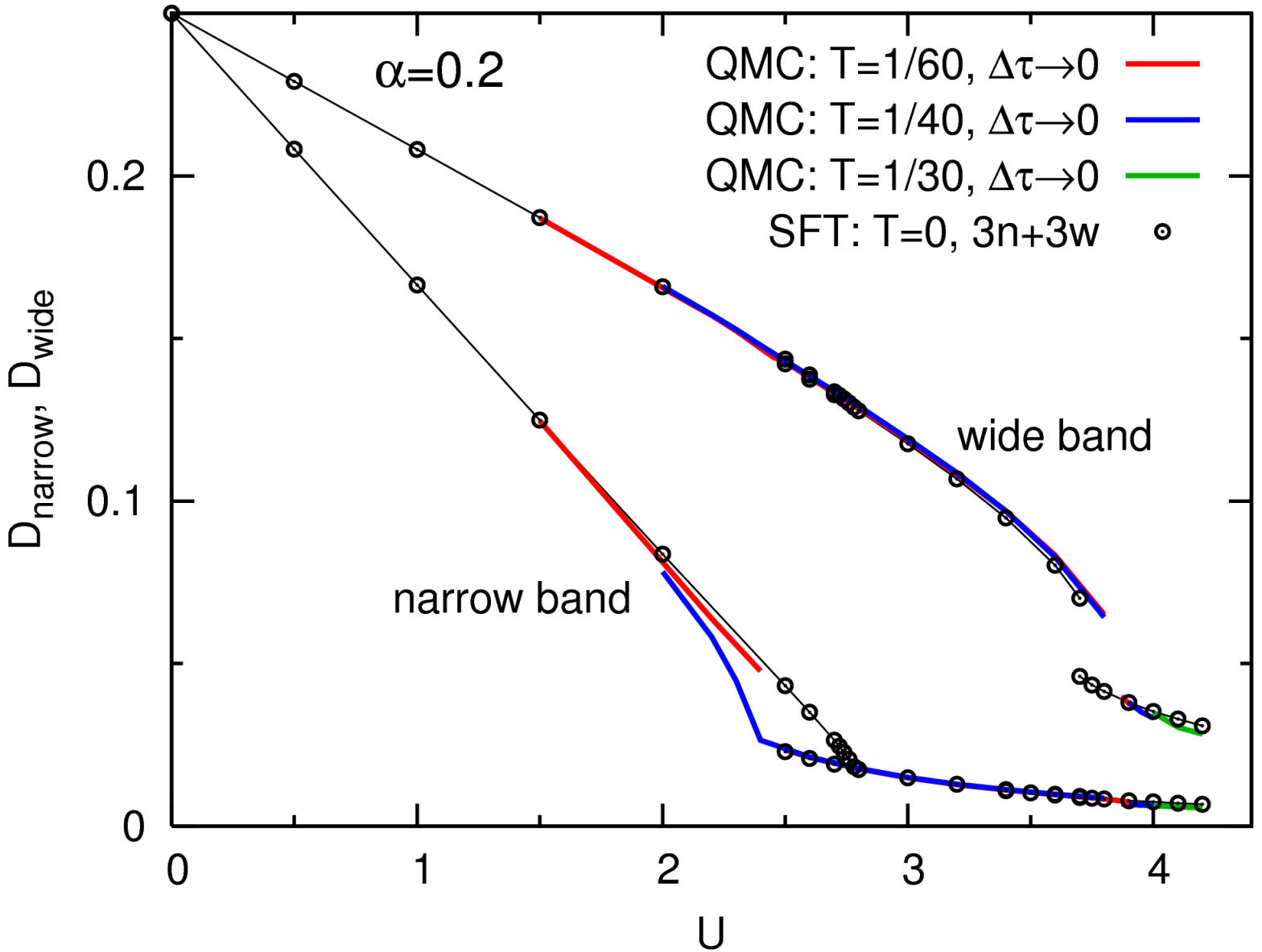

Excellent agreement between SFT and QMC

1st order at $T = 0$ (at least) for $0 < \alpha \leq 0.2$

Efficiency of Quantum Monte Carlo DMFT solvers

New development: continuous-time QMC algorithms

1. weak-coupling expansion

[Rubtsov, Savkin, Lichtenstein, PRB (2005)]

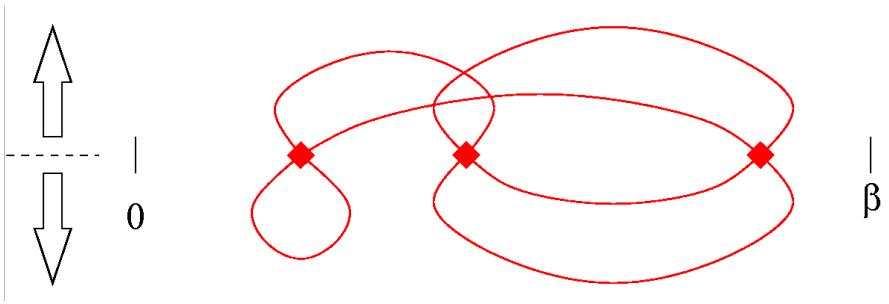

2. hybridization expansion

[Werner et al., PRL (2006)]

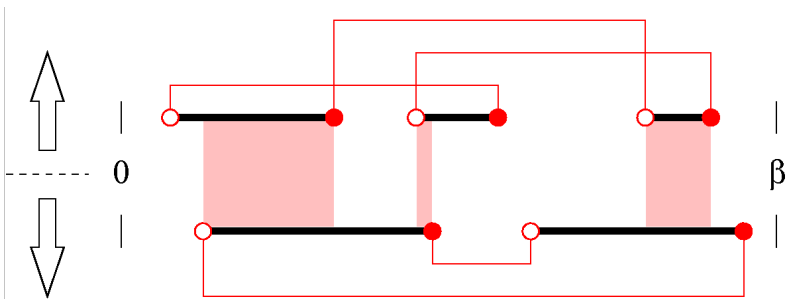

Efficiency of Quantum Monte Carlo DMFT solvers

New development: continuous-time QMC algorithms

1. weak-coupling expansion

[Rubtsov, Savkin, Lichtenstein, PRB (2005)]

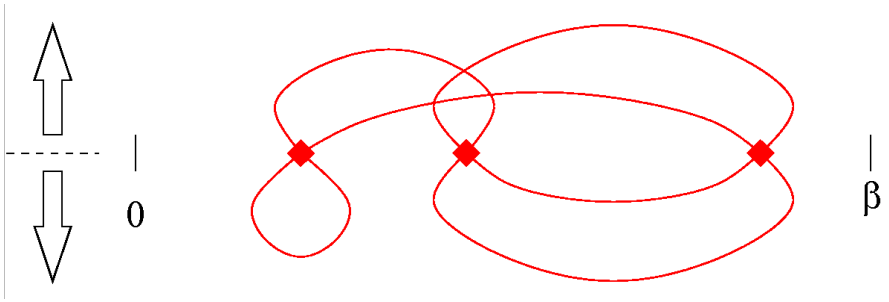

2. hybridization expansion

[Werner et al., PRL (2006)]

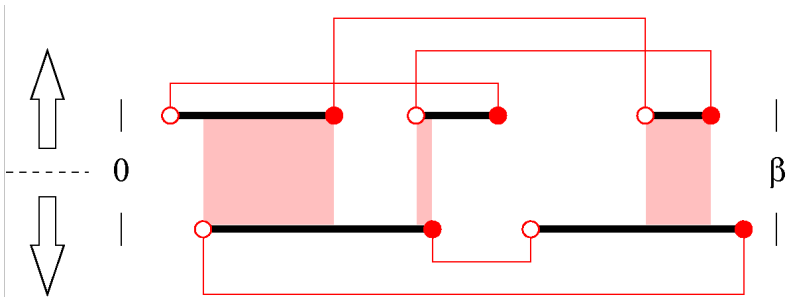

CT-QMC methods: smaller matrices

All QMC methods: effort $\propto \Lambda^3$

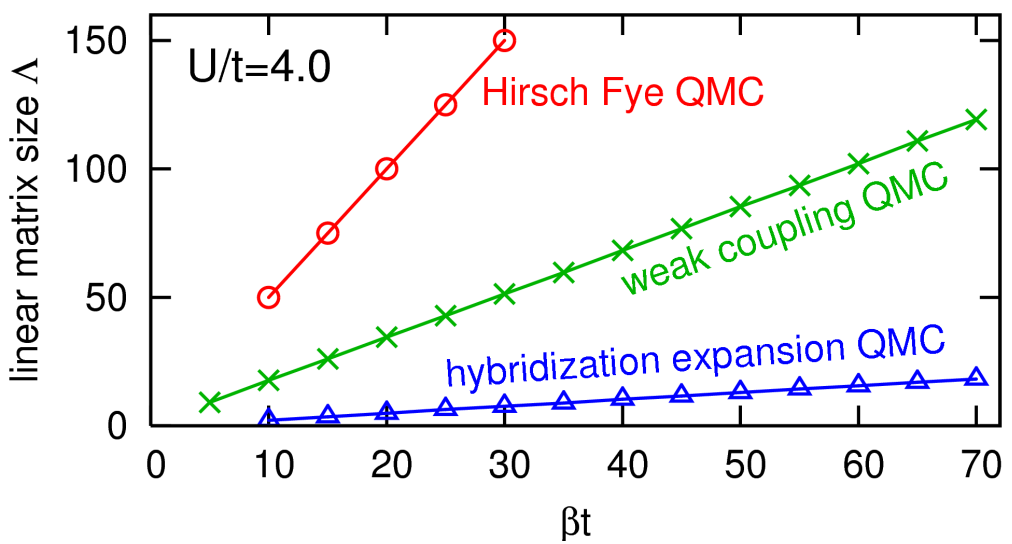

Efficiency of Quantum Monte Carlo DMFT solvers

New development: continuous-time QMC algorithms

1. weak-coupling expansion

[Rubtsov, Savkin, Lichtenstein, PRB (2005)]

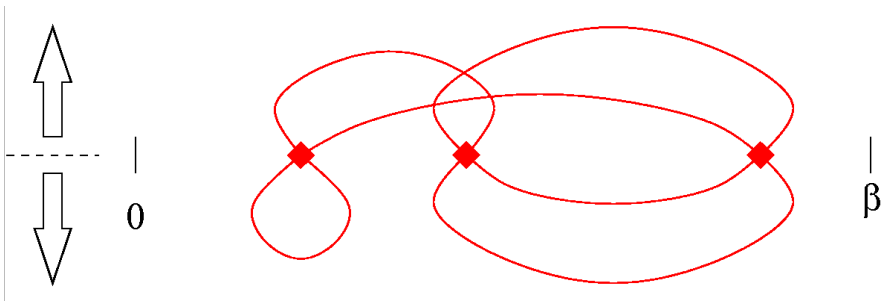

2. hybridization expansion

[Werner et al., PRL (2006)]

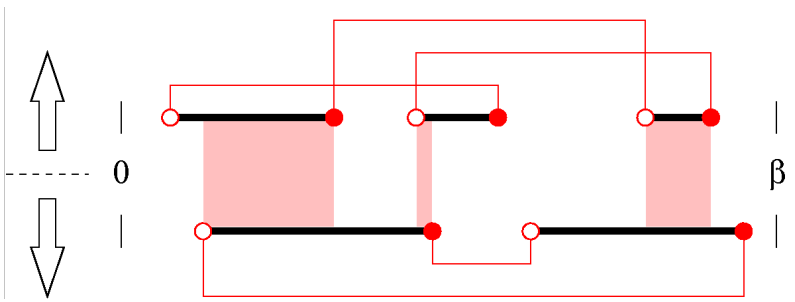

CT-QMC methods: smaller matrices

All QMC methods: effort $\propto \Lambda^3$

Claim [Troyer (2006)]:
CT-QMC more efficient than
HF-QMC by orders of magnitude

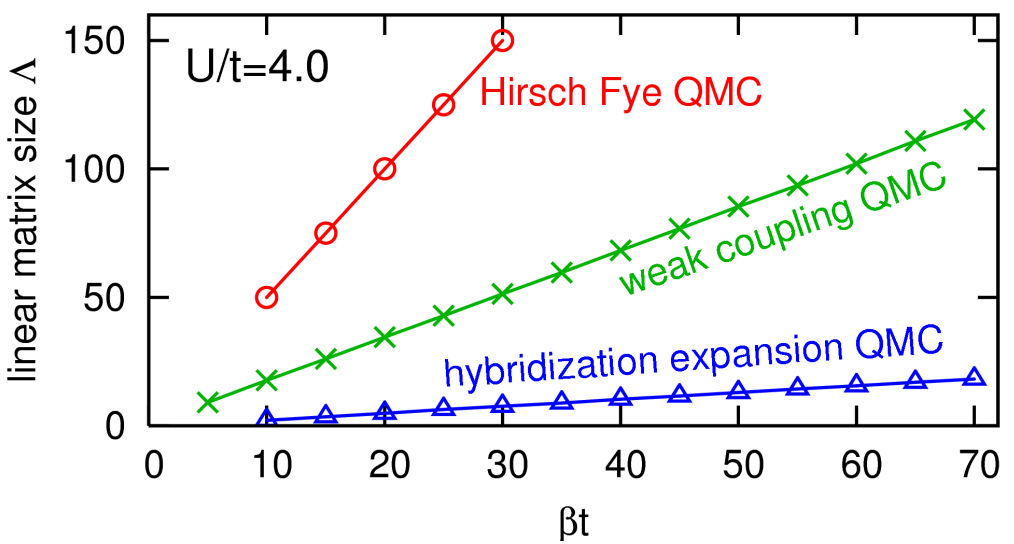

Kinetic energy vs. squared temperature ($U/t = 4.0$)

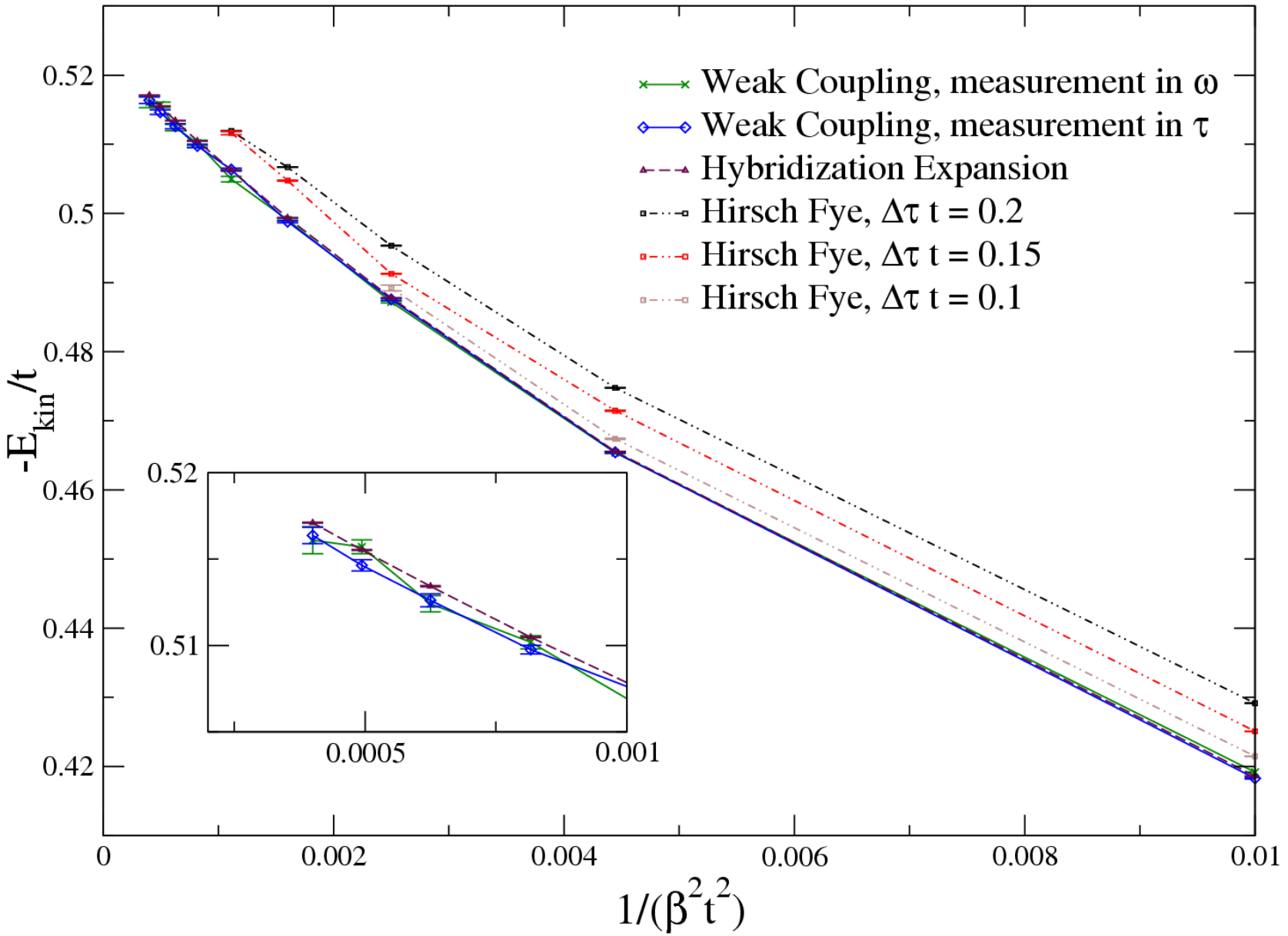

[Gull et al., cond-mat/0609438]

HF-QMC useless at small T!?

Performance analysis: CT-QMC methods versus HF-QMC

Performance analysis of continuous-time solvers for quantum impurity models

Emanuel Gull,[1] Philipp Werner,[2] Andrew Millis,[2] and Matthias Troyer[1]

[1] *Institut für theoretische Physik, ETH Zürich, CH-8093 Zürich, Switzerland*
[2] *Columbia University, 538 West, 120th Street, New York, NY 10027, USA*

Impurity solvers play an essential role in the numerical investigation of strongly correlated electrons systems within the "dynamical mean field" approximation. Recently, a new class of continuous-time solvers has been developed, based on a diagrammatic expansion of the partition function in either the interactions or the impurity-bath hybridization. We investigate the performance of these two complimentary approaches and compare them to the well-established Hirsch-Fye method. The results show that the continuous-time methods, and in particular the version which expands in the hybridization, provide substantial gains in computational efficiency.

PACS numbers: 71.10.-w, 71.10.Fd, 71.28.+d, 71.30.+h

[cond-mat/0609438]

Performance analysis: CT-QMC methods versus HF-QMC

Performance analysis of continuous-time solvers for quantum impurity models

Emanuel Gull,[1] Philipp Werner,[2] Andrew Millis,[2] and Matthias Troyer[1]

[1] *Institut für theoretische Physik, ETH Zürich, CH-8093 Zürich, Switzerland*
[2] *Columbia University, 538 West, 120th Street, New York, NY 10027, USA*

Impurity solvers play an essential role in the numerical investigation of strongly correlated electrons systems within the "dynamical mean field" approximation. Recently, a new class of continuous-time solvers has been developed, based on a diagrammatic expansion of the partition function in either the interactions or the impurity-bath hybridization. We investigate the performance of these two complimentary approaches and compare them to the well-established Hirsch-Fye method. The results show that the continuous-time methods, and in particular the version which expands in the hybridization, provide substantial gains in computational efficiency.

PACS numbers: 71.10.-w, 71.10.Fd, 71.28.+d, 71.30.+h

[cond-mat/0609438]

- Test case: 1-band Hubbard model (semi-elliptic DOS, $n = 1$, $W = 4$) for $U = 4$
- Focus on low temperatures: $T = 1/45$
- Additional results for doped model (also different U)

Performance analysis: CT-QMC methods versus HF-QMC

Performance analysis of continuous-time solvers for quantum impurity models

Emanuel Gull,[1] Philipp Werner,[2] Andrew Millis,[2] and Matthias Troyer[1]

[1] *Institut für theoretische Physik, ETH Zürich, CH-8093 Zürich, Switzerland*
[2] *Columbia University, 538 West, 120th Street, New York, NY 10027, USA*

Impurity solvers play an essential role in the numerical investigation of strongly correlated electrons systems within the "dynamical mean field" approximation. Recently, a new class of continuous-time solvers has been developed, based on a diagrammatic expansion of the partition function in either the interactions or the impurity-bath hybridization. We investigate the performance of these two complimentary approaches and compare them to the well-established Hirsch-Fye method. The results show that the continuous-time methods, and in particular the version which expands in the hybridization, provide substantial gains in computational efficiency.

PACS numbers: 71.10.-w, 71.10.Fd, 71.28.+d, 71.30.+h

[cond-mat/0609438]

- Test case: 1-band Hubbard model (semi-elliptic DOS, $n = 1$, $W = 4$) for $U = 4$
- Focus on low temperatures: $T = 1/45$
- Additional results for doped model (also different U)

Good Hirsch-Fye implementation? Fair comparison? Precision of results?

Principles of weak-coupling CT-QMC

Decouple action into quadratic part

$$S_0 = -\int_0^\beta d\tau d\tau' \sum_\sigma c_\sigma(\tau) F_\sigma(\tau - \tau') c_\sigma^\dagger(\tau') - \mu \int_0^\beta d\tau (n_\uparrow + n_\downarrow)$$

and an interaction part

$$S_U = U \int_0^\beta d\tau n_\uparrow n_\downarrow,$$

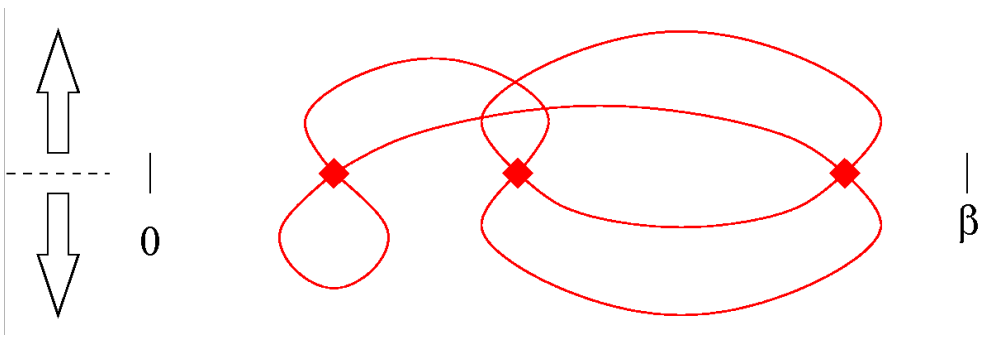

[Gull et al. cond-mat/0609438]

where $\mathcal{G}_{0,\sigma}^{-1}(i\omega) = i\omega + \mu - F_\sigma(-i\omega)$.

$$Z = \sum_k \frac{(-U)^k}{k!} \int d\tau_1 \ldots d\tau_k \, Tr T_\tau e^{-S_0} \quad n_\uparrow(\tau_1) n_\downarrow(\tau_1) \ldots n_\uparrow(\tau_k) n_\downarrow(\tau_k)$$

is sampled by random insertions/removals of vertices. Trick: avoid sign problem

[Rubtsov, Savkin, Lichtenstein, PRB **72**, 035122 (2005)]

Principles of hybridization expansion CT-QMC

Decompose action into local part

$$S_L = -\mu \int_0^\beta d\tau (n_\uparrow + n_\downarrow) + U \int_0^\beta d\tau n_\uparrow n_\downarrow$$

and hybridization part

$$S_F = -\int_0^\beta d\tau d\tau' \sum_\sigma c_\sigma(\tau) F_\sigma(\tau - \tau') c_\sigma^\dagger(\tau');$$

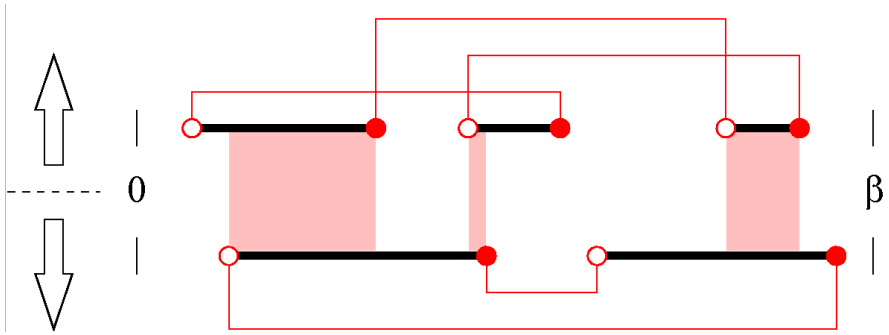

[Gull et al. cond-mat/0609438]

expanding the partition function in powers of F_σ leads to:

$$\begin{aligned} Z &= Tr T_\tau e^{-S_L} \prod_\sigma \sum_{k_\sigma} \frac{1}{k_\sigma!} \int_0^\beta d\tau_1^\sigma \ldots d\tau_{k_\sigma}^\sigma \int_0^\beta d\tilde{\tau}_1^\sigma \ldots d\tilde{\tau}_{k_\sigma}^\sigma \\ &\times \left[c_\sigma(\tau_1) F_\sigma(\tau_1 - \tilde{\tau}_1) c_\sigma^\dagger(\tilde{\tau}_1) \ldots c_\sigma(\tau_{k_\sigma}) F_\sigma(\tau_{k_\sigma} - \tilde{\tau}_{k_\sigma}) c_\sigma^\dagger(\tilde{\tau}_{k_\sigma}) \right]. \end{aligned}$$

Express combined weight corresponding to given collection $\{c_\sigma^\dagger(\tilde{\tau}_i), c_\sigma(\tau_i)\}_{i=1,\ldots,k_\sigma}$ of creation and annihilation operators as the determinant of a matrix $D_{F,\sigma}$, sample . . . [Werner et al., PRL **97**, 076405 (2006); Werner and Millis, PRB **76**, 1 (2006)]

Self-energy

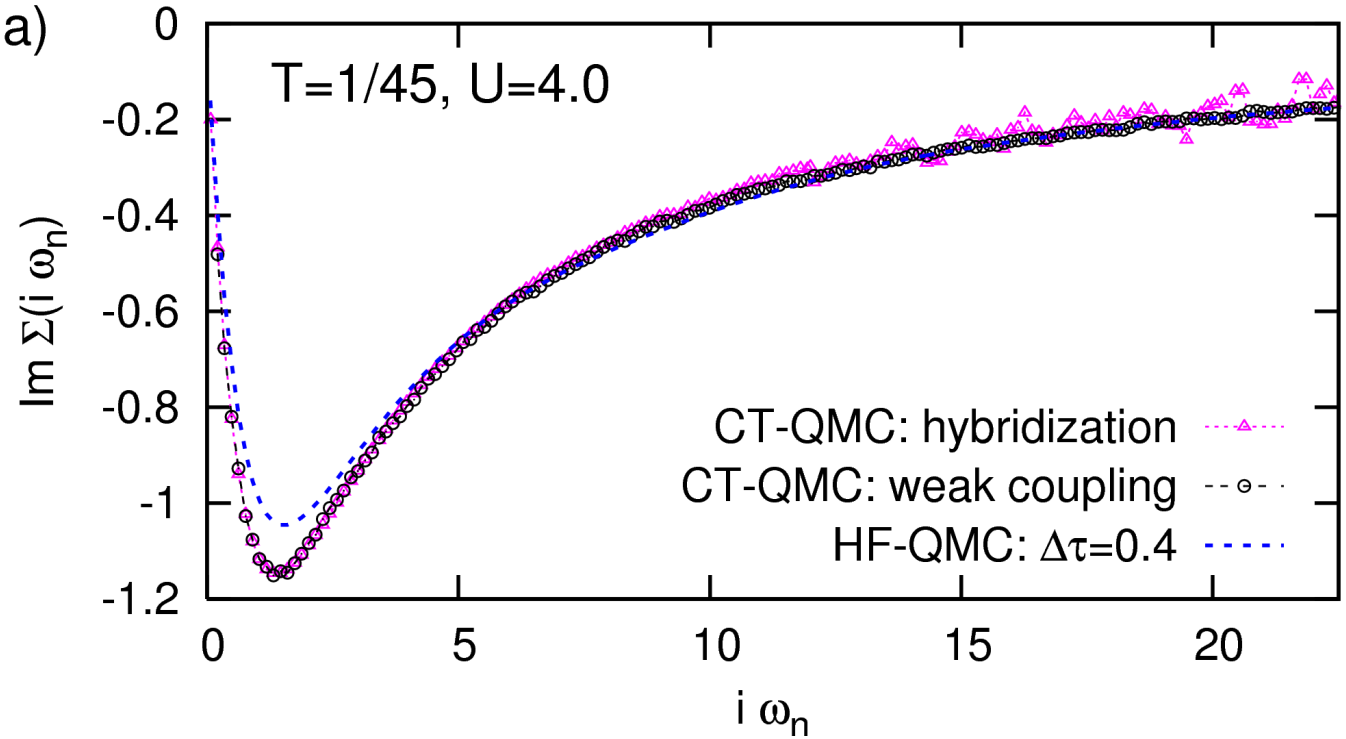
a)
T=1/45, U=4.0
Im Σ(i ω_n)
i ω_n
0
-0.2
-0.4
-0.6
-0.8
-1
-1.2
0
5
10
15
20
CT-QMC: hybridization
CT-QMC: weak coupling
HF-QMC: Δτ=0.4

Self-energy

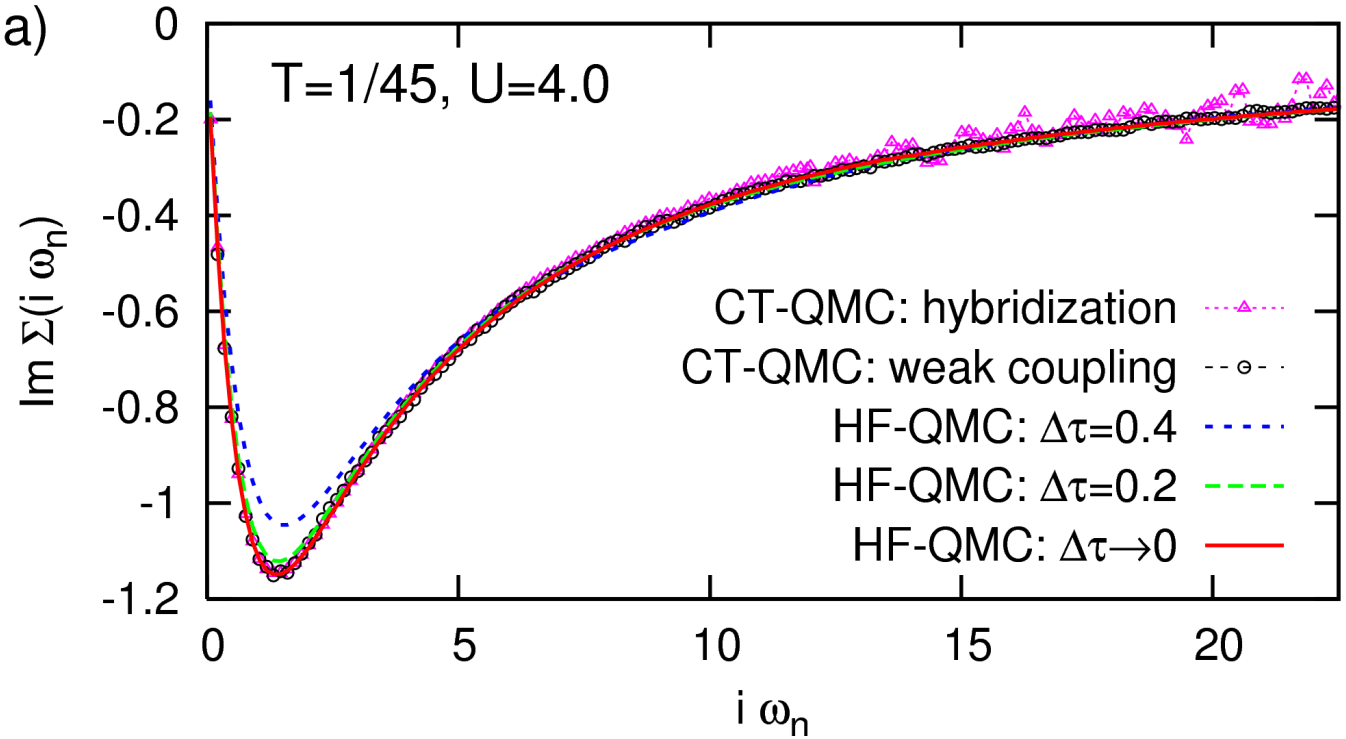
a)
T=1/45, U=4.0
Im Σ(i ω_n)
i ω_n
0
-0.2
-0.4
-0.6
-0.8
-1
-1.2
0
5
10
15
20
CT-QMC: hybridization
CT-QMC: weak coupling
HF-QMC: Δτ=0.4
HF-QMC: Δτ=0.2
HF-QMC: Δτ→0

Self-energy

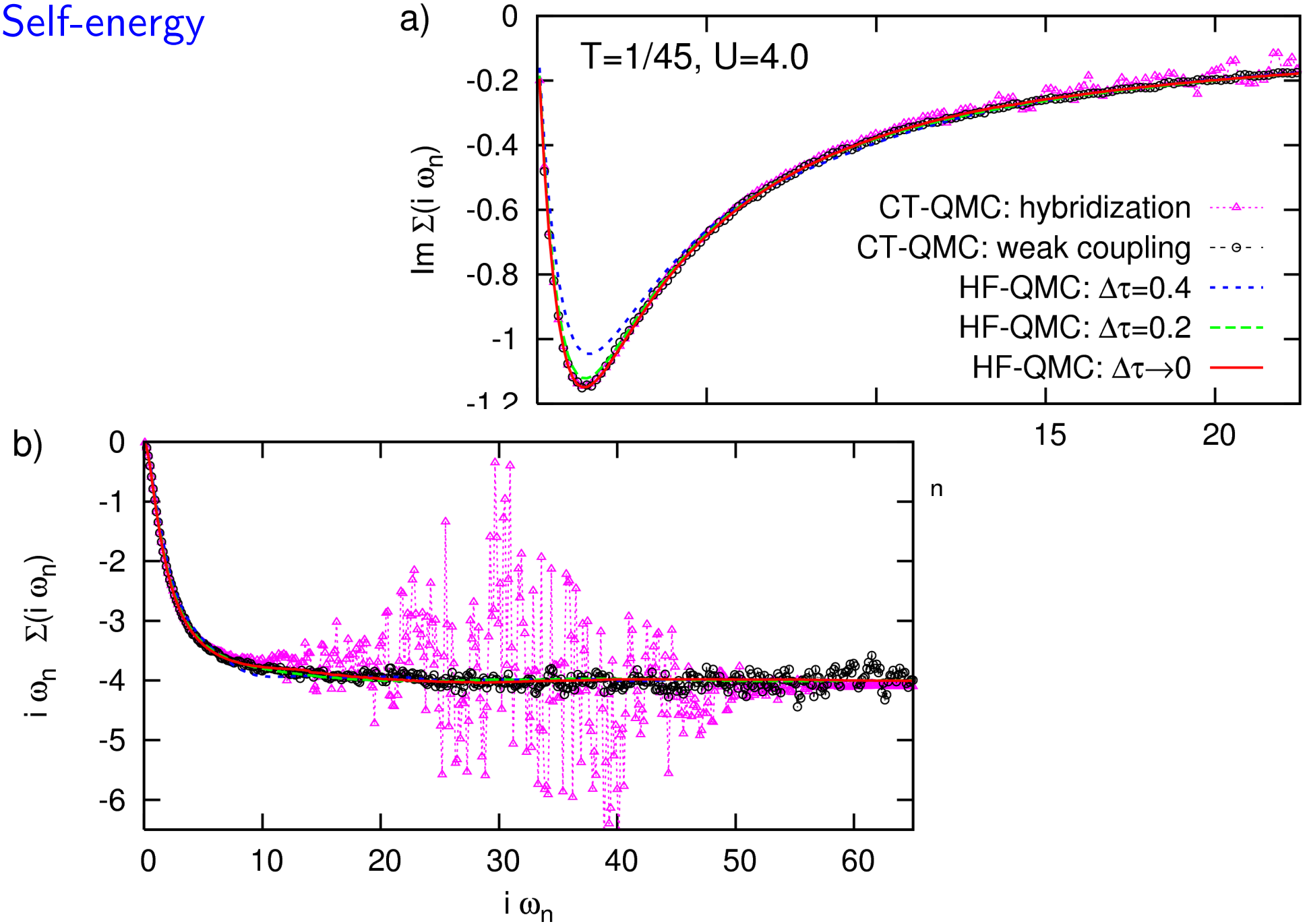
a)
T=1/45, U=4.0
Im Σ(i ω_n)
0
-0.2
-0.4
-0.6
-0.8
-1
15
20
CT-QMC: hybridization
CT-QMC: weak coupling
HF-QMC: Δτ=0.4
HF-QMC: Δτ=0.2
HF-QMC: Δτ→0
b)
i ω_n Σ(i ω_n)
0
-1
-2
-3
-4
-5
-6
0
10
20
30
40
50
60
i ω_n
n

Self-energy: $\mathrm{Im}\Sigma(i\omega_0)/\omega_0 = 1 - 1/Z$ for $U = 4$

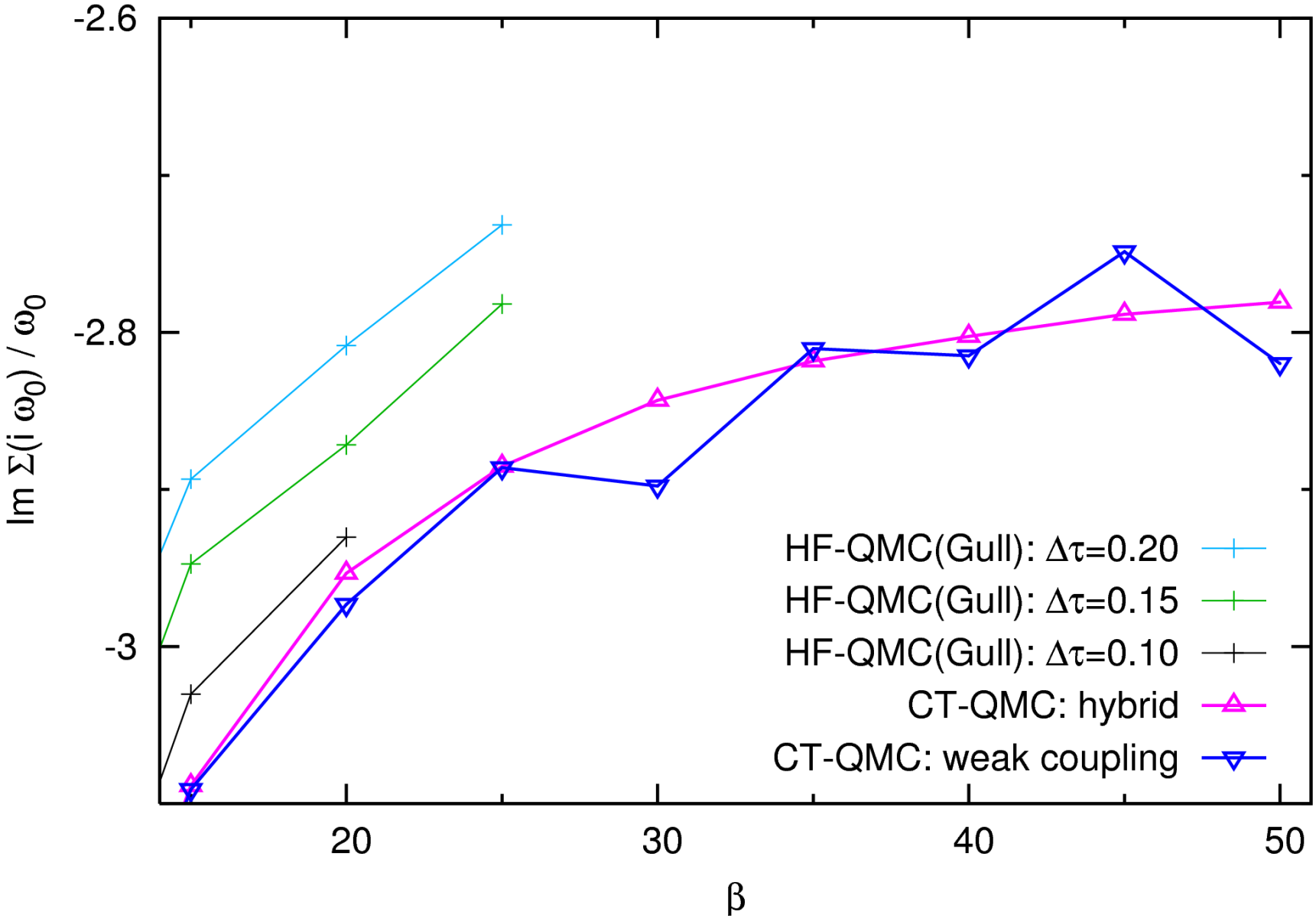

Self-energy: $\mathrm{Im}\Sigma(i\omega_0)/\omega_0 = 1 - 1/Z$ for $U = 4$

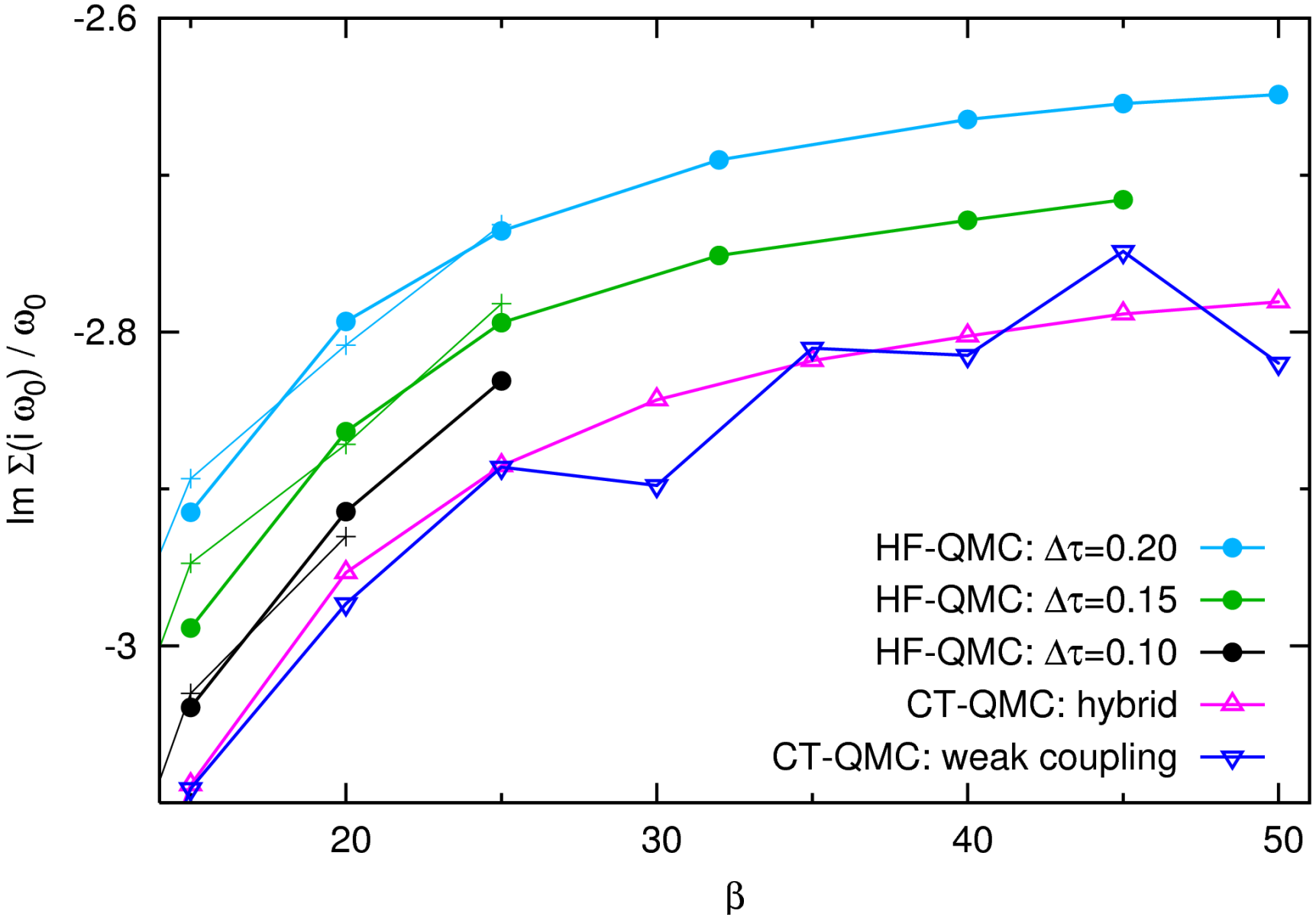

Self-energy: $\mathrm{Im}\Sigma(i\omega_0)/\omega_0 = 1 - 1/Z$ for $U = 4$

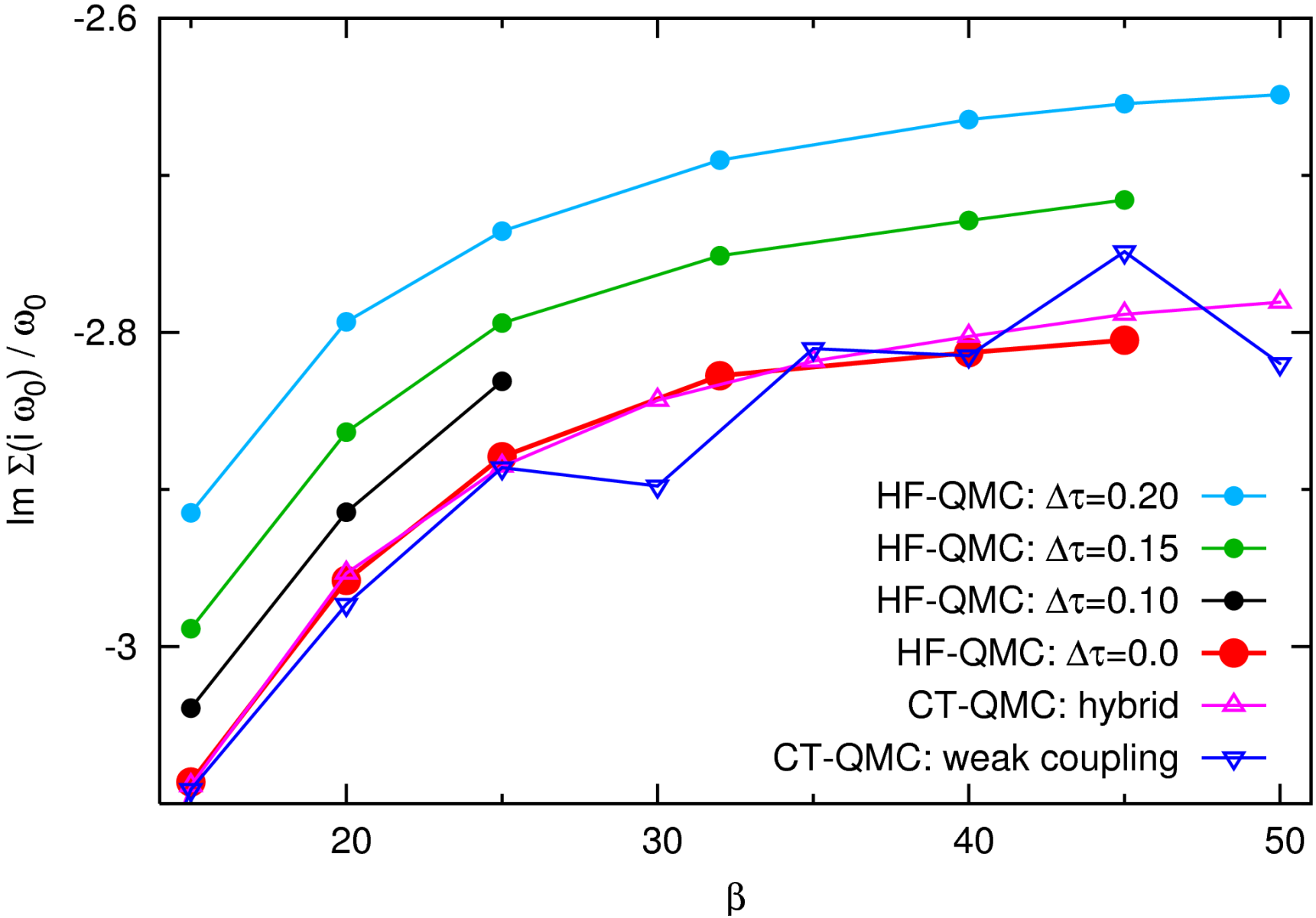

Energetics: kinetic energy for $U = 4$

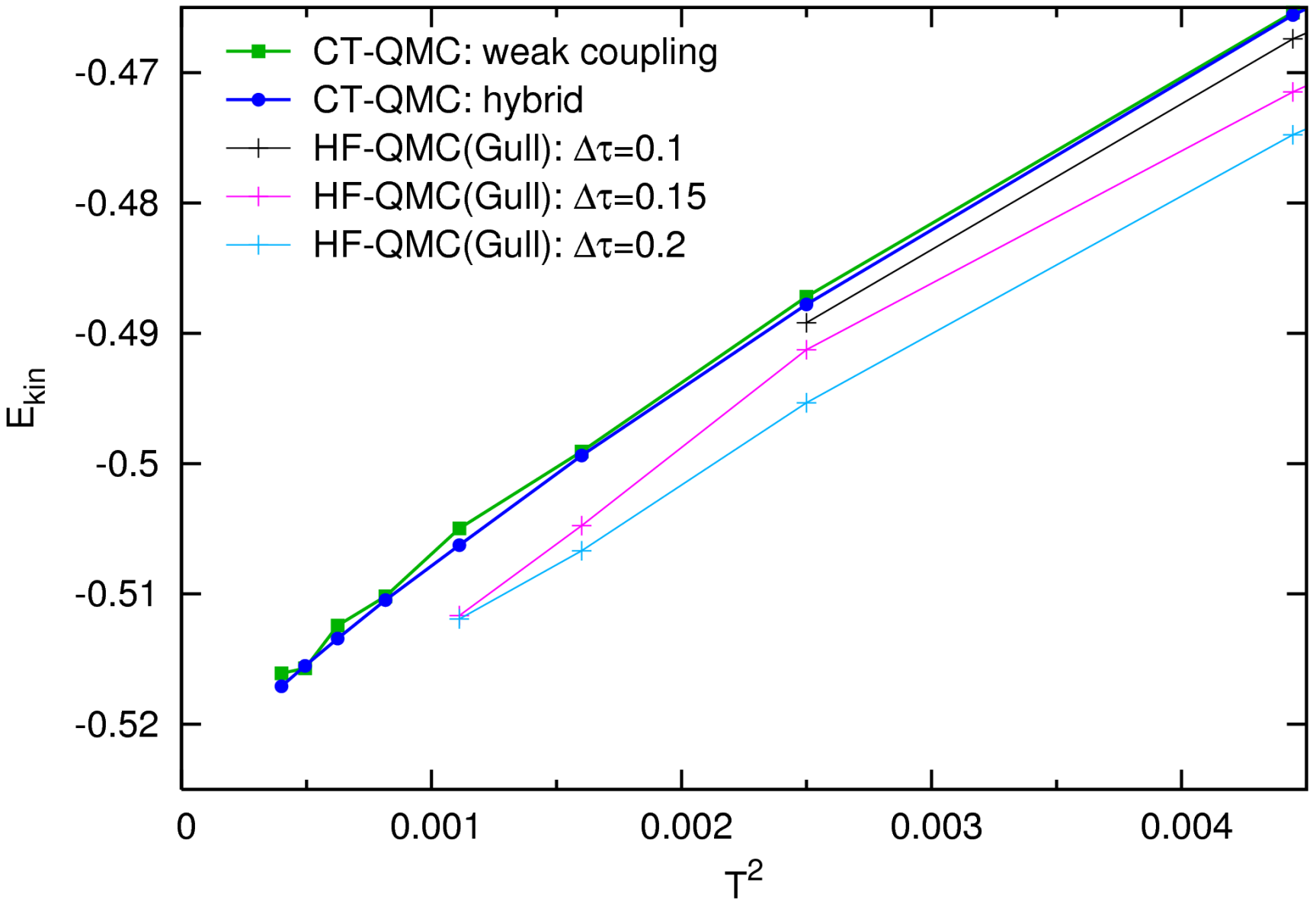

Energetics: kinetic energy for $U = 4$

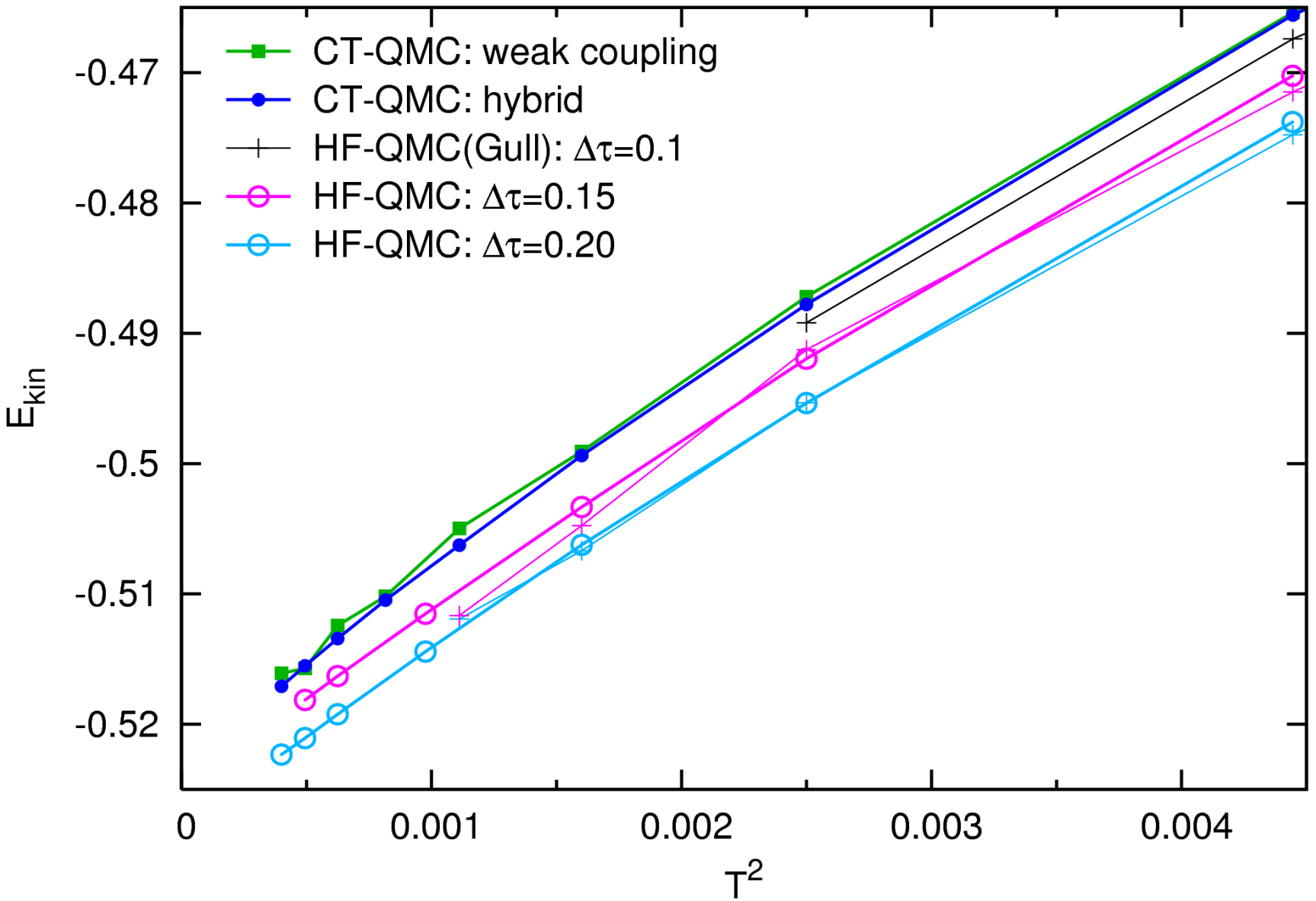

Energetics: kinetic energy for $U = 4$

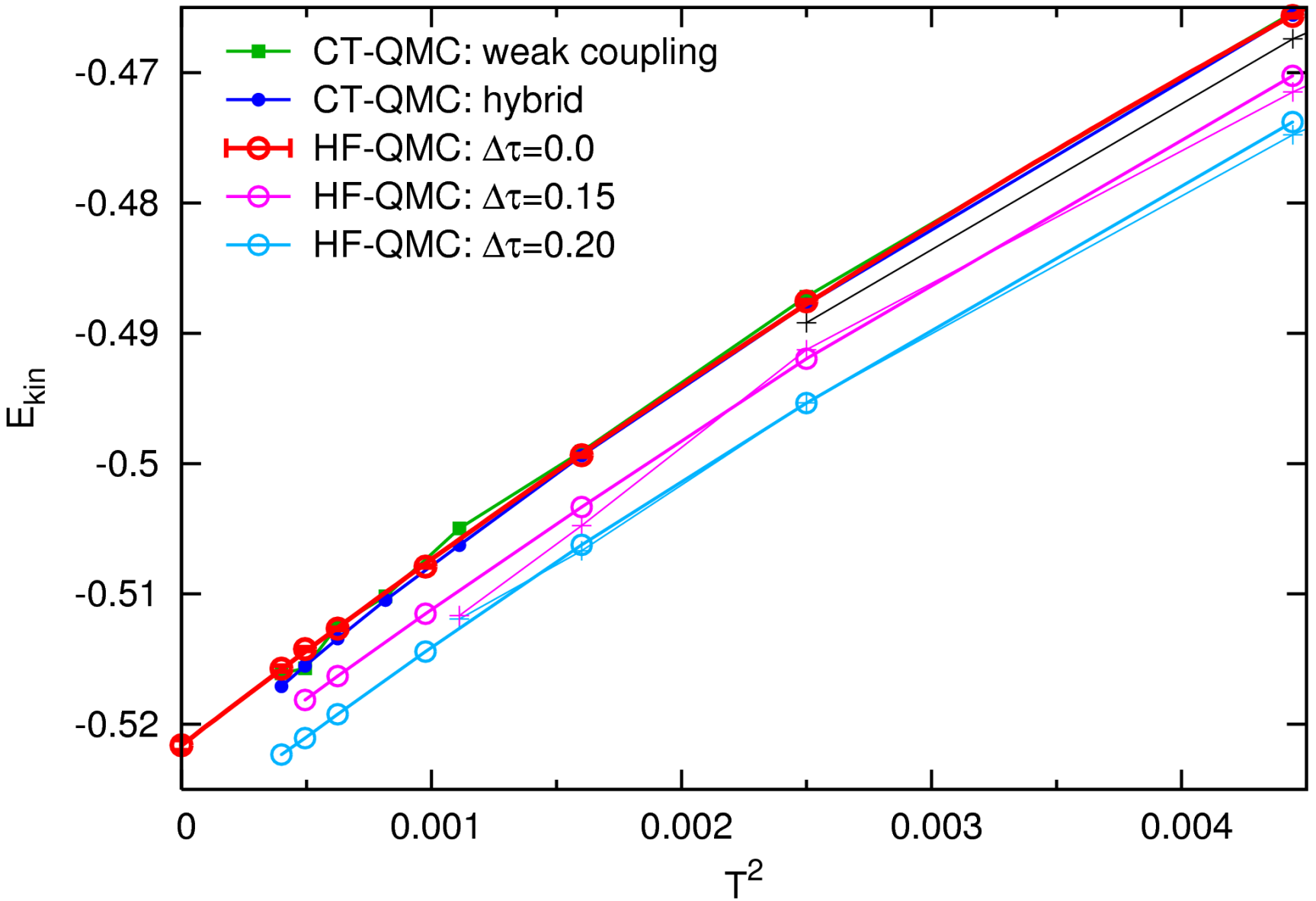

Energetics: kinetic energy for $U = 4$

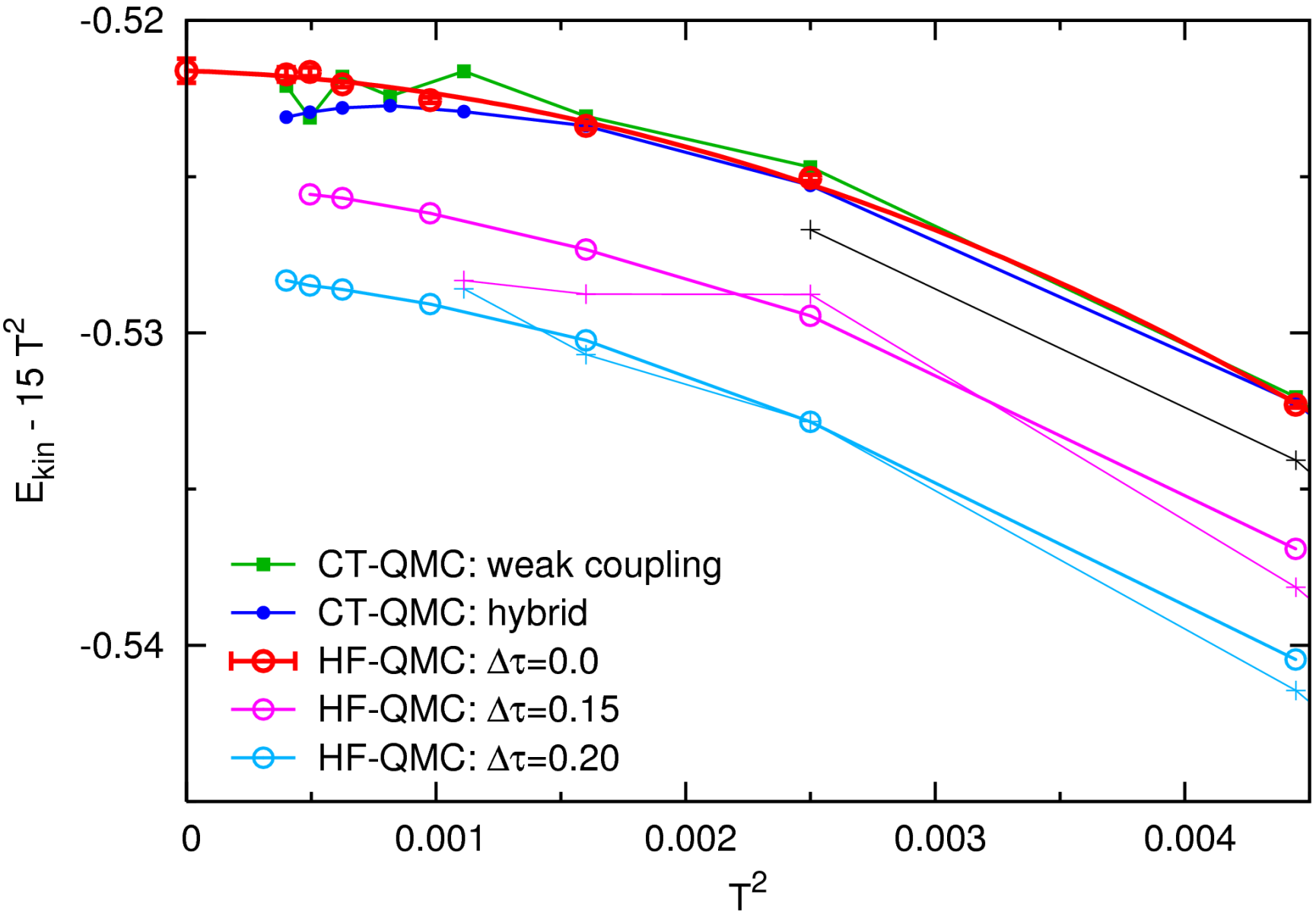

Essential step in HF-QMC: extrapolation $\Delta\tau \to 0$

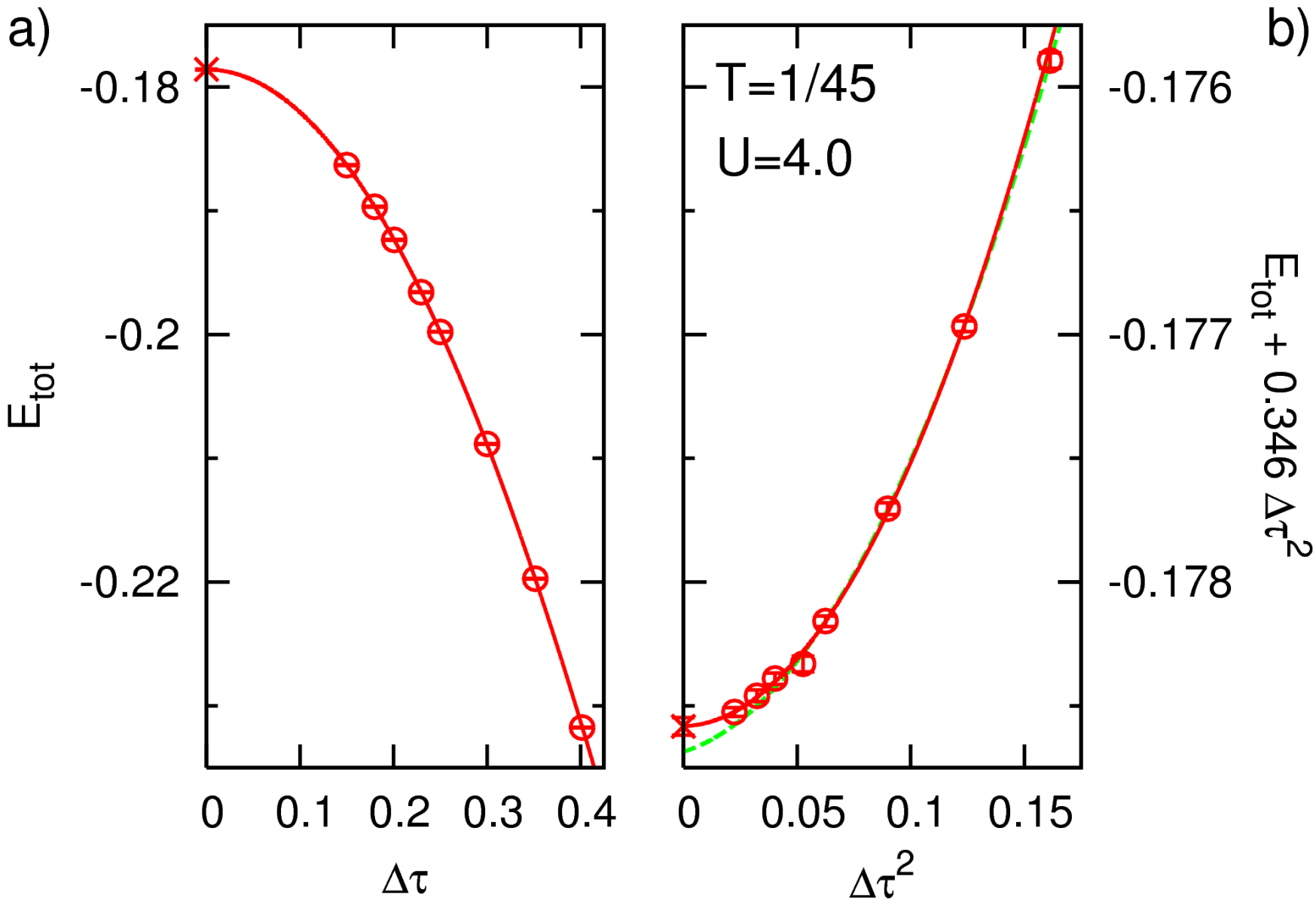

$\Delta\tau$ dependence very regular (except at phase transition)

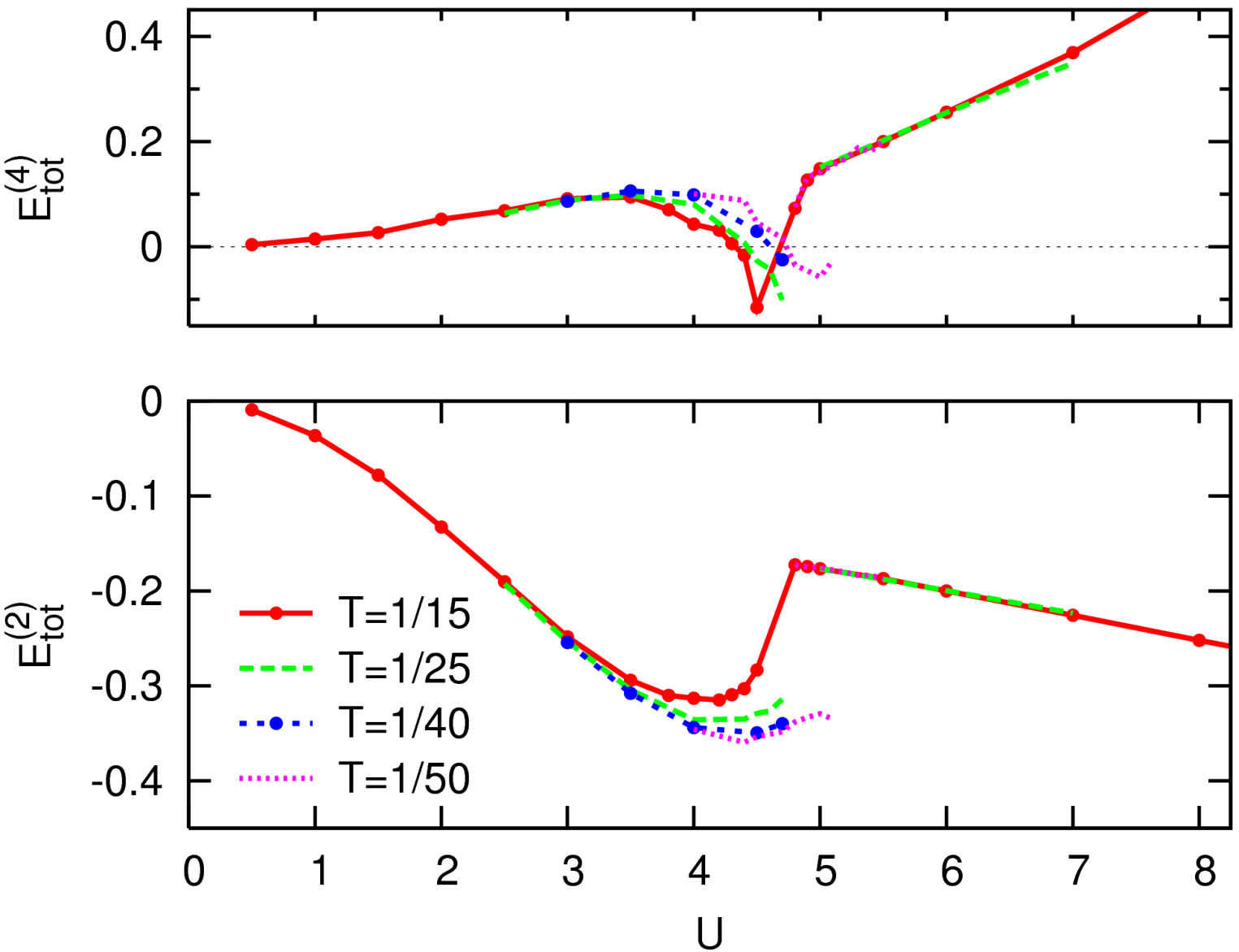

Comparison for total energy

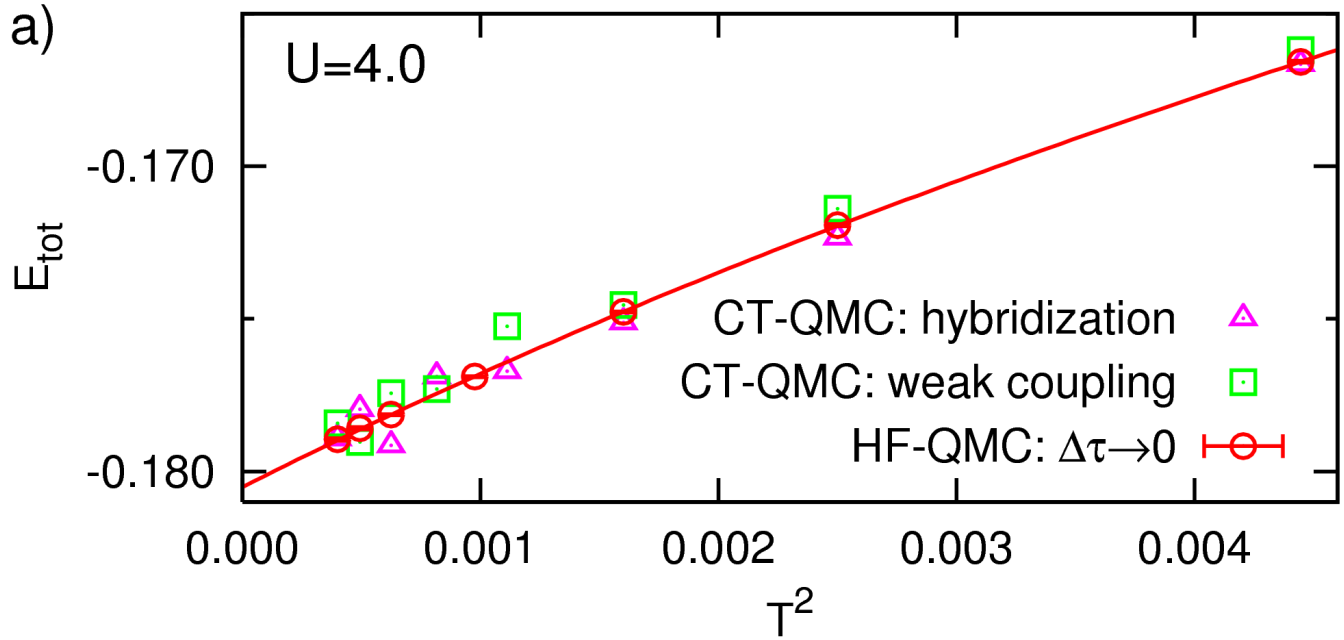

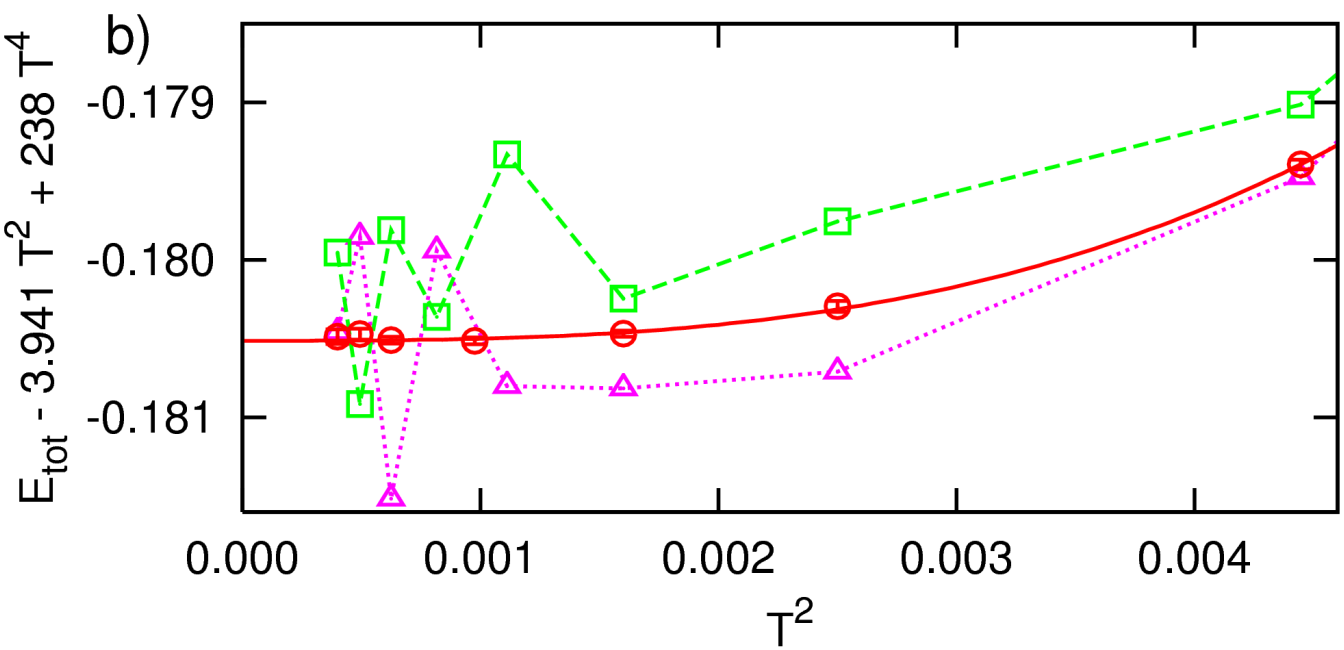

HF-QMC is more efficient (much higher precision at slightly higher cost)

Precision: HF-QMC vs. ground state methods

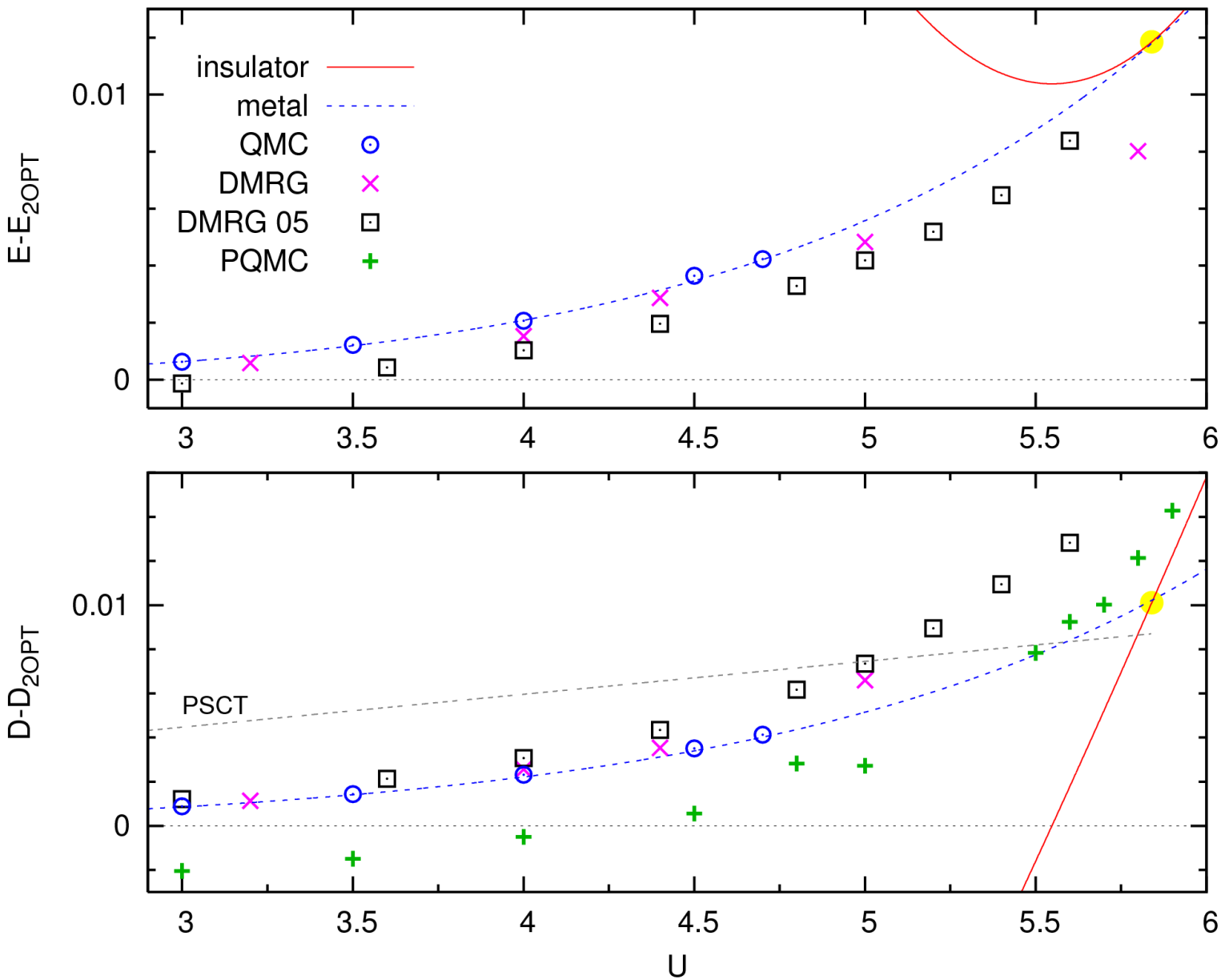

Summary

Cooperative phenomena in correlated electron systems

Theoretical approaches: (multi-band) Hubbard models, DMFT

High-precision Hirsch-Fye quantum Monte-Carlo algorithm

Orbital-selective Mott transitions: 1^{st} order for wide band

Efficiency: HF-QMC competitive with continuous-time QMC

Summary

Cooperative phenomena in correlated electron systems

Theoretical approaches: (multi-band) Hubbard models, DMFT

High-precision Hirsch-Fye quantum Monte-Carlo algorithm

Orbital-selective Mott transitions: 1^{st} order for wide band

Efficiency: HF-QMC competitive with continuous-time QMC

Not covered: Critical exponents from QMC and strong-coupling PT
Theory of half-metallic double perovskites
Realistic material-specific calculations with LDA+DMFT

Summary

Cooperative phenomena in correlated electron systems

Theoretical approaches: (multi-band) Hubbard models, DMFT

High-precision Hirsch-Fye quantum Monte-Carlo algorithm

Orbital-selective Mott transitions: 1^{st} order for wide band

Efficiency: HF-QMC competitive with continuous-time QMC

Not covered: Critical exponents from QMC and strong-coupling PT
Theory of half-metallic double perovskites
Realistic material-specific calculations with LDA+DMFT

Outlook

Band structure calculations for correlated systems

Cluster extensions of DMFT

Ultracold quantum gases on optical lattices

Starting in 7/2007: SFB/TRR 49 (Frankfurt - Kaiserslautern - Mainz)

Condensed matter systems with variable many-body interactions

A1 [Bloch] – Ultracold Fermi mixtures in optical lattices
A2 [Kuhr/Bloch] – Spatially addressable quantum gases in optical lattices
A3 [Hofstetter] – Inhomogeneous quantum phases in ultracold gases with strong correlations
A5 [Fleischhauer/Eggert] – Advanced numerical methods for correlated quantum gases
A6 [Blümer] – Flavour-selective Mott transitions of ultracold quantum gases on optical lattices
A7 [Hillebrands/Serha] – Collective effects and instabilities of a magnon gas
A8 [Kopietz] – Interacting magnons and critical behaviour of bosons

project area B: real materials

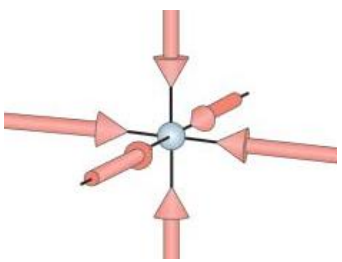

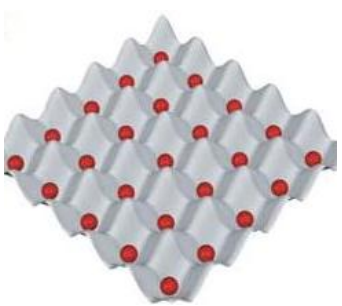

A1 + A6: flavor selectivity in Fermi mixtures of different

- atomic species: ^{6}Li and ^{40}K
- hyperfine states
- vibrational levels

on optical lattices

Hopping amplitudes tunable and flavor-dependent!

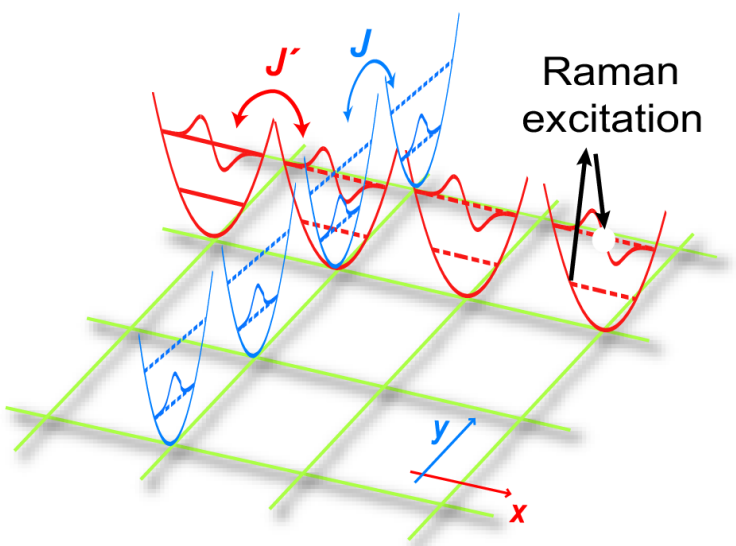

[Müller, Fölling, Widera, Bloch (2007)]